PHENOMIC, GENOMIC AND TRANSCRIPTOMIC STUDIES OF QUORUM SENSING *Enterobacter asburiae* L1 FROM FRESH VEGETABLES

LAU YIN YIN

FACULTY OF SCIENCE
UNIVERSITY OF MALAYA
KUALA LUMPUR

2017

PHENOMIC, GENOMIC AND TRANSCRIPTOMIC STUDIES OF QUORUM SENSING *Enterobacter asburiae* L1 FROM FRESH VEGETABLES

LAU YIN YIN

THESIS SUBMITTED IN FULFILMENT OF THE REQUIREMENTS FOR THE DEGREE OF DOCTOR OF PHILOSOPHY

FACULTY OF SCIENCE
UNIVERSITY OF MALAYA
KUALA LUMPUR

2017

UNIVERSITY OF MALAYA

ORIGINAL LITERARY WORK DECLARATION

Name of Candidate: Lau Yin Yin (I.C/Passport No: [redacted])

Matric No: SHC140102

Name of Degree: Doctor of Philosophy

Title of Thesis: Phenomic, Genomic and Transcriptomic Studies of Quorum Sensing *Enterobacter asburiae* L1 from Fresh Vegetables

Field of Study: Microbiology

I do solemnly and sincerely declare that:

(1) I am the sole author/writer of this Work;
(2) This Work is original;
(3) Any use of any work in which copyright exists was done by way of fair dealing and for permitted purposes and any excerpt or extract from, or reference to or reproduction of any copyright work has been disclosed expressly and sufficiently and the title of the Work and its authorship have been acknowledged in this Work;
(4) I do not have any actual knowledge nor do I ought reasonably to know that the making of this work constitutes an infringement of any copyright work;
(5) I hereby assign all and every rights in the copyright to this Work to the University of Malaya ("UM"), who henceforth shall be owner of the copyright in this Work and that any reproduction or use in any form or by any means whatsoever is prohibited without the written consent of UM having been first had and obtained;
(6) I am fully aware that if in the course of making this Work I have infringed any copyright whether intentionally or otherwise, I may be subject to legal action or any other action as may be determined by UM.

Candidate's Signature Date:

Subscribed and solemnly declared before,

Witness's Signature Date:

Name:

Designation:

ABSTRACT

Bacterial communication or quorum sensing (QS) is achieved via sensing of QS signalling molecules consisting of *N*-acyl homoserine lactones (AHL) in most Gram-negative bacteria. In this study, Enterobacteriaceae isolates from fresh vegetables were screened for AHLs production. A total of twenty different bacterial colonies were isolated and identified by matrix-assisted laser desorption ionization-time of flight mass spectrometry. Preliminary screening demonstrated that one out of twenty isolates produces short chain AHLs. This AHL-producing bacterium which is known as *Enterobacter asburiae* L1 was isolated from Batavia lettuce leaves and was selected for further study. High-resolution triple quadrupole liquid-chromatography mass spectrometry (LC-MS/MS) analysis on *E. asburiae* L1 spent culture supernatant confirmed the production of *N*-butanoyl homoserine lactone (C4-HSL) and *N*–hexanoyl homoserine lactone (C6-HSL). To the best of my knowledge, this is the first report of AHL production by *E. asburiae*. To characterize the *luxI/R* homologues of *E. asburiae* L1, the complete genome of *E. asburiae* L1 (4.5Mbp in size) was sequenced using the single molecule real time sequencer and the whole genome sequence accuracy was verified by optical genome mapping technology. *In silico* analysis of the *E. asburiae* L1 genome revealed the presence of a pair of *luxR* and *luxI* homologues, designated as *easR* and *easI*. The 639 bp *easI* gene was cloned and overexpressed in *Escherichia coli* BL21 (DE3)pLysS. Heterologously expressed EasI protein (~25 kDa) activated AHL biosensor *Chromobacterium violaceum* CV026, indicating this EasI is a functional AHL synthase. LC-MS/MS analysis confirmed the production of C4-HSL and C6-HSL from spent culture supernatant of induced *E. coli* BL21 (DE3)pLysS harbouring the recombinant EasI, suggesting that EasI is indeed the AHL synthase of *E. asburiae* L1. A mutant *E. asburiae* L1 with deletion of the *easI* gene was constructed using Lambda Red

recombination method. With the constructed L1-Δ*easI*::Kan mutant strain, whole transcriptomic sequencing was performed using RNA-seq. Based on the RNA-seq data, a total of 128 genes and 112 genes were being significantly downregulated and upregulated, respectively in L1-Δ*easI*::Kan strain. The *easI* null mutant was shown to be impaired in biofilm formation in comparison to its wildtype strain. In addition, phenotypic microarray (PM) was applied to obtain full metabolic profiles of *E. asburiae* L1 wildtype and mutant strains. The *easI* null mutant was found metabolically less active than wildtype strain when the peptide nitrogen source was utilized. Besides, L1-Δ*easI*::Kan strain has gained more resistance towards several antimicrobial substances. The current study has laid the foundation for developing a deeper understanding in elucidating the roles of AHLs in *E. asburiae* L1 and to study the interaction of EasI with compounds demonstrating anti-QS properties. This could possibly provide a model for bacterial cell-cell communication among *E. asburiae* strains.

ABSTRAK

Komunikasi antara bakteria atau kuorum sensing (QS) boleh dicapai melalui penerimaan isyarat molekul QS yang terdiri daripada *N*-acil homoserine lakton (AHL) yang digunakan oleh kebanyakan bakteria Gram-negatif. Dalam penyelidikan ini, isolat Enterobacteriaceae dari sayur-sayuran segar telah dikaji untuk produksi AHLs. Sebanyak dua puluh koloni bakteria yang berbeza telah diisolat dan identiti bakteria telah dikenal pasti oleh spektrometri matriks bantuan laser desorption pengionan masa jisim penerbangan. Kajian awal menunjukkan bahawa salah satu daripada dua puluh isolat menunjukkan produksi rantaian pendek AHLs. Sejenis bakteria yang menghasilkan AHL iaitu *Enterobacter asburiae* L1, telah diisolat dari daun salad Batavia, dipilih untuk kajian lanjut. Analisis spektrometri jisim kromatografi cecair resolusi tinggi triple quadrupole (LC-MS/MS) pada *E. asburiae* L1 mengesahkan produksi *N*-butanoyl homoserine lakton (C4-HSL) dan *N*–hexanoyl homoserine lakton (C6-HSL). Sepanjang pengetahuan saya, ini adalah laporan pertama mengenai produksi AHL oleh *E. asburiae*. Untuk mencirikan homolog *luxI/R E. asburiae* L1, genom lengkap *E. asburiae* L1 (bersaiz 4.5Mbp) telah melalui jujukan menggunakan sequencer tunggal molekul masa sebenar dan ketepatan seluruh turutan genom telah disahkan oleh teknologi pemetaan optik genom. Analisis *in silico* menujukkan kewujudan sepasang homolog *luxR* dan *luxI* dalam genom *E. asburiae* L1, dan telah dinamakan sebagai *easR* dan *easI*. Gen *easI* (639 bp) telah diklon dan diekpres dalam *Escherichia coli* BL21 (DE3) pLysS. Protein yang diekspress secara heterologus, EasI (~25 kDa) telah mengaktifkan biosensor AHL *Chromobacterium violaceum* CV026, membuktikan EasI adalah synthase AHL yang berfungsi. Analisis LC-MS/MS pada supernatan kultur mengesahkan produksi C4-HSL dan C6-HSL dalam induksi *E. coli* BL21 (DE3) pLysS yang mempaparkan rekombinan EasI. Sehubungan dengan itu, ia membuktikan bahawa EasI ialah synthase AHL *E. asburiae* L1. Dengan menggunakan kaedah penggabungan semula Lambda Merah, mutan *E. asburiae* L1 dengan penyingkiran gen *easI* telah dicipta. Dengan L1-

Δ*easI*::Kan mutan yang dibina, penjujukan seluruh transkriptomik telah dilakukan dengan menggunakan RNA-seq. Berdasarkan data RNA-seq, sebanyak 128 gen mengalami penurunan regulasi dan 112 gen mengalami kanaikan regulasi dalam mutan L1-Δ*easI*::Kan. Pembentukan biofilm bagi mutan null *easI* telah terganggu jika dibandingkan dengan strain wildtype. Selain itu, mikroarray fenotipik (PM) telah digunakan untuk mendapatkan profil penuh metabolik *E. asburiae* L1 strain wildtype dan mutan. Metabolik mutan null *easI* ditemui kurang aktif jika dibandingkan dengan wildtype ketika sumber peptida nitrogen digunakan. Mutan L1-Δ*easI*::Kan juga ditemui menunjukkan lebih rintangan kepada bahan-bahan antimikrob. Kajian ini telah menjadi dasar bagi memahami peranan AHLs di *E. asburiae* L1 dan juga penyelidikan interaksi EasI dengan kompaun yang menunjukkan ciri-ciri anti-QS. Dengan ini, *E. asburiae* L1 mungkin boleh menjadi model untuk memahami komunikasi antara sel-sel bakteria bagi strain *E. asburiae*.

ACKNOWLEDGEMENTS

First and foremost, I would like to express my heartiest appreciation to my supervisor, A/P Dr Chan Kok Gan for his dedicated efforts in providing new ideas, valuable guidance, and constant encouragement from the process of preparation and throughout the completion of my Ph.D research and thesis. My sincere thanks also go to my lab manager, Miss Yin Wai Fong for her well-organization in the lab. She helps to manage the financial and always ensures sufficient supplies of necessity as well as the reasonable working and storage area in the lab that provide us a comfortable working environment.

My appreciation also goes to University of Malaya for providing sufficient financial support which included High Impact Research grants, PPP Grant and Graduate Research Assistantship Scheme (GRAS) as well as all the necessary infra-structural facilities throughout the commencement of this research.

Besides, I would like to express my gratitude to all my fellow lab mates and friends for their moral support, and assistance in various ways during the periods of research. Lastly, I would like to thank my dearest family members especially my parents for their unconditional moral support and love they have given to me throughout my study.

TABLE OF CONTENTS

LIST OF FIGURES

LIST OF TABLES

LIST OF SYMBOLS AND ABBREVIATIONS

%	Percent
<	Less than
≤	Less than or equal
>	More than
≥	More than or equal
× *g*	Times gravity
×	Times
3OH-PAME	3-hydroxypalmitic acid methyl ester
3-oxo-C6-HSL	3-oxo-hexanoyl-HSL
A factor	2-isocapryloyl-3R-hydroxymethyl-γ-butyrolactone
ACN	Acetonitrile
ACP	Acyl carrier protein
AGE	Agarose gel electrophoresis
AHLs	*N*-acyl homoserine lactones
AHQs	2-Alkyl-4-quinolones
AIs	Autoinducers
Amp	Ampicillin
ANI	Average nucleotide identity analysis
BHIB	Brain heart infusion broth
bp	Base pair
BR	Broad range
C10-HSL	*N*-decanoyl-L-homoserine lactone
C12-HSL	*N*-dodecanoyl-L-homoserine lactone
C4-HSL	*N*-butanoyl homoserine lactone
C6-HSL	*N*–hexanoyl homoserine lactone
$CaCl_2$	Calcium chloride
cDNA	Complementary deoxyribonucleic acid
CDS	Coding sequence
CFD	Channel-forming device
cm	Centimetre
Cm	Chloramphenicol
DKP	Diketopiperazines
DNA	Deoxyribonucleic acid

DPD	4,5-dihydroxy-2,3-pentandione
dsDNA	Double-stranded deoxyribonucleic acid
DSF	Diffusible signal factor
e.g.	Latin term of “exempli gratia” which means “for example”
ESBL	Extended-spectrum β-lactamase
et al.	Latin word of “et alii” which means “and other”
eV	Electronvolt
F	Forward
g	Gram
gff	Gene-finding format
gfp	Green fluorescent protein
GN	Gram-negative
h	Hour
HGAP	Hierarchical genome assembly process
HHQ	2-heptyl-4-quinolone
HMDS	Hexamethyldisilazane
HS	High sensitivity
HT1	Hybridisation buffer
HTH	Helix-turn-helix
i.e.	Latin term of “id est” which means “that is”
IF	Inoculating fluid
IPTG	Isopropyl-β-D-1-thiogalactopyranoside
kb	Kilobyte
kDa	Kilodalton
Km	Kanamycin
KPC	*Klebsiella pneumoniae* carbapenemase
kV	Kilovolt
L	Litre
LB	Luria Bertani
LC-MS/MS	Triple quadrupole liquid-chromatography mass spectrometry
M	Molar
M value	Expression stability value
m/z	Mass-to-charge ratio
MALDI	Matrix-assisted laser desorption ionization
MEGA	Molecular evolutionary genetic analysis

mg	Milligram
min	Minute
mL	Millilitre
mm	Millimetre
mM	Millimolar
MOPS	3-[*N*-morpholino] propanesulfonic acid
MR	Methyl red
Mr	Molecular mass
MS	Mass spectrometry
N	Normality
Na_2CO_3	Sodium carbonate
NaCl	Sodium chloride
NaOH	Sodium hydroxide
NCBI	National centre for biotechnology information
ng	Nanogram
Ni-NTA	Nickel-nitrilotriacetic acid
nm	Nanometre
nM	Nanomolar
NO_2^-	Nitrite
NO_3^-	Nitrate
^oC	Degree Celsius
OD	Optical density
o-NPG	o-nitrophenyl-β-D-galactopyranoside
ORF	Open reading frame
PacBio	Pacific biosciences
PBS	Phosphate buffer saline
pC-HSL	N-(*ρ*-coumaroyl)-HSL
PCR	Polymerase chain reaction
pg	Picogram
pi	Isoelectric point
PM	Phenotypic microarray
pM	Picomolar
PMF	Peptide mass fingerprint
PQS	2-heptyl-3-hydroxy-4-quinolone
psi	Pounds per square inch

qPCR	Real-time PCR
QS	Quorum sensing
^{R}	Resistance
R	Reverse
RAST	Rapid annotations using subsystems technology
RIN	Ribonucleic acid integrity number
RLU	Relative light units
RNA	Ribonucleic acid
rpm	Revolutions per minute
rRNA	Ribosomal ribonucleic acid
RTC	Real time classification
s	Second
SAM	S-adenosylmethionine
SDS-PAGE	Sodium dodecyl sulphate polyacrylamide gel electrophoresis
SEM	Scanning electron microscopy
SMRT	Single molecule real time sequencer
spp.	Species
TA	Toxin-antitoxin
TBE	Tris-boric acid ethylenediaminetetraacetic acid
Tet	Tetracycline
TLC	Thin layer chromatography
TOF	Time of flight
TSA	Trypticase soy agar
UV	Ultraviolet
V	Volt
v/v	Volume/Volume
VP	Voges proskauer
w/v	Weight/Volume
WGS	Whole genome sequencing
X-gal	5-bromo-4-chloro-3-indoyl-β-D-galactopyranoside
A	Alpha
β	Beta
γ	Gamma
λ	Lambda
μg	Microgram

μm	Micrometre
μL	Microliter
μM	Micromolar

LIST OF APPENDICES

CHAPTER 1: INTRODUCTION

Consumers' demand for healthy, garden-fresh, natural and convenience food have been on the rise. The lifestyle change of consumers' eating habit towards convenient, ready-to-eat food products in the meantime has accelerated the incidence and outbreaks of food-borne diseases worldwide (Berger et al., 2010; Heaton & Jones, 2008). It is believed that raw vegetables may represent an important source of risk for human health due to their complex surface and porosity which can facilitate pathogen attachment and survival (El Said Said, 2012; Harris et al., 2003; Park et al., 2012). Therefore, it is of interest to study the factors contributing to the transmission of pathogenic microorganisms on vegetables and the epidemiology of food-borne diseases (Altekruse & Swerdlow, 1996; Burnett & Beuchat, 2001).

In nature, bacteria function less as individual cells and more as groups, enabling them to inhabit multiple ecological niches. Bacterial cell-to-cell communication or quorum sensing (QS) is achieved via sensing of QS signalling molecules consisting of *N*-acyl homoserine lactone (AHL) in most Gram-negative bacteria, resulting in regulation of gene expression in response to surrounding bacterial cell density (Dong & Zhang, 2005; Fuqua, Parsek, & Greenberg, 2001; Waters & Bassler, 2005; Williams, 2007). Some physiological activities regulated by QS include symbiosis, virulence, competence, conjugation, antibiotic production, motility, sporulation, and biofilm formation (Miller & Bassler, 2001; Williams, 2007). As it is believed that bacteria can employ QS to gain maximum competition advantages in different environments, study on the potential roles of QS in phyllosphere environment might provide an important insight into food microbiology. Besides, advanced research on AHL signalling system might provide a promising target for developing novel approaches to interfere with microbial QS by regulating the virulence properties of the microbial communities (How et al., 2015).

Enterobacteriaceae is a large family of Gram-negative, rod-shaped, non-spore forming bacteria classified as facultative anaerobes (Zaitseva Iu, Popova, & Khmel, 2014). Members of the family Enterobacteriaceae (e.g. *Enterobacter* spp.) colonization has been reported to cause gastrointestinal illnesses around the world and these outbreaks have been commonly connected to consumption of contaminated vegetable and fruit products (Mandrell, 2009; Teplitski, Warriner, Bartz, & Schneider, 2011). The relation of food-borne illnesses with enteric bacteria has caused an increase in multidisciplinary interest in researching the production of signalling molecules (i.e. QS signalling molecules) to better understand how these interactions may affect food safety and cause infection.

In this research, studies were focused on the isolation of the bacterial community from the Enterobacteriaceae family in six different fresh salad vegetables that are popular among Malaysian population. The isolates were screened for the AHLs production using the bacterial biosensor CV026, followed by characterization of AHL molecules using high-resolution triple quadrupole liquid-chromatography mass spectrometry (LC-MS/MS). In addition, the whole genome sequencing and functional genome of the QS bacteria isolated were investigated before subjecting to the phenotypic and transcriptomic studies.

The objectives of this research include the following:

1) To isolate and identify the isolated strains using MALDI-TOF-MS,
2) To determine QS properties of the isolated bacterial strains,
3) To perform whole genome sequencing of the QS bacteria,
4) To study the functional genome of the QS bacteria,
5) To perform phenotypic study of the QS bacteria,
6) To study transcriptome profile of QS bacterium and its QS knock-out mutant.

CHAPTER 2: LITERATURE REVIEW

2.1 Enterobacteriaceae

The Enterobacteriaceae is a family of non-spore forming, Gram-negative bacilli bacteria, typically 1 to 5 μm in length. They normally inhabit the intestines of humans and animals. According to ILSI Europe Report, only 12 genera and 36 species of Enterobacteriaceae was reported in 1974. Over the decades, the number of genera and species has increased to at least 53 genera, 219 species and 41 sub-species in the family and the number are expected to keep growing. Some of the important genera in this family include *Escherichia*, *Salmonella*, *Shigella*, *Klebsiella*, *Proteus*, *Enterobacter*, *Serratia* and *Yersinia* (Hornick, Allen, Horn, & Clegg, 1991).

Members of the Enterobacteriaceae are widely distributed, ranging from harmless commensals to important human, plant and animal pathogens. Numerous species of the Enterobacteriaceae are pathogenic and cause various infections such as pneumonia, chronic infantile diarrhoea and urinary tract infections (Guentzel, 1996). Apart from those well-known pathogens in Enterobacteriaceae family, some members such as *Enterobacter* spp., *Serratia* spp., *Klebsiella* spp. and *Citrobacter* spp. have been found to involve in human diseases and are well-known as the major cause of wound infections and other hospital acquired (nosocomial) infections. In addition to this, members of this family (e.g. *Enterobacter* spp.) have been reported to cause gastrointestinal illnesses (Swartz, 2002) worldwide and these outbreaks have been frequently related to vegetables and fruits produce. Due to their ubiquitous distribution, it is unavoidable that some members of the Enterobacteriaceae can be found in the edible food. They are commonly present either as the natural microflora reside in certain foods or can be introduced due to post-process contamination (Guentzel, 1996). For instance, studies revealed that some of the food-borne pathogens in this family (e.g. *Salmonella* spp., *Proteus* spp. and

Escherichia spp.) have been recognized to colonize meat and poultry via faecal contamination (Swartz, 2002).

In recent years, the more worrying problem related to Enterobacteriaceae is the emergence of Enterobacteriaceae resistant to 3rd and 4th generation cephalosporins. This resistance has been demonstrated to be related to extended-spectrum β-lactamase (ESBL) production (Li, Mehrotra, Ghimire, & Adewoye, 2007). By this, the mortality rates in patients have increased due to the complications triggered by failure of oral antibiotic to treat many simpler infections, leading to severe infections (Wellington et al., 2013).

Undoubtable, Enterobacteriaceae is definitely one of the most important groups of bacteria closely related to human infections. However, there are still a lot of unsolved mystery about them. Therefore, continuous and extensive studies on members of Enterobacteriaceae will definitely path a better way to understand the pathogenicity of Enterobacteriaceae, in the hope to find ultimate solutions to control infections.

2.2 QS

Over the last two decades, bacteria are assumed to survive as an individual living unicellular organism that sought nutrients for survival and can multiply independently from other members of their species (Atkinson & Williams, 2009). The perspective on bacteria has been replaced with the discovery that bacterial are capable to communicate with one another to form a complex community. These confer on a bacterial population the ability to provoke a collective behavioural change due to environmental challenges. This population-dependent adaptive behaviour will be triggered when bacteria communicate to one another using a mechanism known as QS (Atkinson & Williams, 2009).

QS, a term first introduced by Fuqua et al. (1994), describes the bacterial cell–cell communication process by which bacterial cells are able to identify and response to the accumulation of extracellular signalling molecules namely autoinducers (AIs) (Rutherford & Bassler, 2012; Sifri, 2008). AIs are synthesized in response to the environmental changes or at specific stages of growth and the concerted response will be induced once a critical concentration has been reached (González & Marketon, 2003). Bacterial cells apply QS to count themselves, monitor when they have reached an optimal cell density before change their behaviour synchronously for activities that request a group of cells coordinating together (Whitehead, Barnard, Slater, Simpson, & Salmond, 2001). This communication is crucial for bacteria to adapt better in different environments by defencing against other microorganisms which may compete for the same nutrients and avoid those toxic compounds that might be dangerous for the bacteria (Williams, 2007). Processes controlled by QS include bioluminescence, motility, symbiosis, virulence factor secretion, sporulation, competence, antibiotic production, biofilm formation, and conjugation (Rutherford & Bassler, 2012; Sifri, 2008).

QS system was first described in the bioluminescent marine bacterium, *Vibrio fischeri*. *V. fisheri* is a symbiotic species which colonize the light organ of *Euprymna scolopes* (Hawaiian bobtail squid) to provide its marine eukaryotic hosts with light. Basically, the light emission depends on transcription of the luciferase operon, which occurs when the cell-population density reaches its threshold concentration of a secreted autoinducer. During day time, the luminescence was "turned off" by the squid by pumping out large number of bacteria from its light organ, causing insufficient signalling molecules production in the bacteria, hence the production of luciferase is prohibited (Dunlap, 1999; Waters & Bassler, 2005). However, the bacteria population and the signalling molecules that trigger the luciferase expression will gradually increase over the time. At night, the luminescence will once again "turned on" when the signalling molecules have reached the threshold concentration. This bioluminescence was crucial for the squid to counter-illuminate its shadow and avoid predation at night (Callahan & Dunlap, 2000; Defoirdt, Boon, Sorgeloos, Verstraete, & Bossier, 2008). By using *V. fischeri* as a model, the mechanism of QS circuits was summarized in Figure 2.1.

Generally, the mechanism of AHL-mediated QS circuits in Gram-negative bacteria involves two regulatory components: (1) the AI molecule produced by the autoinducer synthase (known as LuxI) and (2) the transcriptional regulator (known as LuxR). Accumulation of AI occurs in a cell-density-dependent manner in order to regulate the expression of certain genes (Fuqua et al., 2001). At low cell density, signalling molecules synthesized by LuxI will diffuse away rapidly due to the concentration of the signalling molecules is below the required threshold concentration. In contrast, at high cell density, the signalling molecules will diffuse back into the cell upon attaining a threshold concentration and bind to the cognate LuxR that exist in the cytoplasm or in the membrane to mediate a collective behaviour in the bacterial population (Cooley, Chhabra, & Williams, 2008; Fuqua et al., 2001).

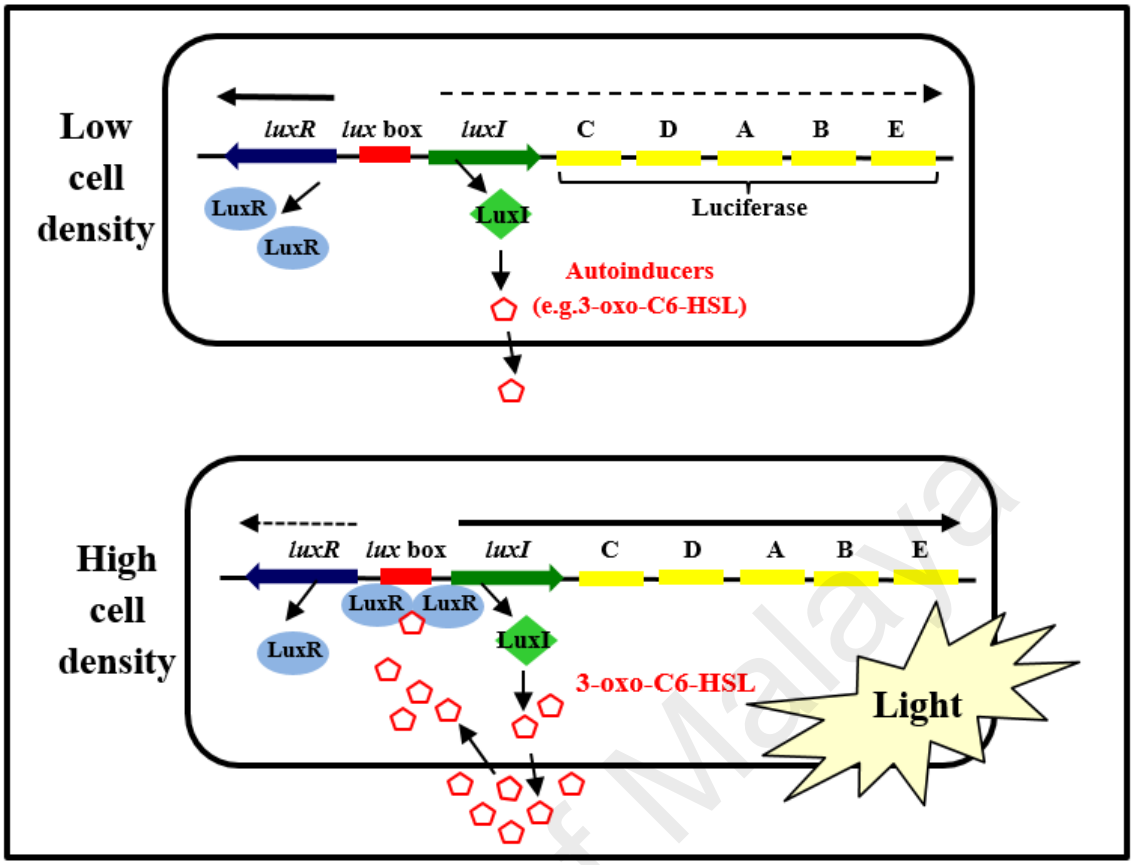

Figure 2.1: Mechanism of QS circuits. Bioluminescence activation in *V. fischeri* by the LuxI/R QS system was displayed. At low cell density, AHL synthesized by LuxI diffuses away rapidly due to the concentration of the signalling molecule is below the required threshold concentration. At high cell density, the AHL binds to LuxR. LuxR in complex with AHL then activates transcription of itself and the luciferase operon. This leads to regulation of bacterial virulence, such as biofilm formation, iron binding, the production of extracellular polysaccharides and innate bactericidal activities.

2.3 QS Signalling Molecules

For true QS-based communication to occur among bacteria, one or few individuals must produce a signal that can be recognized by other individuals as "cues", and the perceivers must alter their behaviour in response to this signal produced (Keller & Surette, 2006). According to Winzer et al. (2002), there are four principle characteristics of QS signals: (1) The production of QS signal occurs in response to specific environmental changes or during specific stages of growth; (2) Recognition and binding of the QS signal that accumulates in the extracellular environment by a specific receptor; (3) The accumulation of the QS signal to a critical threshold concentration in order to trigger a concerted or coordinated response; (4) The cellular response extends beyond the physiological changes required to metabolize or detoxify the molecule (Diggle, Gardner, West, & Griffin, 2007; Winzer, Hardie, & Williams, 2002)

To date, there are numerous types of QS signalling molecules being identified. Bacterial QS signal molecules are structurally and chemically diverse. Some examples of intercellular signalling molecules included AHL; 2-Alkyl-4-quinolones (AHQs) (i.e: 2-heptyl-3-hydroxy-4-quinolone (PQS) and 2-heptyl-4-quinolone (HHQ), termed as *Pseudomonas* quinolone signal) (Fletcher, Diggle, Camara, & Williams, 2007; Pesci et al., 1999); diketopiperazines (DKP); 2-isocapryloyl-3R-hydroxymethyl-γ-butyrolactone (A factor), *cis*-11-methyl-2-dodecenoic acid (diffusible signal factor) (DSF), furanosyl borate diester (autoinducer-2) (AI-2) (Barber et al., 1997); 3-hydroxypalmitic acid methyl ester (3OH-PAME) (Flavier, Clough, Schell, & Denny, 1997); bradyoxetin (Loh, Carlson, York, & Stacey, 2002); and 4,5-dihydroxy-2,3-pentandione (DPD) (Atkinson & Williams, 2009; Williams, 2007). The structure of these different classes of QS signalling molecules are shown in Figure 2.2.

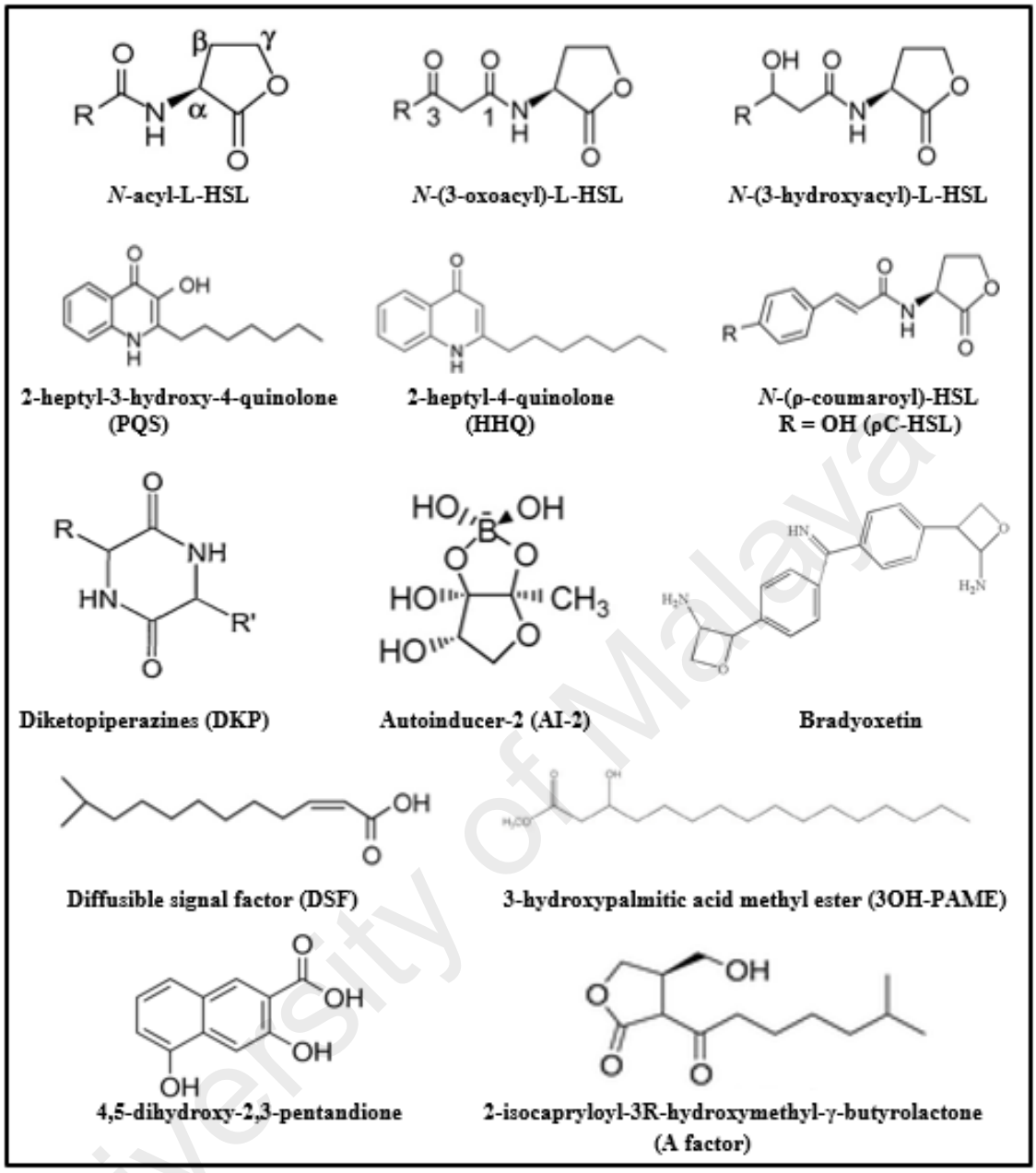

Figure 2.2: Different classes of QS signalling molecules.

2.3.1 AHL

In QS, signalling via AHL (*N*-acyl-L-HSL, *N*-(3-oxoacyl)-L-HSL and *N*-(3-hydroxyacyl)-L-HSL, *N*-(*ρ*-coumaroyl)-HSL) is widely-used among Proteobacteria (Miller & Bassler, 2001; Schaefer et al., 2008). AHL is also the most well-studied and characterized QS signalling molecule. AHL is highly-conserved signalling molecule, each consisting of a homoserine lactone ring unsubstituted in the β- and γ-positions but *N*-acylated at the α-position with a fatty acyl group. The latter moiety comprises 4- to 18-carbon side chain and either an oxo, a hydroxy, or no substitution at the C3 position (Figure 2.2) (Pearson, Van Delden, & Iglewski, 1999). AHLs are synthesized by AHL synthase (LuxI homologue) using *S*-adenosylmethionine (SAM) and acylated acyl carrier protein (Acyl-ACP) as the substrates (Figure 2.3) (Schauder & Bassler, 2001; Swift et al., 1997). SAM usually acts as a methyl donor, whereas acyl-ACPs are components of the fatty acid biosynthetic pathway and act as acyl chain donors in AHL. synthesis (More et al., 1996).

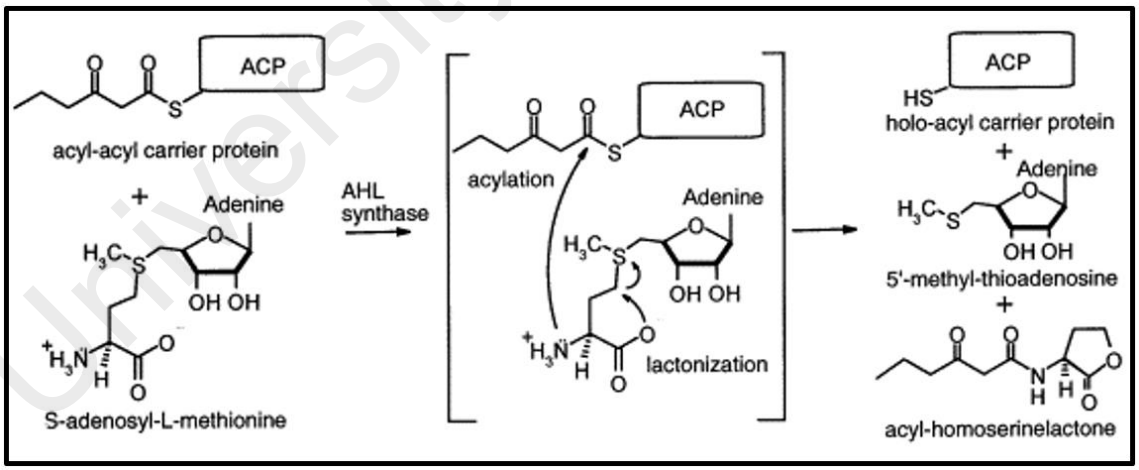

Figure 2.3: Schematic diagram of the AHL synthesis reaction. Two substrates, acyl-ACP and SAM, bind to the enzyme. After the acylation and lactonization reactions, the product AHL and by-products holo-ACP and 5′-methylthioadenosine are released (Watson, Minogue, Val, von Bodman, & Churchill, 2002).

On the other hand, LuxR, members of FixJ-NarL superfamily (Kahn & Ditta, 1991) has two principle conserved domains, an N-terminal AHL-binding domain and a C-terminal DNA binding helix-turn-helix (HTH) domain (Choi & Greenberg, 1991; Hanzelka & Greenberg, 1995). When AHLs concentration has reached its threshold level, the cognate AHL binds to the N-terminal AHL binding site, causing the LuxR conformation changes and promote the multimerization. LuxR then binds to a DNA binding site called a *lux* box, which is normally a 20 bp in length and centred 42.5 nucleotides upstream of the transcription start site (Devine, Shadel, & Baldwin, 1989; Urbanowski, Lostroh, & Greenberg, 2004). The *lux* box sequence has imperfect dyad symmetry, suggesting that the DNA binding domains are multimeric and have a corresponding two-fold rotational symmetry (Antunes, Ferreira, Lostroh, & Greenberg, 2008). Activation of the *lux* box leads to a rapid rise in the levels of AHL and creates a positive-feedback loop. Following this, a complex that stimulates the expression of numerous downstream target genes will form and hence, activates the physiological functions of the cells (How et al., 2015; Parsek & Greenberg, 2000).

The AHL-based QS system was first discovered and characterized in *V. fischeri* which produce 3-oxo-C6-HSL (Figure 2.1) (Eberhard et al., 1981; Schaefer, Val, Hanzelka, Cronan, & Greenberg, 1996). Subsequently, the presence of LuxI/R homologues have been identified in more than 100 Gram-negative bacterial species together with their implications in regulating different cellular responses and phenotypes (Case, Labbate, & Kjelleberg, 2008; Rutherford & Bassler, 2012). These included marine vibrios, rhizosphere bacteria, phototrophic purple non-sulphur bacteria, enteric commensals and opportunistic pathogens of plants and animals. Genetic organization of LuxI/R homologues are as diverse as their function. Homologues of *luxI/R* genes have been identified both on bacterial chromosomes and on extrachromosomal elements. In most cases, they are located adjacently to each other either divergently or convergently

(Gray & Garey, 2001). Studies revealed that numerous bacterial species contain multiple LuxI and/or LuxR homologues for the production or detection of multiple, distinct signals. Besides, multiple LuxR homologues also have been reported to work independently to activate different gene expression in response to a single autoinducer signal (Subramoni & Venturi, 2009; Venturi & Ahmer, 2015). Examples of bacteria utilizing the AHLs as the signalling molecules are summarized in Table 2.1.

Table 2.1: AHLs-producing bacteria and the QS-regulated behaviours

Organism	QS Systems	AHLs	Target Genes and Phenotypes	References
Aeromonas hydrophila	AhyI/R	C4-HSL, C6-HSL	Serine protease, metalloprotease production and biofilm formation	(Lynch et al., 2002; Swift et al., 1997)
Aeromonas salmonicida	AsaI/R	C4-HSL	Production of serine protease	(Swift et al., 1997)
Agrobacterium tumefaciens	TraI/R	3-oxo-C8-HSL	Conjugation	(Piper, Beck Von Bodman, Hwang, & Farrand, 1999; Zhang, Murphy, Kerr, & Tate, 1993)
Agrobacterium vitis	AvsI/R	C16:1-HSL, 3-oxo-C16:1-HSL	Virulence	(Hao & Burr, 2006)
Acidithiobacillus ferrooxidans	AfeI/R	C14-HSL	Biofilm formation, response to iron	(Rivas, Seeger, Jedlicki, & Holmes, 2007)
Acinetobacter baumannii	AbaI/R	3-hydroxy-C12-HSL	*csu*-ecoded chaperone-usher pilus assembly system and the Bap protein for biofilm formation	(Niu, Clemmer, Bonomo, & Rather, 2008)
Burkholderia cepacia	CepI/R	C6-HSL, C8-HSL	Swarming motility, biofilm formation and siderophore production	(Huber et al., 2001; Lewenza, Conway, Greenberg, & Sokol, 1999)
Chromobacterium violaceum	CviI/R	C10-HSL	Biofilm formation, chitinase and violacein production	(Stauff & Bassler, 2011)

Table 2.1, continued

Organism	QS Systems	AHLs	Target Genes and Phenotypes	References
Burkholderia cenocepacia	CepI/R; CciI/R	C6-HSL; C8-HSL	Biofilm formation and siderophore production, virulence, exoenzyme	(Malott, Baldwin, Mahenthiralingam, & Sokol, 2005; Sokol et al., 2003)
Burkholderia mallei	BmaI1/R1, BmaI3/R3 BmaR4, BmaR5	C8-HSL, 3-hydroxy-C8-HSL, C10-HSL	Virulence	(Duerkop, Ulrich, & Greenberg, 2007; Ulrich, Deshazer, Hines, & Jeddeloh, 2004)
Burkholderia pseudomallei	PmlI1/R1, PmlI2/R2, PmlI3/R3	C8-HSL, C10-HSL, 3-hydroxy-C8-HSL, 3-hydroxy-C10-HSL, 3-hydroxy-C14-HSL	Virulence, exoproteases	(Ulrich, Deshazer, Brueggemann, et al., 2004; Valade et al., 2004)
Pectobacterium carotovorum	CarI/R	3-oxo-C6-HSL	Biosynthesis of carbapenem antibiotic	(Barnard et al., 2007)
P. carotovorum subsp carotovorum	ExpI/R	3-oxo-C6-HSL	Carbapenem antibiotic production, exoenzymes	(Bainton et al., 1992)
Edwardsiella tarda strain LTB-4	ExpI/R	3-oxo-C6-HSL	Production of extracellular plant cell wall-degrading enzymes	(Koiv & Mae, 2001)
Erwinia chrysanthemi	EagI/R	3-oxo-C6-HSL	ND	(Swift et al., 1993)

Table 2.1, continued

Organism	QS Systems	AHLs	Target Genes and Phenotypes	References
Enterobacter agglomerans	GinI/R	C10-HSL, C12-HSL, C12:1-HSL	*ginA* (growth in ethanol-containing medium, acetic acid production)	(Iida, Ohnishi, & Horinouchi, 2008)
Massilia timonae	ND	5-*cis*-3-oxo-C12-HSL; 5-*cis*-C12-HSL	ND	(Krick et al., 2007)
Mesorhizobium sp.	MrlI1, MrlI2, MrlI3	C12-HSL, 3-oxo-C6-HSL, C8-HSL, C10-HSL	Symbiotic nodulation	(Yang et al., 2009)
Mesorhizobium loti NZP2213	MsaI/R	C6-HSL, C8-HSL	Extrapolysaccharide carbohydrate production	(Penalver, Cantet, Morin, Haras, & Vorholt, 2006)
Obesumbacterium proteus	PagI/R	C4-HSL	*hrpL, hrpS* and *hrc* genes (gall formation in plant; IAA & cytokinin in regulation	(Chalupowicz, Barash, Panijel, Sessa, & Manulis-Sasson, 2009)
Pantoea stewartii	EsaI/R	3-oxo-C6-HSL	Adhesion and host colonization	(Koutsoudis, Tsaltas, Minogue, & von Bodman, 2006)
Pantoea ananatis	EsaI/R	C6-HSL	Biosynthesis of stewartan and EPS	(Koutsoudis et al., 2006)

Table 2.1, continued

Organism	QS Systems	AHLs	Target Genes and Phenotypes	References
Pseudomonas aeruginosa	LasI/R; RhlI/R	3-oxo-C12-HSL	Exoenzymes, biofilm formation, cell-cell spacing	(Chapon-Herve et al., 1997; Glessner, Smith, Iglewski, & Robinson, 1999; Passador, Cook, Gambello, Rust, & Iglewski, 1993)
Pseudomonas aureofaciens	PhzI/R	C6-HSL	Phenazine antibiotic production	(Pierson, Gaffney, Lam, & Gong, 1995)
Pseudomonas putida	PpuI/R	3-oxo-C10-HSL, 3-oxo-C12-HSL	Maturation	(Dubern, Lugtenberg, & Bloemberg, 2006)
Rhodobacter sphaeroides	CerI/R	7-cis-C14-HSL	Community escape	(Puskas, Greenberg, Kaplan, & Schaefer, 1997)
Rhodopseudomonas palustris	RpaI/R	pC-HSL	ND	(Schaefer et al., 2008)
Rhizobium leguminosarum	RhiI/R	3-hydroxy-7-cis-C14-HSL	Nodulation, bacteriocin, stationary phase survival	(Gray, 1997; Rodelas et al., 1999; Thorne & Williams, 1999)
Serratia liquefaciens	SwrI/R	C4-HSL	Biofilm formation	(Labbate et al., 2004)

Table 2.1, continued

Organism	QS Systems	AHLs	Target Genes and Phenotypes	References
Serratia marcescens	SmaI/R	C4-HSL, C6-HSL	Swarming motility; haemolytic activity; production of caseinase and chitinase; biofilm formation	(Coulthurst, Williamson, Harris, Spring, & Salmond, 2006)
Vibrio anguillarum	VanM	3-hydroxy-C6-HSL	Terminal haemorrhagic septicaemia in fish	(Milton et al., 2001)
Vibrio fischeri	AinS; LuxI/R	C8-HSL, 3-oxo-C6-HSL	Bioluminescence	(Eberhard et al., 1981; Hanzelka et al., 1999)
Vibrio harveyi	LuxM	3-hydroxy-C4-HSL	Bioluminescence	(Bassler, Wright, Showalter, & Silverman, 1993)
Yersinia enterocolitica	YpeI/R	3-oxo-C6-HSL, 3-oxo-C8-HSL, C6-HSL	Swimming and swarming motility	(Atkinson, Chang, Sockett, Camara, & Williams, 2006)
Yersinia pseudotuberculosis	YpsI/R and YtbI/R	C6-HSL, 3-oxo-C6-HSL, C8-HSL	Motility, clumping	(Atkinson, Throup, Stewart, & Williams, 1999)

ND: Not detected

2.4 QS in The Context of Food

Food safety hazards especially pathogenic microorganisms, toxic chemicals, and physical hazards are attributed to contaminated fresh produce, particularly salad vegetables. Of these, microbiological hazards are globally considered as the major cause of food-borne diseases (Parish et al., 2003). Extensive studies have shown that microbiological contamination of food products is largely due to the naturally occurring phenomenon of biofilm formation. Food spoilage and biofilm formation by food-borne pathogens are significant and persistence problems in the food industry, leading to serious health problems and causing great economic loss (Bai & Rai, 2011; Kumar & Anand, 1998). It has been reported that biofilm-forming characteristic is mediated by QS. Studies showed that most of the food-borne pathogens have been identified to form biofilms (Annous, Fratamico, & Smith, 2009), allowing them to enjoy advantages such as resistant to antimicrobial and cleaning agents compared to their planktonic counterparts. This leads to difficulty to eliminate them from the environments that they inhabit.

Unfortunately, to date, studies regarding the roles of QS in food microbial ecology are limited. In most of the available studies, various signalling compounds such as AHLs and AI-2 have been reported to be present and/or increase their concentration in different food ecology. Since bacterial QS has been reported to be crucial in pathogenic relationships with eukaryotic hosts, advanced research on AHL signalling system would provide a promising target for developing novel approaches to interfere with microbial QS by regulating the virulence properties of the microbial communities (How et al., 2015). Consequently, the potential roles of QS especially in regulation of biofilm formation by food-borne or potential food-borne pathogens on food contact surface should be extensively elucidated. With the information gained, it is in the hope to discover new research avenues by designing approaches to interrupt the QS signalling pathway to combat microbial infections (Skandamis & Nychas, 2012).

2.5 Detection of AHLs With Biosensors

Identification of bacterial AHL-mediated QS systems has been simplified and quickened with the development of bacterial biosensors that are able to detect the presence of AHL compounds (Farrand, Qin, & Oger, 2002; Llamas, Keshavan, & Gonzalez, 2004; McClean et al., 1997). Most of the QS biosensors are constructed by either modification of the bacterial QS gene or by the insertion of plasmid reporter vector into the bacteria (Steindler & Venturi, 2007; Winson et al., 1998). Generally, these biosensors do not produce AHL molecules but still contain a functional LuxR-family protein cloned together with a cognate target promoter (normally the promoter of the cognate LuxI-synthase), which positively regulates the transcription of a reporter gene that displays phenotypes such as bioluminescence, pigment production and green fluorescent protein (Steindler & Venturi, 2007).

The AHL biosensors can be applied in four ways to investigate the presence of bacterial AHL-mediated QS systems: (1) a plate "T" streak assay, resulting in the expression of the reporter phenotype in a gradient near the tested strain as indicated. The production of exogenous short chain AHL molecules from the tested isolates will triggered the violacein production on the biosensor streak line; (2) a TLC overlay technique after separation of AHLs from a bacterial extract, resulting in the detection of the reporter phenotype at the place where AHLs are found; (3) a quantification assay by measuring levels of the reporter phenotype upon exposure to spent bacterial supernatants and (4) an *in vivo* assay using gfp-based biosensors (Steindler & Venturi, 2007).

One of the widely exploited AHL biosensor is *C. violaceum* CV026, a double mini-Tn5 mutant derived from *C. violaceum* ATCC 31532. *C. violaceum* CV026 is a violacein and AHL-negative strain developed after mini-Tn*5* transposon mutagenesis on *cviI* gene responsible for C6-HSL production while retaining the functionality of *cviR* gene that

induces violacein production. This defect results in formation of white colony mutant that will only produce purple pigmentation upon exposure to exogenous short chain AHLs ranging from C4-HSL to C8-HSL (McClean et al., 1997). By this, *C. violaceum* CV026 can be used as a simple and rapid biosensor for detection of short chain AHLs. This strain is well suited for detection on solid media via a "T" streak analysis as well as the TLC soft-agar overlay technique (Steindler & Venturi, 2007).

On the other hand, there are other biosensors which rely on a constructed plasmid harbouring the *luxCDABE* operon of *Photorhabdus luminescens* resulting in bioluminescence as a reporter system (Winson et al., 1998). These plasmids are usually harboured in *Escherichia coli*, which lack of the ability to produce AHLs. For instance, *E. coli* [pSB401] is one of these biosensors that is most sensitive to cognate C6-3-oxo-AHL and display good detection towards C6-HSL, 3-oxo-C8-HSL and C8-HSL. By this, bioluminescence will be induced with the presence of short chain AHLs. This biosensor can be used in a TLC analysis as well as in "T" streak analysis. However, for "T" streak analysis, photon camera equipment is required to analyse the result (Steindler & Venturi, 2007). Examples of AHL biosensors are summarized in Table 2.2.

Table 2.2: AHL biosensors

Strain/ Plasmid sensor	Host	Based on QS system	Reporter system	Best responds to	Good detection	Commonly used for	Reference
C. violaceum CV026	*C. violaceum*	CviI/R (*C. violaceum*)	Violacein pigment	C6-HSL	3-oxo-C6-HSL; C8-HSL; 3-oxo-C8-HSL; C4-HSL	T.S., TLC	(McClean et al., 1997)
pSB401	*E. coli*	LuxI/R (*V. fisheri*)	*luxCDABE*	3-oxo-C6-HSL	C6-HSL; 3-oxo-C8-HSL; C8-HSL	TLC, Q	(Winson et al., 1998)
pHV200I^{-}	*E. coli*	LuxI/R (*V. fisheri*)	*luxCDABE*	3-oxo-C6-HSL	C6-HSL; 3-oxo-C8-HSL; C8-HSL	TLC, Q	(Pearson et al., 1994)
pSB403	Broad host range	LuxI/R (*V. fisheri*)	*luxCDABE*	3-oxo-C6-HSL	C6-HSL; 3-oxo-C8-HSL; C8-HSL	TLC, Q	(Winson et al., 1998)
pSB536	*E. coli*	AhyI/R (*A. hydrophyla*)	*luxCDABE*	C4-HSL		TLC, Q	(Swift et al., 1997a)
pAL101	*E. coli* (*sdiA* mutant)	RhlI/R (*P. aeruginosa*)	*luxCDABE*	C4-HSL		TLC, Q	(Lindsay & Ahmer, 2005)

Table 2.2, continued

Strain/ Plasmid sensor	Host	Based on QS system	Reporter system	Best responds to	Good detection	Commonly used for	Reference
pSB1075	*E. coli*	LasI/R (*P. aeruginosa*)	*luxCDABE*	3-oxo-C12-HSL	3-oxo-C10-HSL; C12-HSL	TLC, Q	(Winson et al., 1998)
pKDT17	*E. coli*	LasI/R (*P. aeruginosa*)	β-galactosidase	3-oxo-C12-HSL	C12-HSL; C10-HSL; 3-oxo-C10-HSL	TLC, Q	(Pearson et al., 1994)
pZLR4	*A. tumefaciens* NT1	TraI/R (*A. tumefaciens*)	β-galactosidase	3-oxo-C8-HSL	All 3-oxo-AHLs; C6-HSL; C8-HSL; C10-HSL; C12-HSL; C14-HSL; 3-hydroxy-C6-HSL; 3-hydroxy-C8-HSL; 3-hydroxy-C10-HSL	T.S., TLC, Q	(Farrand et al., 2002)

Table 2.2, continued

Strain/ Plasmid sensor	Host	Based on QS system	Reporter system	Best responds to	Good detection	Commonly used for	Reference
pSF105 + pSF107	*P. fluorescens* 1855	PhzI/R (*P. fluorescens* 2-79)	β-glucuronidase β-galactosidase	3-hydroxy-C6-HSL	3-hydroxy-C8-HSL	TLC, Q	(Khan et al., 2005)
S. melilotisinI::*lacZ*	*S. melilotisinI*::*lacZ*	SinI/R (*S. meliloti*)	β-galactosidase	3-oxo-C14-HSL	3-oxo-C16:1-HSL; C16-HSL; C16:1-HSL; C14-HSL	T.S., TLC, Q	(Llamas et al., 2004)
pJNSinR	*S. melilotisinI*::*lacZ*	SinI/R (*S. meliloti*)	β-galactosidase	As above with more sensitivity	As above with more sensitivity	T.S., TLC, Q	(Llamas et al., 2004)
pAS-C8	Broad host range	CepI/R (*B. cepacia*)	gfp	C8-HSL	C10-HSL	Single cell	(Riedel et al., 2001)
pKR-C12	Broad host range	LasI/R (*P. aeruginosa*)	gfp	3-oxo-C12-HSL	3-oxo-C10-HSL	Single cell	(Riedel et al., 2001)
pJBA-132	Broad host range	LuxI/R (*V. fisheri*)	gfp	3-oxo-C6-HSL	C6-HSL; C8-HSL; C10-HSL	Single cell	(Andersen et al., 1998)

T.S. refers to 'T' streak analysis in solid media and Q refers to quantification

2.6 MALDI-TOF-MS

Traditionally, bacterial identification is relied greatly on series of biochemical tests that are lengthy in incubation procedures. In recent years, MALDI-TOF-MS has revolutionized routine identification of bacteria. It is a rapid analytical technology for microbial identification and characterization based on assessment of the mass spectra composed of mass-to-charge ratio (*m/z*) peaks with varying intensities at a relatively low cost (Singhal, Kumar, Kanaujia, & Virdi, 2015). The major advantage of MALDI-TOF-MS technology over conventional diagnostic methods is the ability of this system to identify the unknown isolates in a significantly reduced time span. However, there are some limitations of this system (Cobo, 2013). The advantages and limitations of MALDI-TOF-MS technology are outlined in Table 2.3.

Table 2.3: Advantages and limitations of MALDI-TOF-MS

Advantages	Limitations
1) Rapid turnaround time	1) Requires fresh culture for accurate identification
2) Automated high output (24 or 96 samples per run)	2) Lack of antimicrobial susceptibility information alongside organism identification
3) Reusable steel target plates	3) Inability to differentiate among certain closely related organisms
4) Broad applicability to bacteria and fungi	4) Identifications is limited by reference spectra in database
5) Cost effective	5) Repeat analysis may be required
6) User-expandable database	

Sample characterization by MALDI-TOF MS begins by spotting the sample (i.e. solid or liquid) into a defined indentation on a solid target support plate (Figure 2.4). The sample (i.e. ranging from purified protein to whole-cell microorganisms) is then overlaid with a chemical matrix. Prior to analysis, the completely dry matrix will crystallize, hence, ensure the sample entrapped within the matrix also co-crystallizes (Singhal et al.,

2015). The matrix is crucial to protect sample molecules from fragmentation. The prepared target plate is then placed into the ionization chamber where each sample is irradiated with 240 brief pulses of energy from an ultraviolet nitrogen laser (337 nm). The individual sample and matrix molecules will be desorbed from the target plate and turned into the gas phase and ionization will take place. The protonated ions are then accelerated at a fixed potential, whereby they are separated from each other on the basis of their *m/z*. The positively charged analytes are then detected and measured using the time of flight (TOF) mass analyser. Each generated mass spectrum is identified as a unique protein "fingerprint" or known as peptide mass fingerprint (PMF) profile of the unknown sample (Marvin, Roberts, & Fay, 2003). Based on the PMF profile, identification of the unknown microorganism is carried out by computerized comparison of the acquired spectra to a database of reference spectra composed of previously well-characterized isolates (Cobo, 2013).

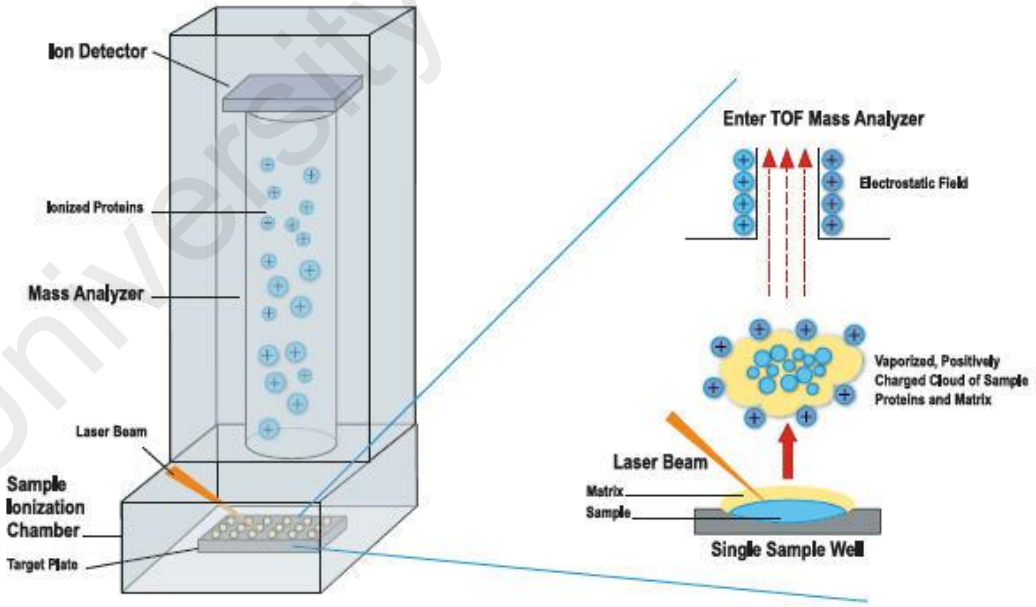

Figure 2.4: MALDI-TOF-MS process.

2.7 Recombineering

Recombineering, also known as recombination-mediated genetic engineering is an efficient *in vivo* genetic engineering that utilizes homologous recombination to edit the genome of prokaryotes and eukaryotes. The recombination is mediated by bacteriophage lambda Red system, which contains three red genes that encode the Gam, Exo and Beta proteins to allow precise insertion, deletion or alteration of any sequence of desired. The Gam protein inhibits the RecBCD exonuclease, which normally degrades linear double-stranded DNA (dsDNA) while Exo protein is a 5' to 3' dsDNA specific exonuclease and is required for dsDNA recombination. The presence of Gam is not absolutely necessary for recombineering; however, its presence helps to increase the frequency of dsDNA recombination about 10-fold. The Beta protein, a single-stranded DNA annealing protein, is the central recombinase in recombineering. Deletions by recombineering can vary in size from a base pair to >10 kb (Sharan, Thomason, Kuznetsov, & Court, 2009).

To perform recombineering, the linear DNA substrates containing the desired knock-out point and short homologies is introduced into the target DNA cells expressing bacteriophage-encoded recombination enzymes. These phage enzymes are expressed either from a heterologous regulated promoter or from their own promoter, confers the advantage of tight regulation and coordinate expression. These enzymes then recombine the linear DNA to the target, yielding higher recombination frequencies, at the same time preventing unwanted rearrangements (Thomason, Sawitzke, Li, Costantino, & Court, 2014). In addition, this technique also brings advantage over the conventional methods as it does not rely on restriction enzymes, hence, the location of restriction sites is no longer an issue to be considered. Consequently, this technique is applied in this study to construct the QS knock-out.

2.8 Phenotype Microarray (PM)

PM is a screening technology that was developed by Biolog Inc. PM technology is a high-throughput platform for simultaneously study the cellular phenotypic activities. A wide range of phenotypic tests are reconfigured in to sets of arrays, whereby each well in the array is designed to test a different phenotype. For instance, wells for PM1 to PM20 are prepared for a total of 1, 920 conditions (Bochner, Gadzinski, & Panomitros, 2001). The cell respiration is measured colourimetrically by using Biolog's patented tetrazolium redox dye. An irreversible purple colour formation will be observed when the dye reduction process takes place in the PM microplate wells. A strong colour formation indicates the cells respire actively in the well. In contrast, if the phenotype is weakly positive or negative, less colour or no colour is formed, indicating slow or no respiration.

Assays of basic cellular nutritional pathways (i.e. catabolism of carbon, nitrogen, phosphorus and sulphur), osmotic, pH and sensitivity, as well as sensitivity to chemical agents (i.e. antibiotics and toxic compounds) are included in the test (Borglin et al., 2012). Many known aspects of cell function can be monitored either directly or indirectly by PM. By this, thousands of cellular phenotypes can be evaluated all at once. This platform also allowed comprehensive and precise quantification of cellular phenotype. As a result, researchers are able to evaluate and obtain an unbiased perspective regarding the effect on cells due to genetic differences, environmental change, and exposure to toxin and chemicals. Commonly, PM assay is applied to assess the phenotypic effects of mutations. A change in genotype of a cell normally lead to one or more changes in phenotype. This provides an easier and rapid way to evaluate the biological changes that occurred consequent to genetic changes in the knock-out or knock-in mutants. In addition, the other common application of PM is phenotypic characterization of a collection of related strains (Bochner et al., 2001).

CHAPTER 3: MATERIALS AND METHODS

3.1 Materials

3.1.1 Equipment and Instruments

Instruments used during the course of this study included -20ºC freezer (Liebherr, UK); 2100 Bioanalyzer (Agilent Technologies, USA); 4ºC chiller (Thermo Scientific, USA); -80ºC freezer (Gaia Science, Singapore); agarose gel electrophoresis (AGE) (Biorad, USA); autoclave machine (Hirayama, USA); automated Argus system (OpGen Inc., USA); belly dancer orbital mixer (IBI Scientific, USA); centrifuge machine (Eppendorf, North America); CFX96 Touch™ real-time PCR detection system (Biorad, USA); class II biosafety cabinet (Thermo Scientific, USA); eco real-time PCR system (Illumina, USA); eco-spin microcentrifuge (Elmi, Latvia); fume hood (Esco Technologies, USA); gel documentary image analyser (UVP, USA); GenePulser Xcell™ electroporation system (Biorad, USA); high performance UV transilluminator (UVP, USA); high-resolution triple quadrupole liquid-chromatography mass spectrometry (LC-MS/MS) (Agilent Technologies, USA); HiSeq 2000 next generation DNA platform (Illumina, USA); ice maker (Nuove Tecnologie Del Freddo, Italy); incubator (Memmert, Germany); infinite M200 luminometer-spectrophotometer (Tecan, Switzerland); laminar flow cabinet (Esco, Technologies, USA); magnetic stirrer hot plate (Labmart, USA); matrix-assisted laser desorption ionization time-of-flight mass spectrometry (MALDI-TOF-MS) (Bruker, Germany); milli-Q® integral water purification system (Merck, Germany); MiSeq personal sequencer (Illumina, USA); nanodrop spectrophotometer (Thermo Scientific, USA); Olympus™ IX71 inverted microscope (Olympus, Japan); Omnilog® reader (Biolog, USA); pH meter (Sartorius, Germany); polymerase chain reaction (PCR) T100 thermal cycler (Biorad, USA); Qubit® 2.0 fluorometer (Invitrogen, USA); SDS-

polyacrylamide gel electrophoresis (Biorad, USA); shaking incubator (Sartorius, Germany); single molecule real time sequencer (SMRT) (Pacific Biosciences, USA); spectrophotometer (Biochrom, USA); stomacher® 400 circulator (Seward, UK); thermomixer (Eppendorf, North America); TM3000 analytical tabletop microscope (Hitachi, USA); turbidimeter (Biolog Inc., USA); vortex mixer (Core Life Sciences, CA); water bath (Benchmark, USA); and weighing machine (Sartorius, Germany).

Equipment used in this study included disposable petri dishes; inoculating loop; hockey stick spreader; laboratory glassware (Schott's bottles, conical flasks, volumetric flasks, universal bottles, measuring cylinder, beaker, test tubes); syringe (Terumo, USA); syringe filter (0.22 µm pore size) (Sartorius, Germany); polypropylene tubes (15 mL and 50 mL); pipettes (Eppendorf, North America), pipette tips (Eppendorf, North America) and microtiter plate (6-well and 96-well).

3.1.2 Commercial Kits

The commercial kits used in the study are described in Table 3.1.

Table 3.1: Commercial kits used in this study

Kit (Manufacturer)	Application
10 kb SMRTbell Library Template Preparation Kit (Pacific Biosciences, USA)	Preparation of PacBio DNA sequencing template
12% Precise Tris-Glycine Gels (Thermo Scientific, USA)	For the separation of proteins by polyacrylamide gel electrophoresis
Agencourt RNAClean™ XP Kit (Beckman Coulter, USA)	Purifying RNA before proceed to ScriptSeq library preparation
Agilent DNA 7500 and DNA 12000 Kit (Agilent Technologies, USA)	Validating the quality sizing analysis of DNA library
Agilent 2100 High Sensitivity DNA Kit (Agilent Technologies, USA)	Examining the quality of the extracted nucleic acid
Agilent RNA 6000 Nano Kit (Agilent Technologies, USA)	Examining the quality of the extracted RNA (i.e. RNA Integrity Number)
Agilent RNA 6000 Pico Kit (Agilent Technologies, USA)	Examining the depletion of 16S and 23S in the rRNA to ensure the quality of the RiboZero treated RNA
AMPure XP Beads (Beckman Coulter, USA)	Purifying cDNA synthesis and RNA-seq library in ScriptSeq library preparation
BugBuster® Protein Extraction Reagent (Novagen, Germany)	Protein extraction
Kapa SYBR Fast qPCR Master Mix (Kapa Biosystems, USA)	Real-time PCR (qPCR) amplification
Masterpure™ DNA Purification Kit (Illumina, USA)	Genomic DNA extraction
Nextera Index Kit (Illumina, USA)	Barcode to identify the pooled samples
Nickel-nitrilotriacetic Acid (Ni-NTA) Fast Start Kit (Qiagen, Germany)	Purification of Protein
NucleoSpin RNA Isolation Kit (Macherey-Nagel GmbH & Co. KG, Germany)	RNA extraction

Table 3.1, continued

Kit (Manufacturer)	Application
OneTaq® DNA Polymerase (NEB, USA)	PCR amplification
QIAamp® Gel Extraction Kit (Qiagen, Germany)	Purification of DNA from agarose gel
Qiagen RNAprotect Bacterial Reagent (Qiagen, USA)	Immediate stabilization of RNA prior to RNA isolation procedures
QIAprep Spin Miniprep Kit (Qiagen, Germany)	Plasmid DNA extraction
QuantiTect Reverse Transcription Kit (Qiagen, Germany)	cDNA synthesis with integrated genomic DNA removal
Qubit® dsDNA BR Assay Kit (Life Technologies, USA)	Quantifying the amount of dsDNA for initial sample concentrations ranging from 100 pg/µL to 1000 ng/µL
Quick Start™ Bradford Protein Assay Kit (Bio-Rad, USA)	Determining the concentration of protein in solution
Ribo-Zero™ Magnetic Kit (Illumina, USA)	Removing unwanted ribosomal RNA prior sequencing
ScriptSeq™ v2 RNA-seq Library Preparation Kit (Illumina, USA)	Preparation of RNA-seq library

3.1.3 Markers and Ladders

DNA ladders used were 1 kb (Promega, USA) and 100 bp (Fermentas, Thermo Fisher Scientific, USA) DNA markers. Molecular weight marker used was PageRuler™ prestained protein ladder, 10 to 180 kDa (Fermentas, Thermo Fisher Scientific, USA)

3.1.4 Growth Medium

All media were obtained from Merck, Germany and subjected to autoclave at 15 psi, 121^{o}C for 15 min. Heat-labile solutions were filter-sterilized with minisart syringe filter (0.22 µm pore size) (Sartorius, Germany).

3.1.5 Chemical Reagents

All the chemical used in this study is of analytical grade purchased from Merck, Germany; Thermo Fisher Scientific, USA; Sigma, USA; Promega Ltd, USA; Amresco, USA; Invitrogen Corp., USA and BD Difco^{TM} Laboratories, USA. Solvents used in this work were supplied by Merck, USA and Thermo Fisher Scientific, UK.

3.1.6 Buffer Solutions

3.1.6.1 Phosphate Buffer Saline (PBS)

The 10× PBS stock solution was prepared by mixing 115 g of Na_2HPO_4, 23 g of NaH_2PO4, and 90 g of NaCl in 1 L of distilled water. The pH of the solution was adjusted to 6.5 prior to autoclave sterilization at 15 psi, 121^oC for 15 min.

3.1.6.2 Tris-Boric Acid Ethylenediaminetetraacetic Acid (TBE)

The 10× TBE stock solution was prepared by mixing 108 g Tris base, 55 g boric acid and 40 mL 0.5 M $Na_2EDTA.2H_2O$ in 1 L of distilled water with pH adjusted to 8.0 before subjected to autoclave at 15 psi, 121^oC for 15 min.

3.1.6.3 Z Buffer

Z buffer was prepared by mixing 0.06 M $Na_2HPO_4.7H_2O$, 0.04 M $NaH_2PO_4.H_2O$, 0.01 M KCl and 0.001 M $MgSO_4$ in 1 L of distilled water with pH adjusted to 7.0. The buffer was filter-sterilized with minisart syringe filter (0.22 µm pore size) and keep in 4^oC. Before use, 0.05 M β-mercapthoethanol was added.

3.1.7 Stock Solutions

3.1.7.1 Synthetic AHLs

Synthetic AHLs were obtained from Cayman, UK and Sigma-Aldrich®, USA. Powder of synthetic AHLs were suspended with acetonitrile (ACN) to the desired concentration and stored at -20°C.

3.1.7.2 Antibiotics

Antibiotics stocks were obtained from Sigma-Aldrich®, USA and Amresco, USA. When indicated, Luria Bertani (LB) was supplemented with antibiotics in the following concentrations: 100 μg/mL ampicillin, 30 μg/mL kanamycin, 34 μg/mL chloramphenicol or 10 μg/mL tetracycline.

3.1.7.3 5-bromo-4-chloro-3-indoyl-β-D-galactopyranoside (X-gal)

X-gal powder was obtained from Amresco, USA. It was used for blue/white colony screening during transformation step. The stock solution at concentration of 50 mg/mL was prepared by dissolving the X-gal powder with N,N'-dimethyl-formamide and filter sterilized with minisart syringe filter (Sartorius, Germany) at pore size of 0.22 μm and stored at -20°C. When indicated, X-gal was added into medium at a final concentration of 80 μg/mL.

3.1.7.4 Isopropyl-β-D-1-thiogalactopyranoside (IPTG)

IPTG (Amresco, USA) stock solution at concentration of 0.1 M was prepared and filter sterilized with minisart syringe filter (Sartorius, Germany) at pore size of 0.22 μm and stored at -20°C. Where indicated, IPTG was added to cultures at a final concentration of 0.5 mM or 1.0 mM.

3.1.7.5 L-arabinose

L-arabinose (Amresco, USA) stock solution at concentration of 1.0 M was prepared and filter sterilized. Where indicated, L-arabinose was added to cultures at a final concentration of 1.0 mM.

3.1.7.6 o-Nitrophenyl-β-D-Galactopyranoside (o-NPG)

o-NPG stock was obtained from Amresco, USA. o-NPG stock solution at concentration of 4.0 mg/mL was prepared, filter sterilized and stored at 4°C. It was added to initiate the β-galactosidase assay at final concentration of 0.4 µg/mL.

3.1.8 Oligonucleotide Primers

All oligonucleotide primers were synthesized by Integrated DNA Technologies Pte. Ltd., Singapore (Table 3.2 and Table 3.3).

Table 3.2: Oligonucleotide used in this study

Oligonucleotide	Sequence (5' to 3')	Length (-mer)
L1-*easI*-F	CCA TGG CGA TGA ATT CTG TTA TTG AGT	27
L1-*easI*-R	GGA TCC TAA GTG GCG TAA ATG CTC C	25
L1-*easR*-F	GCA ACA TAT GGA ACA GGA GGC AAG CAA CTC	30
L1-*easR*-R	CAG AGA TCT TCA GTC GTC CAG TAA TCG TAG	30
L1-*easI*-KFR-F	AAA CTT GGA ACA GAA CTA CGA TTA CTG GAC GAC TGA GCC TCA GCC ACT GGT ATG GAC AGC AAG CGA ACC G	70
L1-*easI*-KFR-R	TAA AAG ACA GGG GAT AAT AGT TTC AGG TGT TAT TAT CAG GAA TAA GAG CAT CAG AAG AAC TCG TCA AGA AG	71
Screen_KFR_F	CAC TGA GTT TCA CGA GGA CT	20
Screen_KFR_R	TGA ACG CAC CGT TAA ATT CC	20
pSIM_F	TTA ACT TCC GGA GCC ACA CC	20
pSIM_R	AAA CTC GCG AAG GCA GAG AA	20

Table 3.3: Oligonucleotide used to validate the RNA-seq results via qPCR

Oligonucleotide	Sequence (5' to 3')	Length (-mer)
easI-qF	TCC GAC GAT GAT AAG CGA AA	20
easI-qR	CCT CCC CTT TTT CAG ACA CG	20
recG-qF	ACC TCC ACC ATC GAC GAA CT	20
recG-qR	TGA ACC AGA CCC ACG TTC AG	20
gapA-qF	CAG TCA ATC ATT CCG GTG GA	20
gapA-qR	GTG CGG GTC GTG GTT AAA AT	20
pyrG-qF	TAC TGA AGA CGG CGC TGA AA	20
pyrG-qR	GGA ATG GCA GGG ATT CGA TA	20
*bsmA*_D-qF	TTG CTG GTG TTT CTG CTG AGT	21
*bsmA*_D-qR	GTC CCG TTA TGA TGG TTT CGT	21
*lsrD*_D-qF	TTG GCC GTC ATC TGT TTT TG	20
*lsrD*_D-qR	AAC CTG ACC CGC CGT AGA TA	20
*lsrB*_D-qF	CCG CAG CAT CTA CAT CAA CC	20
*lsrB*_D-qR	GGA TTT GGT GGC GTC GTT AT	20
*ompD*_U_qF	CCA GGG TAA AAA CGA CCG TAA	21
*ompD*_U_qR	CAT GTT GCG GGT TTC AGA GTA	21
*sdaB*_U-qF	GAG GTT GAA TTC CCG GTT GA	20
*sdaB*_U-qR	TGT GAA GTG CCA GCT CGT TT	20
26kDa_U-qF	TAA AGC GGC GAT TGA TGA TG	20
26kDa_U-qR	TAG CCG CCT CAG TTT GTT GA	20

3.1.9 Polymerase Chain Reaction (PCR) Master Mix for Gene Amplification

PCR was carried out in a final reaction volume of 25 µL containing the final concentration listed in Table 3.4. The thermocycler was programmed and performed in a thermal cycler according to the manufacturer instructions.

Table 3.4: PCR mixture of Q5® High-fidelity DNA polymerase

PCR Component	Volume per sample (µL)	Final Concentration
Q5® High-Fidelity 2× Master Mix	12.50	1×
10 µM Forward Primer	1.25	0.5 µM
10 µM Reverse Primer	1.25	0.5 µM
Template DNA	1.00	< 1,000 ng
Nuclease-Free Water	9.00	-
Total Volume	25.00	-

3.1.10 AGE

DNA fragments (PCR products or digested DNA) were separated by AGE. To separate DNA fragments smaller than 250 bp, 2% (w/v) of agarose gel was used; otherwise 1% (w/v) of agarose gel was used. First, 10 µL of DNA samples were mixed with 2 µL of 6× bromophenol blue loading dye onto an agarose gel along with an appropriate DNA size marker (100 bp or 1 kb DNA ladder). The loaded gel was subjected to electrophoresis in 1× TBE buffer at 75 V until the loading dye front approached about 1.0 cm from the edge of the gel (~60 min). The gel was pre-stained with 0.5× GelStar™ Nucleic Acid Gel Stain (Lonza, USA). The stained agarose gel was visualized and digitally photographed with gel documentary image analyser (UVP, USA). The desired DNA band(s) was determined by comparing the size of DNA band to the DNA ladder.

3.1.11 Purification of DNA Fragments from Agarose Gels

The desired PCR-amplified DNA bands were excised from the agarose gel with a clean scalpel under UV transilluminator (UVP, USA) and transferred to a 1.5 mL microfuge tube. DNA fragments (PCR products) were purified from agarose gels using the QIAamp® Gel Extraction Kit (Qiagen, Germany) according to the manufacturer's protocol.

3.2 Bacterial Strains, Biosensors, Plasmids and Culturing Conditions

3.2.1 Bacterial Strains and Biosensors

All bacterial strains and biosensors used in this study are listed in Table 3.5.

Table 3.5: Bacterial strains and biosensors used in this study

Strain / Biosensor	Genotype / Description	Source / Reference
Enterobacter asburiae L1	Lettuce isolate. QS strain with the formation of purple violacein pigment in the presence of short chain exogenous AHL molecules.	This study
Enterobacter asburiae L1-Δ*easI*::Kan	LuxI mutant derived from *E. asburiae* L1. The *easI* gene (~639 bp) of *E. asburiae* L1 was replaced with kanamycin gene (~950 bp).	This study
Chromobacterium violaceum CV026	A biosensor with mini-Tn5 mutant derived from *C. violaceum* ATCC 31532. In the presence of short chain exogenous AHL molecules, it triggers the purple violacein pigment.	(McClean et al., 1997)
Pectobacterium carotovorum GS101 (previously known as *Erwinia carotovora*)	Acts as positive control for biosensors. It produces short chain AHLs to activate biosensor *C. violaceum* CV026.	(McGowan et al., 1995)
Pectobacterium carotovorum PNP22	Acts as negative control for biosensors. It does not produce AHL molecules to activate biosensor *C. violaceum* CV026.	(McGowan et al., 1995)
Escherichia coli [pSB401]	Short chain AHL biosensor, LuxR receptor cognate AHL=3-oxo-C6-HSL, Tet^R.	(Winson et al., 1998)

Table 3.5, continued

Strain / Biosensor	Genotype / Description	Source / Reference
Escherichia coli DH5α	Host without presence of plasmid that yield high quality and concentration of inserted plasmid. d*lacZ*ΔM15 Δ(*lacZYA-argF*)U169 *rec*A1 *end*A1 hsdR17(rK^-mK^+) *supE*44 *thi-1 gyrA96 relA1*.	Invitrogen, USA
Escherichia coli BL21 (DE3)pLysS	DE3 lysogen expresses T7 polymerase upon IPTG induction. The pLysS plasmid produces T7 lysozyme to reduce basal level expression of the gene of interest. F^- *ompT gal dcm lon* $hsdS_B(r_B^- m_B^-)$ λ(DE3 [*lacI lacUV5-T7p07 ind1 sam7 nin5*]) $[malB^+]_{K-12}(\lambda^S)$ pLysS[*T7p20* ori_{p15A}]; Cm^R.	Novagen, Germany
Escherichia coli TOP10	Host without presence of plasmid that yield high quality and concentration of inserted plasmid. F- *mcrA* Δ(*mrr-hsd*RMS-*mcr*BC) ϕ80*lacZ*ΔM15 Δ*lac*X74 *rec*A1 *ara*D139 Δ(*ara*A-leu)7697 *gal*U *gal*K *rps*L (Str^R) *end*A1 *nup*G.	Invitrogen, USA
Escherichia coli TKC	Drug cassette for Recombineering system. Template for tetracycline, kanamycin and chloramphenicol.	Court lab (court@ncifcrf.gov)

Amp^R, Cm^R, Km^R, and Tet^R indicate resistance to ampicillin, chloramphenicol, kanamycin, and tetracycline respectively

3.2.2 Plasmids

All plasmids used in this study are listed in Table 3.6.

Table 3.6: Plasmids used in this study

Plasmid	Genotype / Description	Source / Reference
pGEM®-T	Toxin-antitoxin (TA) cloning vector, Amp^R. The vector map is displayed in Appendix A.	Promega, USA
pGEM®-T -*easI*	pGEM®-T containing 639 bp of *easI* with NcoI-BamHI sites; Amp^R.	This study
pET-28a(+)	Circle plasmid carrying N-terminal His-tag / thrombin / enterokinase configuration plus an optional C-terminal His tag sequence; Km^R. The vector map is displayed in Appendix B.	Novagen, Germany
pET-28a(+)-*easI*	pET-28a(+) containing 639 bp of *easI* cloned into NcoI-BamHI sites; Km^R.	This study
pSIM7	Source of λ Red recombination genes. pBBR1 Gam Exo Bet; Cm^R. The vector map of pSIM7 is shown in Appendix C.	Court lab (court@ncifcrf.gov)
pMULTIAHLPROM	pMP220-derived Broad-host-range plasmid containing 8-*luxI* type promoters *(luxI, cviI, ahlI, rhlI, cepI, phzI, traI and ppuI)* fused to a promoterless *lacZ* gene, Tet^R. The vector map of pMULTIAHLPROM is shown in Appendix D.	(Steindler, Devescovi, Subramoni, & Venturi, 2008)

Table 3.6, continued

Plasmid	Genotype / Description	Source / Reference
pLNBAD	Multiple cloning site; contains PBAD promoter; Cm^R. The vector map of pLNBAD is shown in Appendix E.	(Lemonnier et al., 2003)
pLNBAD-*easR*	pLNBAD containing 693 bp of *easR* with NdeI-BglII sites; Cm^R.	This study
pMBAD-*easR*	pMULTIAHLPROM containing pLNBAD cloned with 693 bp of *easR*; Tet^R and Cm^R.	This study

Amp^R, Cm^R, Km^R, and Tet^R indicate resistance to ampicillin, chloramphenicol, kanamycin, and tetracycline respectively

3.2.3 Culturing Conditions

The growth of *E. asburiae* and *E. coli* were carried out at 37°C in LB media for 18 to 20 h while *C. violaceum* and *P. carotovorum* were cultured in LB media at 28°C. Incubation in broth was done with shaking at 220 rpm unless indicated.

3.3 Methods

3.3.1 Sample Collection and Processing

Six different type of salad vegetables sample (Lettuces, bitter gourds, cabbages, long beans, tomatoes, and chili) were purchased from a local market at Sri Petaling, Malaysia (GPS coordinate: 03°03.81198', 101°41.66502') in a pre-sterilized container. The samples were process within half an hour of sample collection. After the vegetables surface were washed using sterile distilled water, approximately 20 g of each sample was homogenized with Stomacher® 400 circulator (Seward, UK) with 230 rpm agitation for 10 min. Briefly, 10 g of the homogenized sample were placed in 100 mL of Brain Heart Infusion broth (BHIB) (Merck, Germany) to incubate overnight at 37°C agitated at 200 rpm.

3.3.2 Isolation of Bacterial Strains

A 10 µL tenfold serial dilutions (10^{-1}, 10^{-2}, 10^{-3}, 10^{-4} and 10^{-5}) of the overnight culture were plated on MacConkey agar (Merck, Germany). The pure culture is routinely maintained on LB agar (Merck, USA) at 37°C or incubated overnight at 37°C agitated at 220 rpm in LB broth. Isolation procedure was proceeded by selection of single bacterial colonies displaying distinctive morphologies. Each of the identified single colonies is streaked onto LB agar plates until pure cultures were obtained.

3.3.3 Identification of Bacterial Strains

3.3.3.1 Gram Staining

Gram staining was performed by viewing the stained samples under Olympus^{TM} IX71 inverted microscope (Olympus, Japan), at 100 × magnification and the micrographs were captured using Olympus Cell^D imaging system. Briefly, a drop of the suspended bacteria culture was smeared and heat-fixed on a glass slide. The fixed culture sample was stained with crystal violet. After 1 min, excess crystal violet was washed away under the running tap water for 30 s. Following this, iodine solution was added onto the smear and let stand for 1 min before proceeded to rinse off with running tap water. Few drops of decolourizer were added and rinsed off with running tap water after 5 s. Lastly, the sample was counterstained with safranin.

3.3.3.2 MALDI-TOF-MS

Bacterial isolates of interest were identified using MALDI-TOF-MS (Bruker, Germany) (Seng, Drancourt, Gouriet, La Scola, Fournier, Rolain, & Raoult, 2009) extraction method with UV laser wavelength of 337 nm and acceleration voltage of 20 kV. Each spot on the target plate was then measured by the MBT-autoX.axe autoExecute method. The bacterial spectra were analysed in the Bruker MALDI Biotyper Real Time Classification (RTC) Version 3.1 (Build 65) software. The dendrogram was generated with standard MALDI Biotyper MSP creation method.

3.3.4 Whole Genome Sequencing (WGS) of Bacterial Isolates

3.3.4.1 Genomic DNA Extraction

Bacterial isolates were inoculated into LB broth and incubated overnight in a shaking incubator at 220 rpm. The bacteria cells were harvested by centrifugation at 10, 000 × *g* for 10 min. Bacterial genomic DNA was extracted using Masterpure™ DNA purification kit (Illumina, USA) per the manufacturer's instructions. The quality of the extracted DNA was performed with Nanodrop spectrophotometer (Thermo Scientific, USA) and agarose gel electrophoresis while DNA quantification was carried out with Qubit® 2.0 Fluorometer (dsDNA High Sensitivity Assay Kit) (Invitrogen, USA).

3.3.4.2 WGS of Bacterial Isolates

The genomic DNA of bacterial isolates was extracted as stated in Section 3.3.4.1. The extracted DNA was subjected to library preparation with commercial kit. The quality was examined using 2100 Bioanalyzer (Agilent Technologies, USA). The WGS was performed with HiSeq 2000 next generation DNA platform (Illumina, USA). Raw reads from the sequencing were processed using commercial software and freeware. The sequences were trimmed with the limit of 0.001 (Q30). The trimmed sequences were assembled to contigs with lengths of at least 500 bp.

3.3.5 AHLs Detection of Bacterial Isolates

3.3.5.1 *C. violaceum* CV026 Cross Streak

Preliminary screening for AHLs production among the isolates involved the cross streaking with biosensor *C. violaceum* CV026 to detect the presence of exogenous short chain AHLs ranging from four to eight carbons. *Pectobacterium carotovorum* GS101 and *P. carotovorum* PNP22 was used as positive control and negative controls, respectively (McClean et al., 1997). Observation of purple pigments production in CV026 after 18 to 24 h incubation indicate the secretion of short chain AHLs from the isolate.

3.3.5.2 AHLs Extraction

Bacterial isolate that showed positive result for AHLs production was incubated overnight for 18 h in 100 mL buffered LB medium with 50 mM 3-[*N*-morpholino] propanesulfonic acid (MOPS) to pH5.5 to prevent spontaneous degradation of AHLs (Yates et al., 2002) at 37°C with shaking at 220 rpm. The spent culture supernatant was then extracted thrice with an equal volume of acidified ethyl acetate (0.1% v/v glacial acetic acid in ethyl acetate). The extract was dried and stored at -20°C prior to LC-MS/MS analysis.

3.3.5.3 Measurement of Bioluminescence

Cell density bioluminescence measurements were done using an Infinite M200 luminometer-spectrophotometer (Tecan, Switzerland). Aliquots of 200 µL of diluted (1:100) *E. coli* [pSB401] overnight culture in LB supplemented with tetracycline (20 µg/mL) was added with 1 µL of extracted AHL to every well of a 96-well optical bottom microtiter plate (Wong et al., 2012; Yin et al., 2012). Acetonitrile and synthetic 3-oxo-C6-HSL (250 pg/µL) were used as the negative and positive standards, respectively. Results were indicated as Relative Light Units (RLU)/OD495 nm against incubation time.

3.3.5.4 AHLs Identification by Triple Quadrupole LC-MS/MS

Extracted AHL was reconstituted in acetonitrile followed by LC-MS/MS analysis using an Agilent 1290 Infinity LC system (Agilent Technologies, USA) equipped with an Agilent ZORBAX Rapid Resolution High Definition SB-C18 Threaded Column (2.1 mm × 50 mm, 1.8 μm particle size). The flow rate and the temperature were set at 0.3 mL/min and 37°C, respectively. Injection volume was 2 μL. Both mobile phases A and B were 0.1% v/v formic acid in water and 0.1% v/v formic acid in acetonitrile, respectively. The gradient profile was set at A:B 80:20 at 0 min, 50:50 at 7 min, 20:80 at 12 min, and 80:20 at 14 min. Subsequent MS detection of separated compounds was performed on the Agilent 6490 Triple Quadrupole LC-MS/MS system. Precursor ion-scanning analysis were performed in positive ion mode with Q3 set to monitor for *m/z* 102 and Q1 set to scan a mass range of *m/z* 80 to *m/z* 400. Molecular mass of *m/z* 102 refers to the presence of lactone ring, thus indicating presence of AHLs. The MS parameters were as follows: probe capillary voltage set at 3 kV, sheath gas at 11 mL/h, nebulizer pressure of 20 psi and desolvation temperature at 200°C. Nitrogen gas was used as the collision gas in the collisionally-induced dissociation mode for the MS/MS analysis and the collision energy was set at 10 eV. The Agilent MassHunter software was used for the MS data analysis to confirm the presence of AHLs. Analysis was based on the retention index and the comparison of the electron ionization mass spectra with AHL standards.

3.3.6 Bacterial Characterization of QS Bacteria

3.3.6.1 API 20E Test

Biochemical assay of *E. asburiae* L1 was performed using API 20E according to the manufacturer's instruction. Type strain *E. asburiae* ATCC 35953 was included as comparison.

3.3.6.2 IMViC Test

IMViC test was performed by inoculating three different sets of test tubes with tryptone broth (indole test), methyl red-voges proskauer broth (MR-VP broth), and citrate agar. The tests were performed and the results were interpreted based on manufacturer's protocol.

For indole test, formation of a pink to red colour ("cherry-red ring") in the reagent layer on top of the medium within seconds after addition of appropriate reagent indicate positive reaction. No change in colour indicates negative reaction.

For MR-VP tests, positive MR test is indicated by the development of red colour after the addition of methyl red reagent while a negative reaction is indicated by no change in colour. On the other hand, a positive VP test is indicated by the development of red-brown colour after the addition of Barritt's A and Barritt's B reagents while negative test is indicated by lack of colour change.

A citrate positive reaction is indicated by visible growth on the slant surface and the medium will show an intense Prussian blue. In contrast, when organisms show negative citrate reaction, there will be no visible growth on the citrate agar slant surface. In addition, no colour change will occur, so the medium will remain deep forest green colour.

3.3.6.3 Decarboxylation Test

The decarboxylation broth was prepared and aliquoted into individual sterile test tubes. Then, the decarboxylase broth was inoculated with the test organism and overlaid with a layer of mineral oil. After 24 h incubation at 37^{o}C, the preliminary results were determined. The microbe must first use the glucose present to cause the pH to drop. This was indicated by a change from purple to yellow colour. Once the medium has been acidified, the decarboxylase enzyme is activated. The culture was incubated for an additional 24 h at 37^{o}C to allow the microbe to use the enzyme. The final results were recorded by observing colour changes in the tube at 48 h. Purple colour formation after 48 h indicated positive result. Failure to turn yellow at 24 h or to revert back to purple at 48 h indicates a negative result.

3.3.6.4 Nitrate Reduction Test

To perform this test, nitrate broth was prepared and aliquoted into individual sterile test tubes. The test was performed by inoculating the broth with a heavy growth of test organism and incubated at 37^{o}C. After 24 h of incubation, one dropper full of sulphanilic acid and one dropper full of a α-naphthylamine was added to each broth. Positive result is indicated by formation of red colour after addition of nitrate I and nitrate II reagents. If red colour was not observed at this point, the test was proceeded to the next step by adding a small amount of zinc powder to the inoculate. If instead, the tube turns red after the addition of zinc powder, this indicated a negative result. In contrast, if the tube is colourless after the addition of zinc powder, this indicated a positive reaction. If there is no colour change in the tube after the addition of nitrate I and nitrate II, the result is uncertain.

3.3.6.5 Carbohydrate Fermentation Test

Phenol red broth (Proteose peptone 10 g, beef extract 1 g, sodium chloride 5 g carbohydrate 5 g, and phenol red 0.018 g) was prepared and aliquoted into sterile individual test tubes. The phenol red broth was inoculated with the test organism and incubated at 37^{o}C for 24 h. When fermentation occurs, acidic by-products will form. By this, the solution will turn from red to yellow colour which indicated positive reaction.

3.3.6.6 Tabletop Scanning Electron Microscopy (SEM)

SEM observation of QS bacterial was conducted on a TM3000 Analytical Tabletop Microscope (Hitachi, Brisbane, CA, USA). The bacterial pellets were fixed in 2.5% glutaraldehyde for at least 2 h before proceeding with two 0.1 M phosphate buffer washes. The fixed cells were then subjected to post fixation with 1% (v/v) osmium tetroxide for at least an hour. After two post-fixation washes, a graded series of ethanol dehydration steps (50%, 75%, 95%, 100%, 100% v/v ethanol, 10 min each) was performed before immersed the cells in Hexamethyldisilazane (HMDS) (Ted Pella, Redding, CA, USA) for another 10 min. The SEM preparation was completed by decanting the HMDS from the tube and letting the cells air-dry in a desiccator at room temperature. Prior to examination, the dried cells were mounted onto a SEM specimen aluminium stub with a double-sided sticky tape and subjected to gold coating in a SC7620 mini sputter coater (Quorum Technologies, UK).

3.3.6.7 Phenotypic Characterization (GENIII MicroPlate)

E. asburiae L1 was plated on Trypticase Soy Agar (TSA) and incubated overnight at 37°C. Cells were swabbed from the overnight culture and suspended in Biolog inoculating fluid, IF-A to the turbidity of 95% according to the manufacturer's instructions. Cell suspensions were inoculated into each well of the GENIII MicroPlates and incubated for 24 h at 37°C. Results were interpreted with Biolog microplate reader coupled with Biolog's Microbial Identification System software version 3.1.

3.3.7 Sequencing of QS Bacteria Using PacBio SMRT Sequencer

The PacBio RS II sequencing technology was applied in this study to obtain the complete genome of the QS bacteria. Genomic DNA was extracted as stated in Section 3.3.4.1. The quality of the extracted DNA was performed with Nanodrop spectrophotometer (Thermo Scientific, USA) and agarose gel electrophoresis while DNA quantification was carried out with Qubit® 2.0 Fluorometer (dsDNA Broad Range Assay Kit) (Invitrogen, USA). The 10 kb DNA sequencing template of *E. asburiae* L1 was obtained from sheared genomic DNA using the Pacific Bioscience 10 kb SMRTbell library template preparation kit per the manufacturer's instructions (Pacific Biosciences, USA). The quality sizing analysis of DNA library was validated by Bioanalyzer 2100 high sensitivity DNA kit (Agilent Technologies, USA) prior to sequencing. SMRTbell libraries were bound to polymerases using the DNA/Polymerase binding kit P4. Binding calculator version 2.0.1.2 (Pacific Biosciences, USA) was used to calculate the concentration of polymerase-template complex for binding and annealing reaction. These complexes were bound to magbeads using the MagBead Kit (Pacific Biosciences, USA) and the prepared library was sequenced on four SMRT cells (SMRT cells 8Pac version 3; Pacific Biosciences). PacBio RS II sequencing technology (Pacific Biosciences) was used as the sequencing platform.

3.3.8 Whole Genome Optical Mapping of QS Bacteria

Whole genome map of *E. asburiae* L1 was generated from the single DNA molecule with the automated Argus system (OpGen Inc., USA). DNA extraction was performed based on the manufacturer's instructions. Purified DNA was then diluted to the appropriate concentration by performing a quality check using QCard (OpGen Inc., USA). The DNA molecules were filled through all the channels of the channel-forming device (CFD) on MapCards II (OpGen Inc., USA) through capillary action. The four reagent reservoirs were pipetted into their individual load ports according to the labelled with the corresponding reagent on the left side of the MapCard II. Digestion was performed with AflII for 30 min while all the four reagents were dispensed and aspirated from the reaction chamber at appropriate times, volumes, and flow rates in the MapCard Processor. Upon completion, the MapCard II was placed in whole genome mapper to perform whole genome optical mapping.

3.3.9 Bioinformatics Analysis

3.3.9.1 Gene Prediction and Annotation

Raw data obtained from HiSeq 2000 was trimmed to Qscore of 30 and assembled with Genomics Workbench version 6.5 (CLC bio, Denmark). Sequences less than 50 bp were discarded. Minimum contig length was set at 500 bp. On the other hand, raw data obtained from PacBio for QS bacteria, was assembled with Hierarchical Genome Assembly Process (HGAP).

RNAmmer was applied to identify the strains. Genes were predicted using Prodigal 2.60 while gene annotation was performed using SEED-based automated annotation system provided by the Rapid Annotations using Subsystems Technology (RAST) server version 4.0 (Aziz et al., 2008). Circularization of the QS bacterial genome was done using Gepard version 1.3 (Institute of Computational Biology) (Krumsiek, Arnold, & Rattei, 2007).

3.3.9.2 Comparative Genome Analysis of QS Bacteria

Sequence-based comparative analysis of *E. asburiae* L1 with other closely related *E. asburiae* strains was performed with RAST. The genome of *E. asburiae* L1 was used as the reference and was compared with the genome of strains ATCC 35953 (CP011863.1), PDN3 (JUGH00000000.1), GN02073 (LDCE01000001.1), GN02127 (LDCH00000000.1), and 33838 (LAAP00000000.1), which were obtained from NCBI database. In addition, comparative analysis of *E. asburiae* L1 genome with the closest related strains, ATCC 35953 and PDN3 were performed using Mauve software 2.3.1 (Darling, Mau, Blattner, & Perna, 2004), an online Java-based tool for ordering contigs and inspecting assembly statistic.

3.3.9.3 Nucleotide Sequence Analysis of QS Bacteria

The amino acid sequence of EasI was compared with the GenBank *E. asburiae* database (http://www.ncbi.nlm.nih.gov). The amino acid sequences of fourteen different strains of *E. asburiae* which possess LuxI homologues were selected from the protein database. Redundant sequences or bacterial strains with ambiguities were omitted. Multiple sequence alignments of the amino acid sequences were performed using Clustal OMEGA tool with its default parameter settings. A phylogenetic tree of the *easI* gene was then constructed using Molecular Evolutionary Genetic Analysis (MEGA) version 6.0 (Tamura, Stecher, Peterson, Filipski, & Kumar, 2013) The Neighbour-joining algorithm was used with bootstrap value of 1000, expressed as the percentage of 1000 replicates. Meanwhile, searches for open reading frame (ORF) and prediction of nucleotide translational products were performed using the ORF Finder tool while the fundamental properties of the proteins were predicted using by ExPASy.

3.3.10 Cloning

3.3.10.1 Preparation of Chemically-Induced Competent Cells

Pure colony of the bacterial culture (i.e. *E. asburiae* L1, *E. coli* DH5α, *E. coli* TOP10 and *E. coli* BL21 (DE3)pLysS) was inoculated into 10 mL sterile LB broth supplemented with appropriate antibiotics when necessary and incubated overnight at 37°C in a shaking incubator at 250 rpm. A 1 mL aliquot of the overnight culture was inoculated into 50 mL sterile LB broth in a conical flask. The culture was allowed to grow at 37°C with shaking at 250 rpm until OD_{600} ~0.3-0.4. The cells were then placed on ice before harvested in a 4°C refrigerated centrifuge at 8, 000 rpm for 10 min. The supernatant was discarded and the cell pellet was gently resuspended in 25 mL of pre-chilled 0.1 M $CaCl_2$. The resuspended cells were kept on ice for 30 min before subjected to harvest by centrifugation at 8, 000 rpm and at 4°C for 10 min. The resulting cell pellet was then resuspended in 4 mL of pre-chilled $CaCl_2$ solution (68 mM $CaCl_2$ containing 15% glycerol) using chilled tips. The resuspended competent cells were then aliquoted into pre-chilled microfuge tubes (200 µL per tube) and were stored at -80°C until further use.

3.3.10.2 Preparation of Electrocompetent Cells

A 500 µL of a fresh overnight culture was inoculated into 50 mL of sterile LB broth in a conical flask. The cells were incubated at 37°C with shaking at 250 rpm to an OD_{600} ~0.5-0.7. The cells were then incubated on ice for 20 min. For all subsequent steps, the cells were kept as close to 0°C as possible and all tubes and tips were pre-chilled before use. The chilled cells were transferred to a sterile, cold 50 mL falcon tube and centrifuged at 4, 000 × *g* for 15 min at 4°C. The supernatant was carefully discarded. Following that, the pellet was gently resuspended in 50 mL of pre-chilled 10% (v/v) glycerol before subjected to centrifuge at 4, 000 × *g* for 15 min at 4°C again. The supernatant was discarded and the pellet was resuspended in 25 mL of ice-cold 10% (v/v) glycerol. The

centrifugation step was repeated and the pellet was resuspended in 2 mL of pre-chilled 10% (v/v) glycerol. Finally, the cell pellet was resuspended in a final volume of 200 µL of ice-cold 10% (v/v) glycerol after centrifugation step. The resuspended electrocompetent cells were then aliquoted into pre-chilled microfuge tubes (20 µL per tube) and were stored at -80°C until further use.

3.3.10.3 Construction of Recombinant EasI Expression Plasmids

Plasmid DNA for use in sub-cloning was isolated using QIAprep Spin Miniprep Kit (Qiagen, Germany) as recommended by the manufacturer. The genomic DNA of *E. asburiae* L1 was used to amplify the *easI* gene using the following primers: Forward primer, L1-*easI*-F (5' CCATGGCGATGAATTCTGTTATTGAGT 3') and reverse primer, L1-*easI*-R (5' GGATCCTAAGTGGCGTAAATGCTCC 3'). For the forward primer, a NcoI restriction site (underlined) and two non-specific bases CG were added to accommodate the frameshift of the recombinant gene sequence; for the reverse primer, a BamHI restriction site (underlined) was added. PCR was performed using Q5® High-Fidelity DNA polymerase (NEB, USA) as stated in Section 3.1.9. The thermocycler was programmed for an initial denaturation step at 98ºC for 30 s, followed by 27 cycles at 98ºC for 10 s, annealing at 55.5ºC for 30 s, extension at 72ºC for 30 s, a final extension at 72ºC for 2 min and a hold temperature at 4ºC at the end. Sterile deionized water was used as the negative control. The resultant recombinant plasmid (designated pGEM®-T-*easI*) was chemically transformed into *E. coli* DH5α (Sambrook & Russel, 2001). Blue-white colony screening and colony PCR were performed to allow identification and confirmation of the recombinants. The *easI* gene was excised from the plasmid by digestion with FastDigest NcoI and BamHI (Thermo Scientific, USA), followed by gel purification for subsequent ligation with overexpression vector, pET-28a(+) (Novagen, Germany), digested with the same enzymes. This resulting recombinant plasmid was

designated pET-28a(+)-*easI*. Sequence verification of the recombinant plasmid was performed by automated Sanger DNA sequencing.

3.3.10.4 Construction of Recombinant EasR Plasmids

The genomic DNA of *E. asburiae* L1 was used to amplify the *easR* gene using the following primers: Forward primer, L1-*easR*-F (5' GCAACATATGGAACAGGAGGC AAGCAACTC 3') and reverse primer, L1-*easR*-R (5' CAGAGATCTTCAGTCGTC CAGTAATCGTAG 3'). For the forward primer, a NdeI restriction site (underlined) was added while for the reverse primer, a BglII restriction site (underlined) was added. To accommodate the frameshift of the recombinant gene sequence, four non-specific bases GCAA were added to the forward primer while three non-specific bases CAG were added to the reverse primer. PCR was performed using Q5® High-Fidelity DNA polymerase (NEB, USA) following the condition stated in section 3.3.10.3. The annealing temperature was set at 57°C. The resultant recombinant plasmid (designated pGEM®-T-*easR*) was chemically transformed into *E. coli* DH5α (Sambrook & Russel, 2001). Blue-white colony screening and colony PCR were performed to allow identification and confirmation of the recombinants. The *easR* gene was excised from the plasmid by digestion with FastDigest NdeI and BglII (Thermo Scientific, USA), followed by gel purification for subsequent ligation with pLNBAD, digested with the same enzymes. This resulting recombinant plasmid was designated pLNBAD-*easR*. Sequence verification of the recombinant plasmid was performed by automated Sanger DNA sequencing. The resulting constructed recombinant plasmids were chemically transformed into *E. coli* TOP10 that contain pMULTIAHLPROM vector (designated pMBAD-*easR*) and subjected to β-galactosidase assay to study the promoter activities.

3.3.10.5 Heterologous Expression of EasI Protein in *E. coli*

The *E. coli* BL21 (DE3)pLysS (Sambrook & Russel, 2001) which was transformed with pET-28a(+)-*easI*, was cultured in LB medium supplemented with 30 µg/mL kanamycin and 34 µg/mL chloramphenicol at 37ºC. Following this, 1 mL of an overnight culture of the desired clone was inoculated into 50 mL of LB medium supplemented with the same antibiotics and cells were grown in the same condition until it reached OD_{600} of ~0.4-0.5 before IPTG was added at a final concentration of 1.0 mM to induce the expression of the *easI* gene in *E. coli*. After addition of IPTG, the cells were incubated at 25ºC, agitated at 250 rpm for another 8 h before harvested by centrifugation at 10, 000 rpm. *E. coli* harbouring pET-28a(+) alone was used as the negative control. The cells harvested were lysed by BugBuster® Protein Extraction Reagent (Novagen, Germany) with the addition of protease inhibitor cocktail (Thermo Scientific, Pittsburgh, PA, USA). The concentration of the solubilized protein was determined using Quick Start™ Bradford Protein Assay (Bio-Rad, USA).

3.3.10.6 Purification of EasI Protein and Sodium Dodecyl Sulphate Polyacrylamide Gel Electrophoresis (SDS-PAGE) Analysis

The recombinant proteins were purified from cell lysate using Ni-NTA Fast Start Kit (Qiagen, Germany) per manufacturer's instructions. The samples were incubated for 3 min at 95ºC before subjected to 12% Tris-Glycine polyacrylamide gel electrophoresis (Thermo Scientific, USA) using 1× Tris-Glycine-SDS buffer (Thermo Scientific, USA) at 125 V for 15 min followed by 150 V for 60 min. To visualize the protein bands, the gels were stained with Coomassie brilliant blue R250 (CBB; Bio-Rad, USA) for 5 min, followed by destaining step with destaining solution (10% glacial acetic acid; 40% methanol; 50% distilled water) for three times, each 10 min long.

3.3.10.7 AHL Detection, Extraction and Identification

C. violaceum CV026 was used as the AHL biosensor to detect the presence of exogenous short chain AHLs ranging from four to eight carbons. The induced *E. coli* BL21 (DE3)pLysS harbouring pET-28a(+)-*easI* was screened using cross streaking with CV026. *P. carotovorum* GS101 was used as the positive control while *P. carotovorum* PNP22 and *E. coli* harbouring pET-28a(+) alone as the negative controls. AHL extraction of bacterial culture supernatants was performed according to a previously reported method with minor modifications (Lau, Sulaiman, Chen, Yin, & Chan, 2013). The bacterial culture was grown in buffered LB medium, pH 6.5, with MOPS (50 mM, pH 6.5) at 37°C. MOPS was used to prevent degradation of AHLs (Yates et al., 2002). After induction with IPTG for 8 h as described earlier, the spent culture supernatant was then extracted thrice with an equal volume of acidified (0.1% v/v acetate acid) ethyl acetate (Merck, Germany). Extracted AHL was reconstituted in acetonitrile followed by LC-MS/MS analysis using an Agilent 1290 Infinity LC system (Agilent Technologies, Santa Clara, CA, USA) equipped with an Agilent ZORBAX Rapid Resolution High Definition SB-C18 Threaded Column (2.1 mm × 50 mm, 1.8 μm particle size) according to the previously reported method (Lau, Sulaiman, Chen, Yin, & Chan, 2013). Acetonitrile and AHL extract from the culture supernatant of *E. coli* harbouring pET-28a(+) alone were used as the blank and negative control, respectively.

3.3.10.8 Determination of *easR*-regulated Promoter Activities Using β-galactosidase Assay

The recombinant *E. coli* TOP10 clones containing pMULTIAHLPROM fused with pLNBAD (designated pMBAD) or pMBAD-*easR* recombinant plasmids were cultured in 10 mL LB broth supplemented with 10 µg/mL tetracycline and 20 µg/mL chloramphenicol at 30°C with agitation at 250 rpm. An aliquot of the overnight bacterial cultures was inoculated into 10 mL of sterile fresh LB broth supplemented with appropriate antibiotics with starting OD_{600} ~0.02. When indicated, AHLs was added to clones pMBAD or pMBAD-*easR* at a final concentration of 100 µM. Two sets of cultures were prepared for each sample, whereby one set was induced by adding 1.0 mM of L-arabinose and another set was grown without addition of any inducer. All cultures were allowed to grow under the same conditions until mid-log phase (OD_{600} ~0.4-0.6) where they were then placed on ice. A 2 mL aliquot of the bacterial culture was harvested by centrifugation at 3, 500 × *g* for 10 min and the resulting cell pellet was resuspended in 2 mL chilled Z buffer. The OD_{600} of the resuspended cells was measured spectrophotometrically with Z buffer as a blank. To permeabilize the cells, 1 mL cells in Z buffer was transferred into a 2 mL microfuge tube into which 100 µL chloroform and 50 µL 0.1% (w/v) SDS were added. The mixture was then vortexed and equilibrated for 5 min in a 28°C heat block. The β-galactosidase assay is initiated by the addition of 0.2 mL o-NPG (4 mg/mL) as the substrate into the lysate. The tubes were vortexed before incubation in the 28°C heat block and the colour changes was observed. After sufficient yellow colour (as the colour of LB broth) had developed, the reaction was stopped by the addition of 0.5 mL 1.0 M Na_2CO_3 and mixed by vortexing. The addition of Na_2CO_3 will raise the pH of the solution to 11 and thus stop the enzymatic reaction. The time taken from the addition of o-NPG to the stopping of the reaction with Na_2CO_3 was precisely recorded. The mixture was centrifuged at maximum speed for 5 min to remove cellular

debris and chloroform. The OD at 420 nm and at 550 nm for each tube was recorded (blanked against the same mixture but without cells). The units of enzyme activity, expressed as Miller units, were calculated using the following equation (Miller, 1972):

$$\text{Miller Units} = 1000 \times [(OD_{420} - 1.75 \times OD_{550})] / (T \times V \times OD_{600})$$

where:

OD_{420} and OD_{550} were read from the reaction mixture

OD_{600} reflected cell density in the washed cell suspension

T = time of the reaction, in min

V = volume of culture used in the assay, in mL

3.3.11 Construction of *E. asburiae* L1-Δ*easI*::Kan Mutant

Linear DNA substrate for recombineering was constructed through PCR amplification by using the ~70 base hybrid primers. These primers contain 50 bases of homology at the 5' end and 20 bases at the 3' end that will prime synthesis of the TKC drug cassette. Primers with the following sequences were used: L1-*easI*_KFR-F (5' AAACTTGGAACAGAAC TACGATTACTGGACGACTGAGCCTCAGCCACTGGTATGGACAGCAAGCGAA CCG 3') and L1-*easI*_KFR-R: (5' TAAAAGACAGGGGATAATAGTTTCAGGTGTT ATTATCAGGAATAAGAGCATCAGAAGAACTCGTCAAGAAG 3'). Primers belong to the drug cassette (Km^R) was underlined. Meantime, the λ Red recombination genes from pSIM 7 plasmid was introduced into *E. asburiae* L1 genome and sequence verification of the recombinant plasmid was performed by automated Sanger DNA sequencing. The λ recombination genes was then induced at 42°C for recombination functions. Following this, the linear substrates constructed was transformed into the recombineering-ready *E. asburiae* L1 cells. Finally, the recombinant clones were selected and screened by amplified the two junctions to confirm the knockout mutations. Primers with the following sequences were used: Screen_KFR_F (5' CACTGAGTTTCACGAG GACT 3') and Screen_KFR_R (5' TGAACGCACCGTTAAATTCC 3'). The sequence was verified by automated Sanger DNA sequencing. Figure 3.1 illustrates the schematic diagram of the construction of *E. asburiae* L1-Δ*easI*::Kan mutant using recombineering.

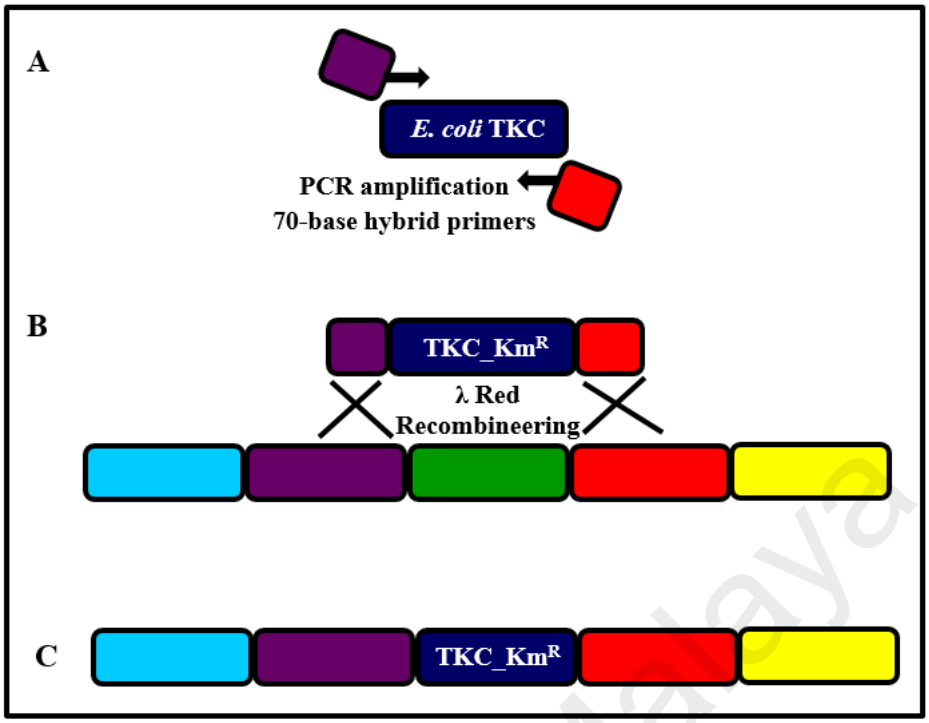

Figure 3.1: Schematic diagram of the construction of *E. asburiae* L1-Δ*easI*::Kan mutant using recombineering. (A) The drug-resistant cassette available from *E. coli* TKC is amplified by PCR using two, ~70 base hybrid primers. The 5' end of the primer has homology to the desired target (50 base) and the 3' end of the primer (~20 base) has sequence to prime the *E. coli* TKC kanamycin resistance gene (TKC_Km^R); (B) The linear TKC_Km^R cassette amplified by PCR is transformed into *E. asburiae* L1 recombination-competent cells and Red-mediated recombination occurs; (C) The final recombinant will be a gene swap between *E. asburiae* L1 *easI* (639 bp) and TKC_Km^R (950 bp), yielding *E. asburiae* L1-Δ*easI*::Kan mutant.

3.3.12 Transcriptomic Studies

3.3.12.1 RNA Extraction

E. asburiae L1 wildtype and mutant cells were grown in LB broth at 37°C. The total RNA was stabilized immediately using Qiagen RNAprotect bacterial reagent (Qiagen, USA) when the OD reached 2.0. Total bacterial RNA was purified using Macherey-Nagel NucleoSpin RNA isolation kit (Macherey-Nagel GmbH & Co. KG, Germany) according to the manufacturer's instructions. Precipitated RNA samples were resuspended in sterile RNase-free water. Total RNA from three biological replicates was prepared from independent cultures to evaluate the reproducibility of RNA-seq data. Purity of RNA samples was assessed using Nanodrop spectrophotometer (Thermo Scientific, USA) while RNA quantification was carried out with Qubit® RNA HS Assay Kit (Invitrogen, USA). The quality of the extracted RNA samples was performed with Agilent RNA 6000 Nano Kit (Agilent Technologies, USA) using 2100 Bioanalyzer.

3.3.12.2 cDNA Synthesis, cDNA Library Preparation and RNA-seq Sequencing

RNA samples with RNA Integrity Number (RIN) of value >7.0 were chosen to proceed to rRNA depeletion using Ribo-Zero™ rRNA Removal Kits (Bacteria) (Epicentre, USA) prior to cDNA synthesis. The quality of the rRNA-depleted RNA was assessed with Agilent RNA6000 Pico Chip (Agilent Technologies, USA) using 2100 Bioanalyzer. Library preparation was performed according to the manufacturer's protocol using the Illumina ScriptSeq™ v2 RNA-Seq Library Preparation Kit (Epicentre, USA). Quality of the RNA-seq transcriptome library was examined by using Agilent 2100 High Sensitivity DNA Kit. Quantification of the library was performed using Qubit® dsDNA HS Assay Kit (Life Technologies, USA) and qPCR (KAPA Biosystems) before subjecting to normalization. The normalised samples (4.0 nM) were denatured with 0.2 N NaOH and diluted 20.0 pM using pre-chilled Hybridisation Buffer (HT1) (Illumina, USA). The 20

pM transcriptome libraries were further diluted to 10 pM with pre-chilled HT1 buffer prior to whole transcriptome sequencing on MiSeq platform.

3.3.12.3 Validation of RNA-seq Results Using qPCR

To quantify and validate the level of *E. asburiae* L1 gene expression that were altered after the *easI* gene was knocked-out, few genes from the upregulated and downregulated gene list obtained from RNA-seq results were selected randomly. The primers for the selected genes were designed using Primer 3 version 0.4.0 (http://bioinfo.ut.ee/primer3-0.4.0/), with the following criteria: product size ranges: 150-300; minimum primer size: 18; maximum primer size: 22; minimum temperature: 60ºC maximum temperature: 63ºC; maximum temperature difference: 3ºC; minimum primer GC%: 40; and maximum primer GC%: 60.

The RNA of *E. asburiae* L1 wildtype and mutant cells were re-extracted to determine the reproducibility of the data. One microgram of total RNA from each sample was used to synthesize the first strand cDNA using the QuantiTect Reverse Transcription Kit (Qiagen, Germany) according to the manufacturer's protocol. The qPCR was carried out in a CFX96 Touch™ Real-Time PCR Detection System using Kapa SYBR Fast qPCR Master Mix (Kapa Biosystems, USA) according to the manufacturer's instructions, under the thermal cycle conditions of an initial denaturation at 95°C for 3 min, followed by 35 cycles of 95°C for 3 s, and annealing at 58°C for 30 s. Each sample was performed in biological triplicates with three technical replicates each.

The expression level of genes was calculated by the delta-delta-Cq method using the Bio-Rad CFX Manager version 3.1. Reference genes with expression stability value (M) of less than 0.7 were selected as reference genes for normalization. The selected reference genes were *recG*, *gapA* and *pyrG*. The downregulated genes that were selected are *bsmA*,

lsrD and *lsrB* while the upregulated *ompD*, *sdaB* genes and 26 kDa periplasmic immunogenic protein precursor were selected.

3.3.12.4 Biofilm Formation and Quantification

E. asburiae L1 wildtype and mutant cells were grown overnight in LB medium at 37°C with agitation. After growth, the culture was diluted with LB medium and adjusted to OD_{600} of 0.1. *E. asburiae* L1 wildtype and mutant cells were incubated statically for 72 h at 37°C. *Pseudomonas aeruginosa* PA01 was used as a positive control. After incubation, planktonic bacteria were discarded, and the biofilms were washed thrice with sterile distilled water and let to air-dry. Crystal violet of 1% (w/v) was then added to each well (1 mL/well), and the plates were incubated at room temperature. After 45 min of staining, the excess crystal violet was discarded, and stained biofilms were washed thrice with 1 mL sterile distilled water. In order to solubilize the crystal violet, 1 mL of 95% (v/v) ethanol was added to the stained biofilms and 200 µL of resulting solution was transferred to a new microtiter plate. The absorbance of the solution was read at 590nm. All experiments were performed in triplicates. The statistical significance of each test ($n = 3$) was evaluated by conducting unpaired *t* tests and using the GraphPad Prism software; a *P* value of ≤ 0.01 was considered significant.

3.3.13 Phenotypic Analysis--Biolog Omnilog® PM Assay

The PM assay were performed using Biolog OmniLog® automated incubator (Hayward, California) based on the PM procedures for *E. coli* and other GN bacteria. In this assay, total of twenty 96-well PM panels that contained different nutrients, chemicals, or inhibitory substances were performed. As described by Bochner, PM plates 1 and 2 utilize carbon source; PM 3, nitrogen source; PM 4, phosphorus and sulphur sources; PM 5, biosynthetic pathway/nutrient stimulation; PM 6–8, peptides and nitrogen sources; PM plates 9 to 10 test for osmotic/ion response and pH effects while PM plates 11 to 20 utilize bacterial chemical sensitivity assays, including antimicrobial agents. To perform this assay, *E. asburiae* L1 wildtype and mutant strains were first plated on TSA and incubated overnight at 37°C. Cells were swabbed from the overnight culture and suspended in appropriate Biolog medium containing Dye Mix A to the turbidity of 85% according to the manufacturer's instructions. IF-0 GN Base was used for PM plates 1 and 2; IF-0 GN Base plus 5.0 mM sodium pyruvate was used for plates 3 to 8 and IF-10 Base plus 1:200 dilution of an 85% transmittance suspension of cells was used for plates 9 to 20. Each well of PM plates 1 to 20 was inoculated with 100 µL of the cells suspension accordingly. After optimizing, plates were incubated in the OmniLog® reader (BioLog Inc., Hayward, California) at 37ºC for 24 h (PM1-2 and PM9-20) or 48 h (PM3-8) with readings taken every 15 min, converting the pixel density in each well to a signal value reflecting cell growth and dye conversion. The tetrazolium redox dye is reduced when bacteria respire, which provides both amplification and quantitation of the phenotype. Data analysis was performed using Kinetic and Parametric software (BioLog Inc., Hayward, California). Phenotypes were determined based on the area difference under the kinetic curve of dye formation between the wildtype and mutant strains and a significant divergent phenotype was identified when a difference in Omnilog™ units of 5, 000 ± 1, 000 or greater between the two strains was obtained.

CHAPTER 4: RESULTS

4.1 Isolation of Bacteria

From the inoculated salad vegetables in BHIB, aliquots were serially diluted (10^{-1}, 10^{-2}, 10^{-3}, 10^{-4} and 10^{-5}) and spread on the MacConkey agar plates. MacConkey agar is the selective media for growing Gram-negative bacteria particularly Enterobacteriaceae while inhibiting any growth of Gram-positive bacteria. From each of the food samples, Enterobacteriaceae bacterial colonies with different morphologies were selected for further experiments. A total of twenty Enterobacteriaceae bacterial colonies with different morphologies were successfully isolated with MacConkey agar. Table 4.1 illustrates a summary of the appearance and morphology of bacterial colonies obtained from LB agar plates.

4.2 Gram Staining

The pure cultures of the twenty bacterial isolates were stained according to the standard Gram staining procedure. Microscopic observations based on the shape and size of each of the bacteria type was done under the light microscope at 1000 × magnification size (with oil emersion). The gram staining results of the bacterial isolates are shown in Table 4.1.

Table 4.1: Morphology of bacterial colonies

Sample Name	Gram reaction	Colour	Size	Opacity	Surface	Form	Elevation	Margin
B1	Negative	Creamy yellow	Medium; 2 mm	Opaque	Smooth	Circular	Raised	Entire
B2	Negative	Pale yellow	Medium; 3 mm	Translucent	Smooth	Circular	Flat	Undulate
B3	Negative	Creamy yellow	Medium; 2 mm	Opaque	Smooth	Circular	Raised	Entire
CB1	Negative	Creamy yellow	Medium; 3 mm	Opaque	Smooth	Circular	Raised	Entire
CB2	Negative	Pale yellow	Medium; 3 mm	Translucent	Smooth	Circular	Flat	Entire
CH1	Negative	Cream	Medium; 2 mm	Translucent	Smooth	Circular	Raised	Entire
CH2	Negative	Cream	Medium; 2 mm	Opaque	Smooth	Circular	Raised	Entire
CH3	Negative	Pale yellow	Medium; 2 mm	Translucent	Smooth	Circular	Raised	Entire
CH4	Negative	Cream	Medium; 3 mm	Opaque	Smooth	Circular	Raised	Entire
CH5	Negative	Cream	Medium; 2 mm	Opaque	Smooth	Circular	Raised	Entire

Table 4.1, continued

Sample Name	Gram reaction	Colour	Size	Opacity	Surface	Form	Elevation	Margin
L1	Negative	Pale yellow	Medium; 2 mm	Translucent	Smooth	Circular	Raised	Entire
L2	Negative	Pale yellow	Medium; 3 mm	Translucent	Smooth	Circular	Flat	Entire
L3	Negative	Creamy yellow	Medium; 2 mm	Translucent	Smooth	Circular	Flat	Entire
L4	Negative	Pale yellow	Medium; 2 mm	Translucent	Smooth	Circular	Flat	Entire
LB1	Negative	Pale yellow	Medium; 2 mm	Translucent	Smooth	Circular	Flat	Entire
LB2	Negative	Pale yellow	Medium; 3 mm	Translucent	Smooth	Circular	Flat	Entire
LB3	Negative	Creamy yellow	Medium; 3 mm	Translucent	Smooth	Circular	Flat	Entire
LB4	Negative	Pale yellow	Medium; 2 mm	Translucent	Smooth	Irregular	Flat	Undulate
T1	Negative	Creamy yellow	Medium; 2 mm	Opaque	Smooth	Circular	Raised	Entire
T2	Negative	Pale yellow	Medium; 3 mm	Translucent	Smooth	Circular	Flat	Undulate

4.3 IDENTIFICATION OF BACTERIAL ISOLATES

4.3.1 MALDI-TOF-MS

Twenty Enterobacteriaceae bacterial colonies were further identified by MALDI-TOF-MS. MALDI-TOF-MS enabled most of the bacterial isolates to be identified to genus level with score value above 2.0. Among the twenty isolates, twelve isolates were able to be identified up to the species level with score values above 2.3. The meaning of the score value was summarized in Table 4.2 while Table 4.3 summarized the strain identity of the bacterial isolates and the score value of each strain from MALDI-TOF-MS. Phylogenetic trees generated on all of the isolates are shown in Figures 4.1 to 4.6.

Table 4.2: Meaning of score values

Range	Description
2.300 - 3.000	Highly probable species identification
2.000 - 2.299	Secure genus identification, probable species identification
1.700 - 1.999	Probable genus identification
0.000 - 1.699	Not reliable identification

Table 4.3: Identification of bacterial isolates and score value by MALDI-TOF-MS

Sample Name	Strain identification	Source	Score Value
B1	*Klebsiella pneumonia*	B	2.474
B2	*Enterobacter cloacae*	B	2.207
B3	*Enterobacter aerogenes*	B	2.482
CB1	*Raoultella ornithinolytica*	CB	2.703
CB2	*Enterobacter cloacae*	CB	2.311
CH1	*Enterobacter cloacae*	CH	2.490
CH2	*Klebsiella oxytoca*	CH	2.249
CH3	*Enterobacter asburiae*	CH	2.285
CH4	*Klebsiella pneumonia*	CH	2.505
CH5	*Klebsiella oxytoca*	CH	2.434
L1	*Enterobacter asburiae*	L	2.461
L2	*Kluyvera cryocrescens*	L	2.071
L3	*Morganella morganii*	L	2.754
L4	*Rahnella aquatilis*	L	2.008
LB1	*Citrobacter freundii*	LB	2.423
LB2	*Morganella morganii*	LB	2.702
LB3	*Enterobacter cloacae*	LB	2.570
LB4	*Salmonella sp.*	LB	1.834
T1	*Enterobacter aerogenes*	T	2.245
T2	*Enterobacter cloacae*	T	2.508

B, Bitter gout; CB, cabbage; CH, chili pepper; L, lettuce; LB, long bean; T, tomato.

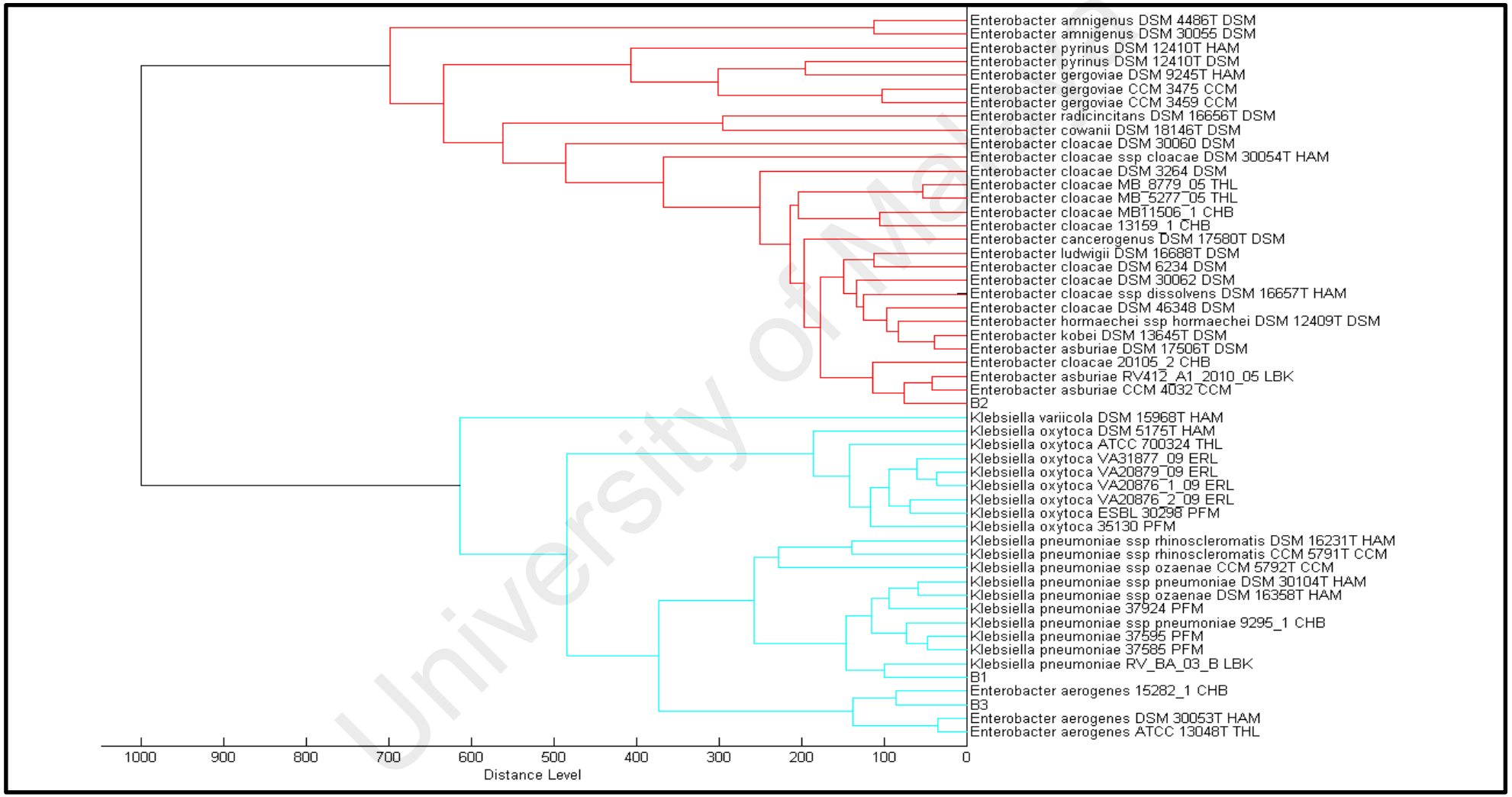

Figure 4.1: Phylogenetic positions of (a) B1, B2 and B3 isolates, visualized using the standard MALDI Biotyper MSP. The different colours of the branches represent distinct clusters among the organisms in the database.

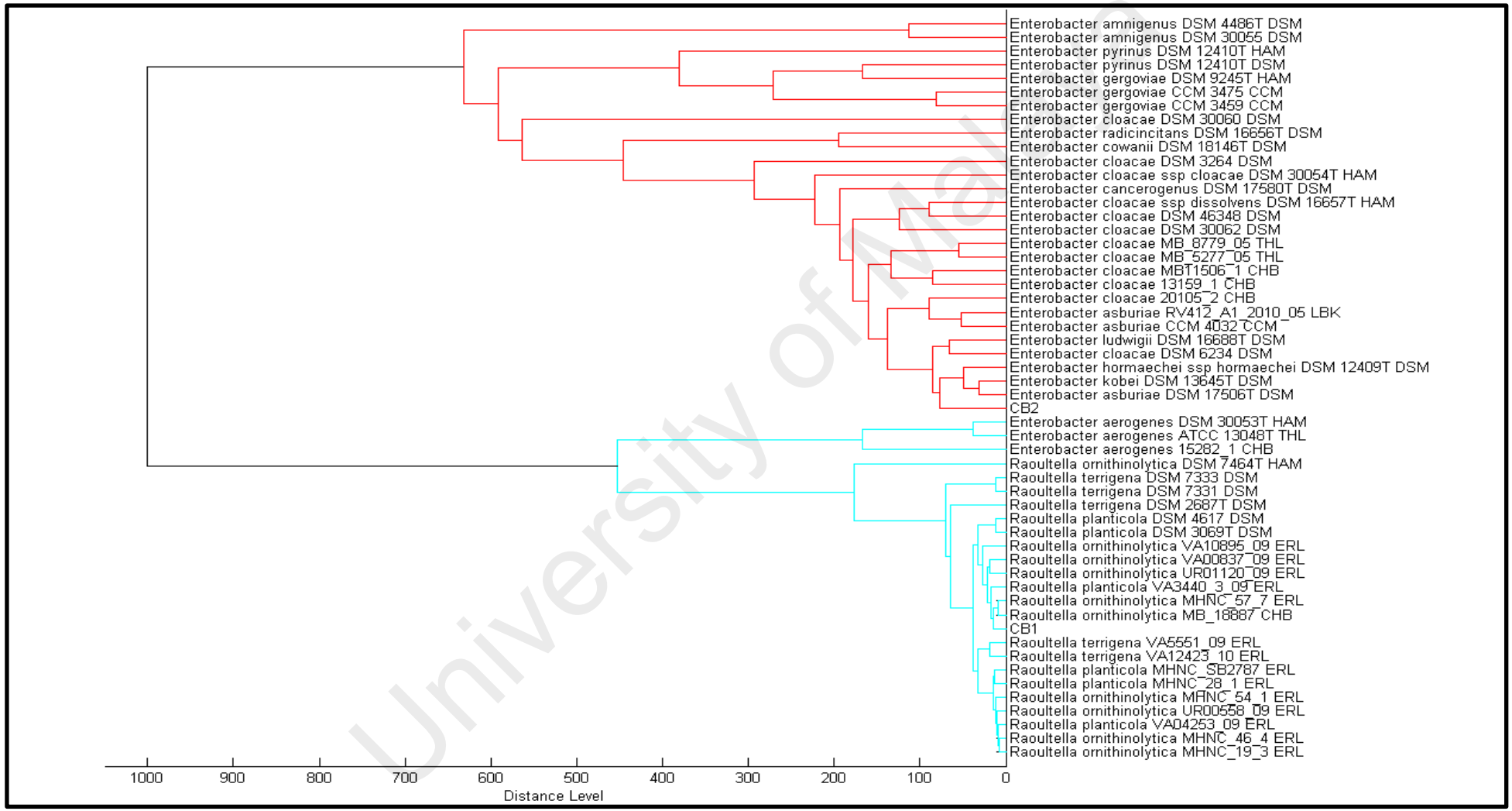

Figure 4.2: Phylogenetic positions of CB1 and CB2 isolates, visualized using the standard MALDI Biotyper MSP. The different colours of the branches represent distinct clusters among the organisms in the database.

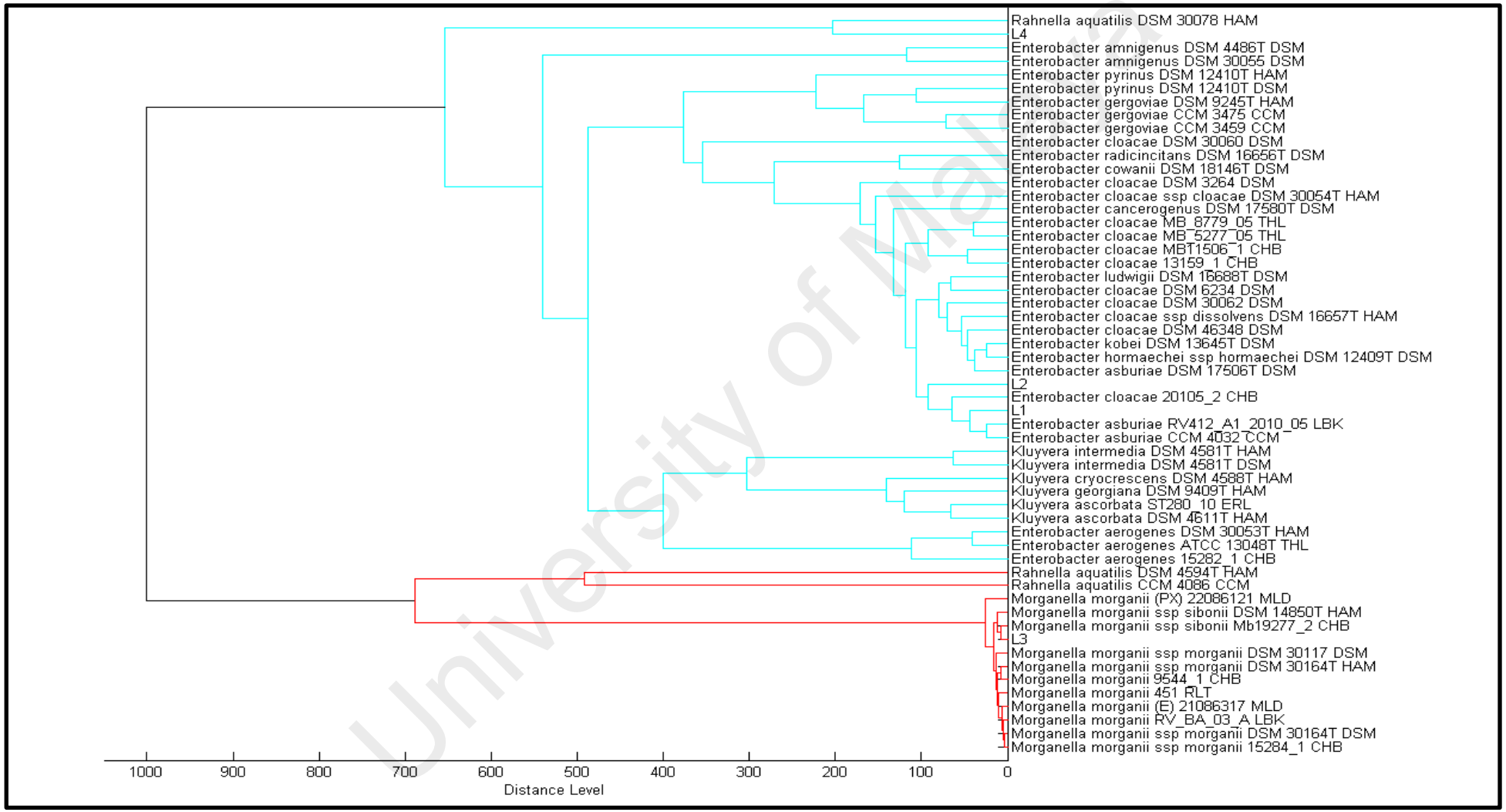

Figure 4.3: Phylogenetic positions of L1, L2, L3 and L4 isolates, visualized using the standard MALDI Biotyper MSP. The different colours of the branches represent distinct clusters among the organisms in the database.

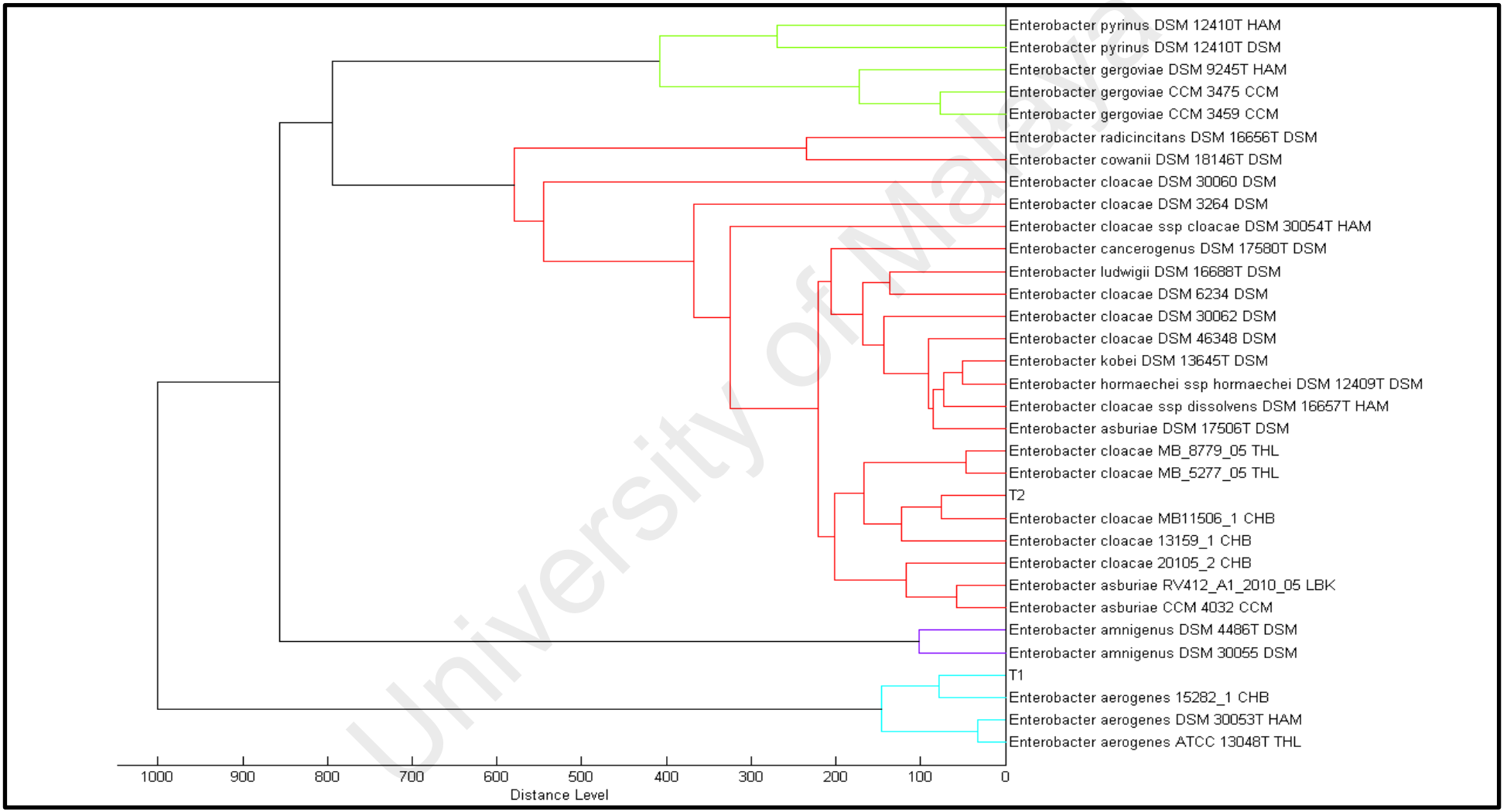

Figure 4.4: Phylogenetic positions of T1 and T2 isolates, visualized using the standard MALDI Biotyper MSP. The different colours of the branches represent distinct clusters among the organisms in the database.

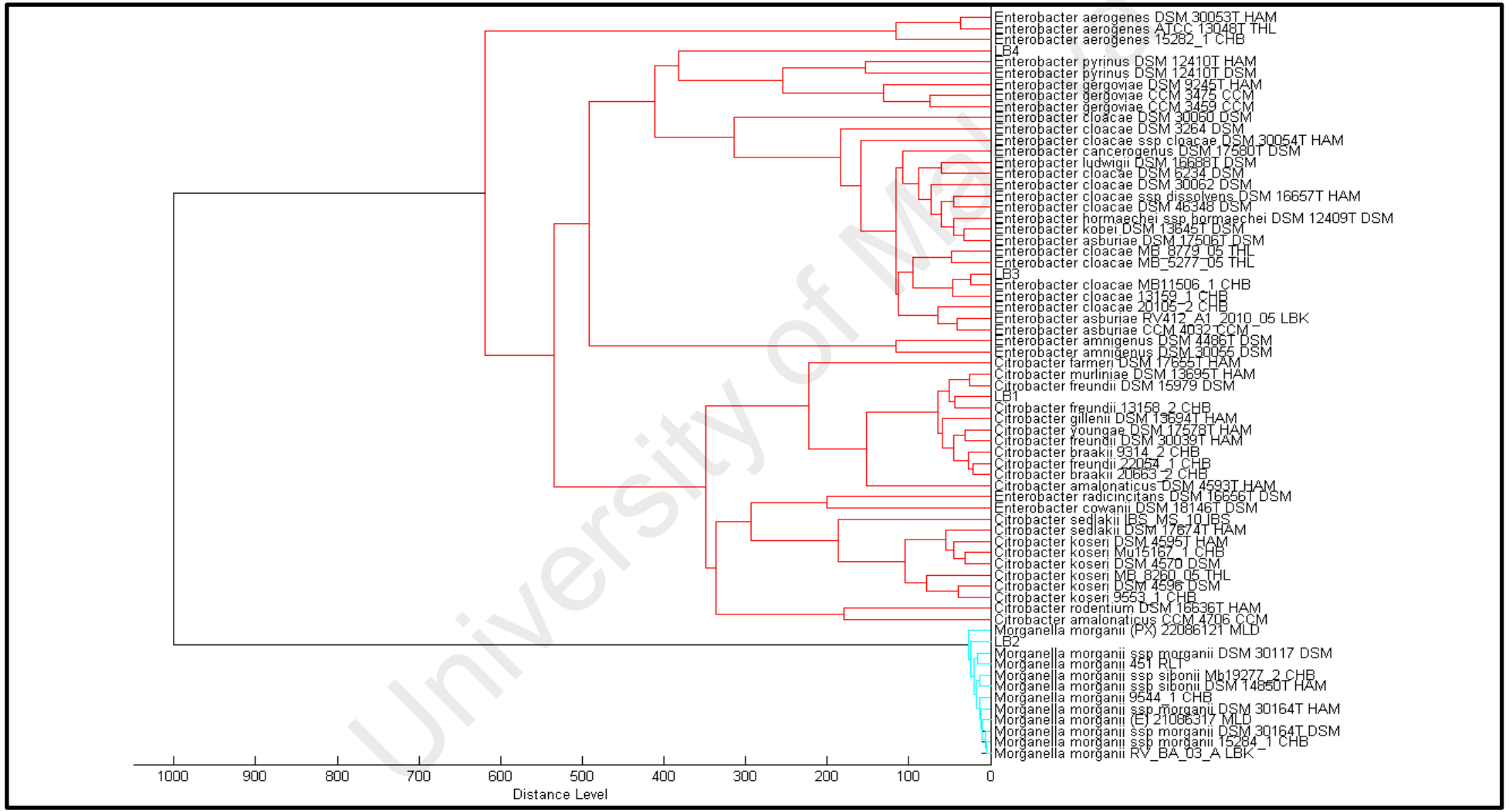

Figure 4.5: Phylogenetic positions of LB1, LB2, LB3 and LB4 isolates, visualized using the standard MALDI Biotyper MSP. The different colours of the branches represent distinct clusters among the organisms in the database.

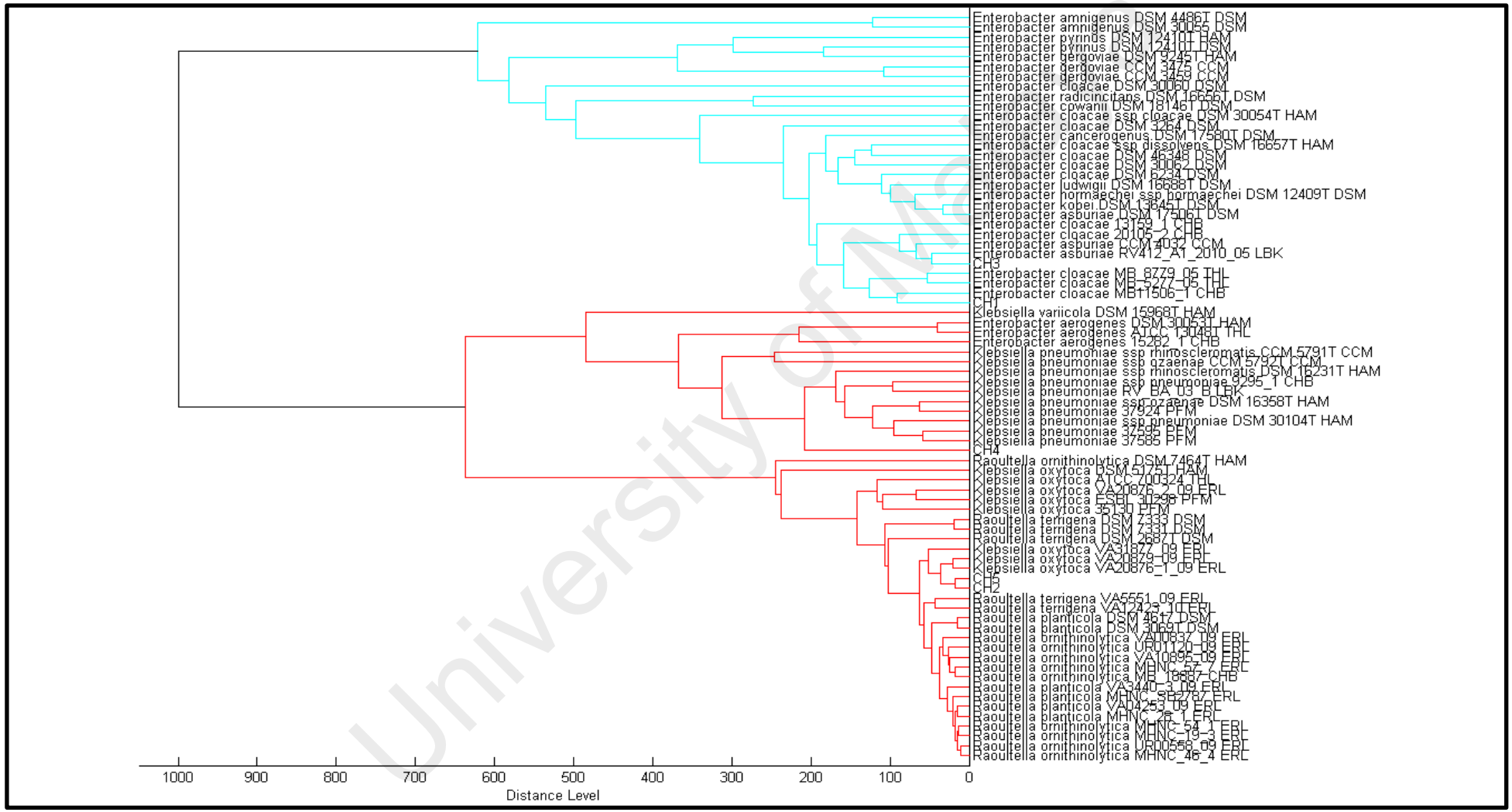

Figure 4.6: Phylogenetic positions of CH1, CH2, CH3, CH4 and CH5 isolates, visualized using the standard MALDI Biotyper MSP. The different colours of the branches represent distinct clusters among the organisms in the database.

4.3.2 Nucleotide Sequence Depositions

The whole genome sequence of the isolates that passed the quality control and possessed less than 200 contigs were deposited in GenBank. The acquired GenBank accession number for each of the deposited sequence are shown in Table 4.4.

Table 4.4: Assigned GenBank accession numbers for the identified isolates

Sample Name	Strain identification	GenBank Accession Number
B1	*Klebsiella pneumonia*	JSWX00000000
B2	*Enterobacter cloacae*	JSWY00000000
B3	*Enterobacter aerogenes*	JSWV00000000
CB1	*Raoultella ornithinolytica*	LFBW00000000
CB2	*Enterobacter cloacae*	LFLG00000000
CH1	*Enterobacter cloacae*	JSWZ00000000
CH2	*Klebsiella oxytoca*	JSWW00000000
CH4	*Klebsiella pneumonia*	JSXA00000000
CH5	*Klebsiella oxytoca*	LFUC00000000
L1	*Enterobacter asburiae*	AWXI00000000
L2	*Kluyvera cryocrescens*	LGHZ00000000
L3	*Morganella morganii*	JSWU00000000
LB2	*Morganella morganii*	LFLH00000000
LB3	*Enterobacter cloacae*	LFHB00000000
T1	*Enterobacter aerogenes*	JSWV00000000

4.4 AHLs Detection of Bacterial Isolates

4.4.1 Screening for Short Chain AHLs Production by Biosensor *C. violaceum* CV026

Preliminary screening for QS activities of the twenty bacterial isolates was performed by cross streaking with biosensor *C. violaceum* CV026. Observation of purple pigment, i.e. violacein on the biosensor streak line would indicate the production of exogenous short chain AHL molecules from the tested isolates (McClean et al., 1997). *P. carotovorum* GS101 which carries *carI* gene that is responsible for the production of 3-oxo-C6-HSL was used as the positive control while the *carI* defect mutant *P. carotovorum* PNP22 served as negative control (McGowan et al., 1995). Among the tested isolates, only *E. asburiae* L1 was positive for the production of short chain AHLs (Figure 4.7), which triggered biosensor *C. violaceum* CV026 violacein production. Cross streak results for bacterial isolates that showed negative violacein production are shown in Appendix F. Table 4.5 indicates the results from the *C. violaceum* CV026 cross streak.

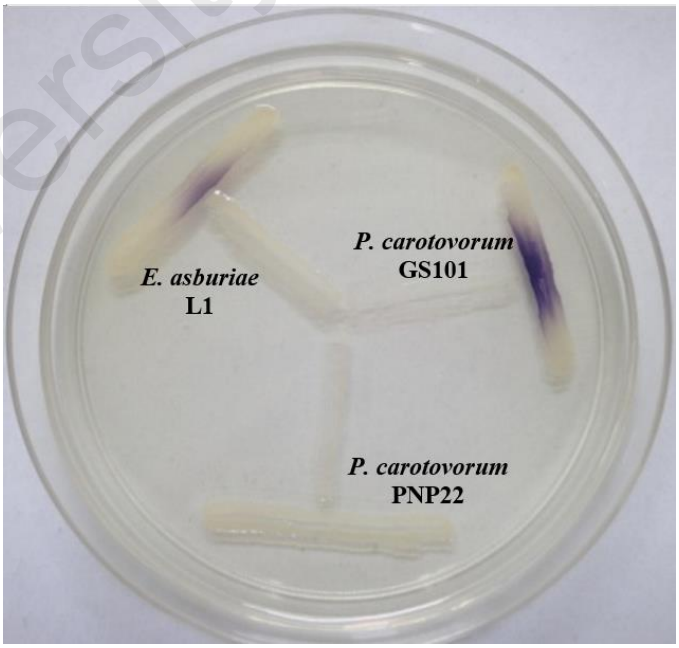

Figure 4.7: Preliminary screening for violacein production using *C. violaceum* CV026 cross streak. *P. carotovorum* GS101 and *P. carotovorum* PNP22 was used as positive and negative controls, respectively. Observation of purple pigment formation on the biosensor indicates the production of exogenous short chain AHL molecules by the *E. asburiae* L1 isolate.

Table 4.5: Results from the preliminary screening for AHLs production among the bacterial isolates using biosensor *C. violaceum* CV026

Bacterial isolates	**Violacein production**
K. pneumonia B1	Negative
E. cloacae B2	Negative
E. aerogenes B3	Negative
R. ornithinolytica CB1	Negative
E. cloacae CB2	Negative
E. cloacae CH1	Negative
K. oxytoca CH2	Negative
E. asburiae CH3	Negative
K. pneumonia CH4	Negative
K. oxytoca CH5	Negative
E. asburiae L1	Positive
K. cryocrescens L2	Negative
M. morganii L3	Negative
R. aquatilis L4	Negative
C. freundii LB1	Negative
M. morganii.LB2	Negative
E. cloacae LB3	Negative
Salmonella sp. LB4	Negative
E. aerogenes T1	Negative
E. cloacae T2	Negative

4.4.2 Measurement of Bioluminescence

The production of AHLs by *E. asburiae* L1 was further confirmed by using the luminometer-spectrophotometer. AHLs extract for *E. asburiae* L1 was cultured with biosensor *E. coli* [pSB401], whereby the activation of bioluminescence of *E. coli* [pSB401] was observed (Figure 4.8).

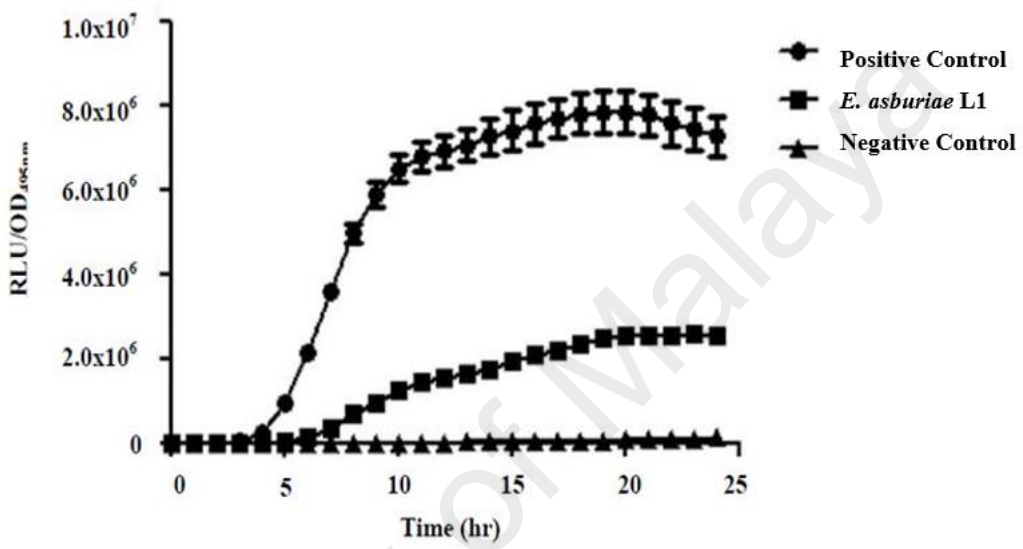

Figure 4.8: Confirmation of AHLs production by *E. asburiae* L1. Bioluminescence measurement was done for 24 h, 37ºC growth in the presence of AHL extracted from spent culture supernatant of *E. asburiae* L1 (square), the positive control, synthetic 3-oxo-C6-HSL (250 pg/µL; circle) and the negative control, acetonitrile (250 pg/µL; triangle). *E. coli* [pSB401] served as the biosensor. Data are presented as means of ± SEM values of triplicates.

4.4.3 AHLs Identification by Triple Quadrupole LC-MS/MS

In order to identify and confirm the AHLs production, overnight cultures of *E. asburiae* L1 was subjected to AHLs extraction as described in Chapter 3.3.4.4. The extract was then analysed with Agilent 1290 Infinity LC system and Agilent MassHunter software was used for the MS data analysis. The results of MS data analysis from the spent culture supernatant of *E. asburiae* L1, presented in Figure 4.9 provided the evidence for the presence of C4-HSL (*m/z* 172.0000) and C6-HSL (*m/z* 200.4000). To the best of my knowledge, this is the first report of AHL production by *E. asburiae*.

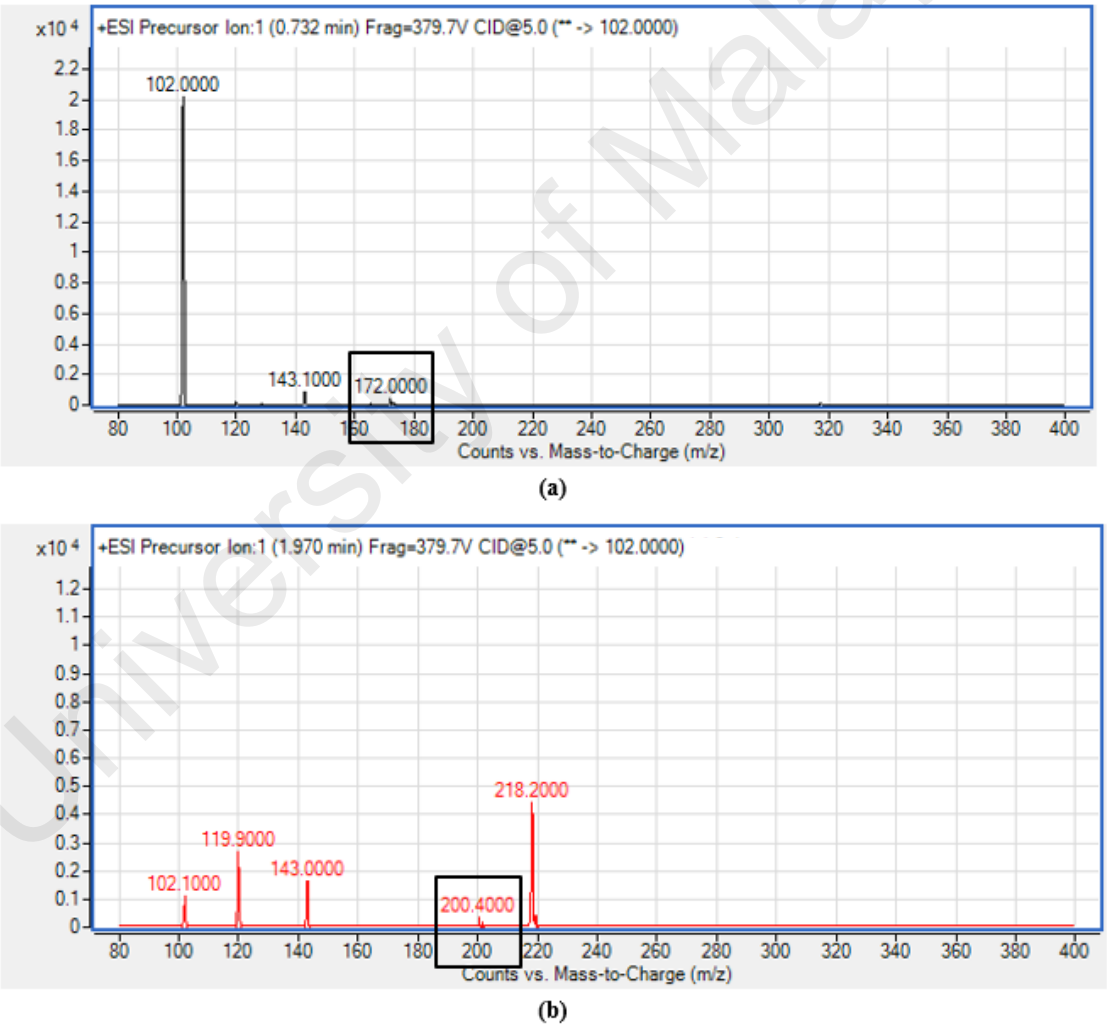

Figure 4.9: Mass spectra analysis of the extracted AHLs from the spent culture supernatant of *E. asburiae* L1. (**a**) C4-HSL (*m/z* 172.0000) and (**b**) C6-HSL (*m/z* 200.4000) (boxed).

4.5 Bacterial Characterization of AHL-Producing Bacterium *E. asburiae* L1

4.5.1 Biochemical Assays

In the subsequent research, only the AHL-producing bacterium *E. asburiae* L1 was selected for further study. The API 20E biochemical assays was performed as a preliminary characterization of *E. asburiae* L1. In addition to this, a few commonly applied biochemical tests for characterization of Enterobacteriaceae were carried out independently to validate the results obtained from API 20E biochemical assay. For all the biochemical assays performed, type strain *E. asburiae* ATCC 35953 was included for comparison.

4.5.1.1 API Biochemical Assay Analysis

The biochemical reactions for *E. asburiae* L1 and *E. asburiae* ATCC 35953 are summarized in Table 4.6.

Table 4.6: API 20E biochemical assays

Biochemical tests	***E. asburiae* L1**	***E. asburiae* ATCC 35953**
ONPG, β-Galactosidase	Positive	Positive
ADH, Arginine dihydrolase	Positive	Negative
LDC, Lysine decarboxylase	Negative	Negative
ODC, Ornithine decarboxylase	Positive	Positive
CIT, Citrate utilization	Positive	Positive
H2S, H_2S production	Negative	Negative
URE, Urease	Negative	Negative
TDA, Tryptophane deaminase	Positive	Positive
IND, Indole production	Negative	Negative
VP, Voges–Proskauer	Positive	Positive
MAN, Mannitol	Positive	Positive
GEL, Gelatinase	Negative	Negative

Table 4.6, continued

Biochemical tests	***E. asburiae* L1**	***E. asburiae* ATCC 35953**
GLU, Glucose	Positive	Positive
INO, Inositol	Negative	Negative
SOR, Sobitol	Positive	Positive
RHA, Rhamnose	Negative	Negative
SAC, Saccharose	Positive	Positive
MEL, Melibiose	Negative	Negative
AMY, Amygdalin	Positive	Positive
ARA, Arabinose	Positive	Positive
OX, Cytochrome Oxidase	Negative	Negative

4.5.1.2 IMViC Test

IMViC is an acronym that stands for four different tests. This test consists of indole test, MR-VP tests and citrate utilization test. Indole test determines the ability of organisms to split amino acid tryptophan to form the compound indole. MR test determines whether the microbes perform mixed acids fermentation when supplied glucose while the VP test detects organisms that utilize the butylene glycol pathway and produce acetoin. The citrate test screens for the ability of organisms to utilize citrate as its carbon and energy source. Figure 4.10 shows the IMViC test result of *E. asburiae* L1 and *E. asburiae* ATCC 35953.

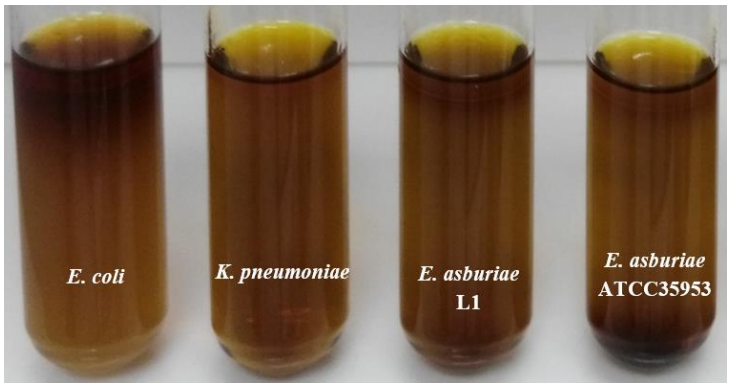

(A)

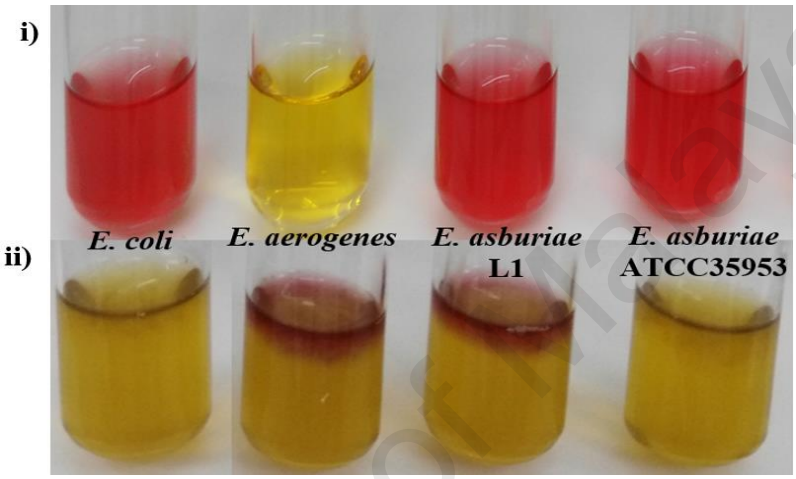

(B)

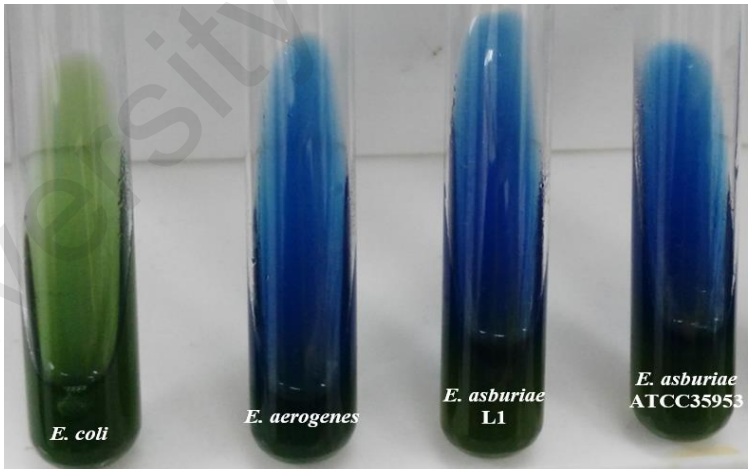

(C)

Figure 4.10: IMViC test. (A) Indole test. Absence of cherry-red ring on top of the medium indicated that *E. asburiae* L1 and *E. asburiae* ATCC 35953 (type strain) showed negative indole reaction. *E. coli* and *K. pneumoniae* acted as positive (cherry-red ring) and negative control (colourless ring), respectively. (B) MR-VP tests. Both *E. asburiae* L1 and *E. asburiae* ATCC 35953 showed positive reaction for (i) MR test. For (ii)VP test, *E. asburiae* L1 and *E. asburiae* ATCC 35953 showed positive and negative reaction, respectively. *E. coli* acted as positive control for MR test and negative control for VP test while *E. aerogenes* served as negative control for MR test and positive control for VP test. (C) Citrate test. The colour changes from green to dark blue indicated positive citrate reaction in *E. asburiae* L1 and *E. asburiae* ATCC 35953. *E. coli* and *E. aerogenes* served as negative and positive controls, respectively.

4.5.1.3 Decarboxylation Test

This biochemical tests examine the production of the enzyme decarboxylase, which removes the carboxyl group from an amino acid. Lysine, ornithine, and arginine were the three amino acids routinely tested in the identification of Enterobacteriaceae. Therefore, they were included in this test.

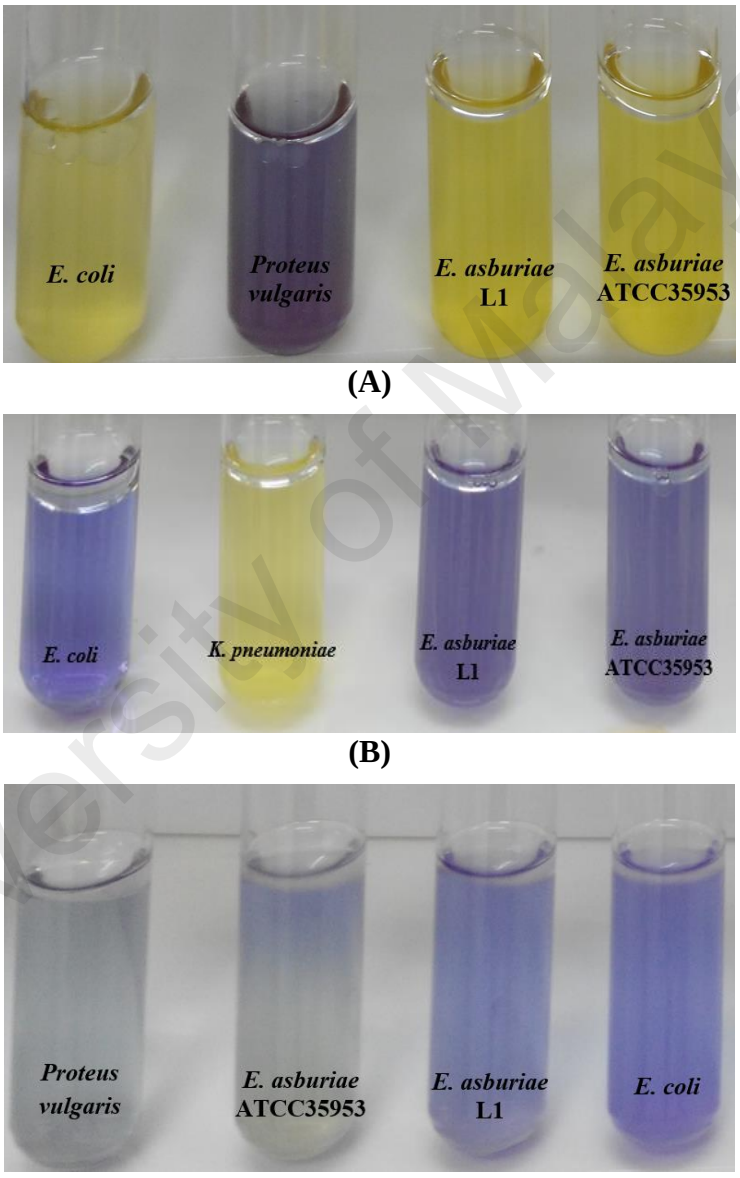

Figure 4.11: (A) Lysine (B) ornithine and (C) arginine decarboxylation tests. *E. asburiae* L1 showed negative, positive and positive reactions for lysine, ornithine and arginine decarboxylation tests. *E. asburiae* ATCC 35953 showed negative reactions for all the decarboxylation tests.

4.5.1.4 Nitrate Reduction Test

Nitrate reduction test is performed to examine the ability of *E. asburiae* L1 to produce nitrate reductase enzyme that hydrolyse nitrate (NO_3^-) to nitrite (NO_2^-) and then be degraded to various nitrogen products such as nitrogen oxide, nitrous oxide and ammonia. Figure 4.12 displays the nitrate reduction test result of *E. asburiae* L1 and ATCC 35953. Table 4.7 summarizes the biochemical reactions of *E. asburiae* L1 and ATCC 35953 for IMViC, decarboxylation and nitrate reduction tests.

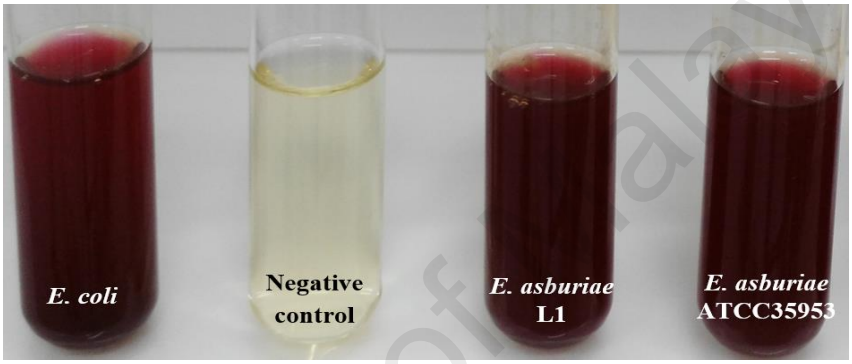

Figure 4.12: Nitrate reduction test. *E. asburiae* L1 and ATCC 35953 showed positive nitrate reduction reaction. Red colour was observed after addition of nitrate I and nitrate II reagents. *E. coli* and uninoculated medium was included as positive and negative controls, respectively.

Table 4.7: Biochemical reactions of *E. asburiae* L1 and *E. asburiae* ATCC 35953

Biochemical tests	***E. asburiae* L1**	***E. asburiae* ATCC 35953**
IMViC		
Indole	Negative	Negative
MR	Positive	Positive
VP	Positive	Negative
Citrate utilization	Positive	Positive
Decarboxylation		
Lysine	Negative	Negative
Ornithine	Positive	Positive
Arginine	Positive	Negative
Nitrate Reduction	Positive	Positive

4.5.1.5 Carbohydrate Fermentation Test

The **c**arbohydrate fermentation test evaluates the fermentation of different sugars. Phenol red broths were prepared and supplemented with different sugars (i.e. lactose, L-arabinose, L-rhamnose, maltose, mannitol, sorbitol, sucrose and xylose). When fermentation occurs, acidic by-products are formed, whereby the solution will turn from red to yellow. The positive and negative reactions were illustrated in Figure 4.13. Table 4.8 indicates the carbohydrate fermentation test result.

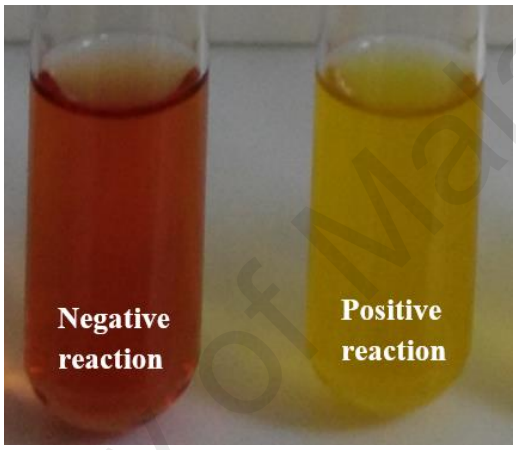

Figure 4.13: Representative result of carbohydrate fermentation test.

Table 4.8: Carbohydrate fermentation test result of *E. asburiae* L1 and *E. asburiae* ATCC 35953

Biochemical tests	***E. asburiae* L1**	***E. asburiae* ATCC 35953**
Lactose	Negative	Positive
L-arabinose	Positive	Positive
L-rhamnose	Negative	Negative
Maltose	Positive	Positive
Mannitol	Positive	Positive
Sorbitol	Positive	Positive
Sucrose	Positive	Positive
Xylose	Positive	Positive

4.5.2 Tabletop SEM

E. asburiae L1 is a non-motile bacterial strain isolated from the Batavia lettuce leaves. Similar to other species classified under Enterobacteriaceae family, *E. asburiae* L1 is a rod-shaped bacterium with approximately 1.32 μm in size (Figure 4.14). *E. asburiae* L1 lives in the mesophilic environment with its optimal temperature at 37°C.

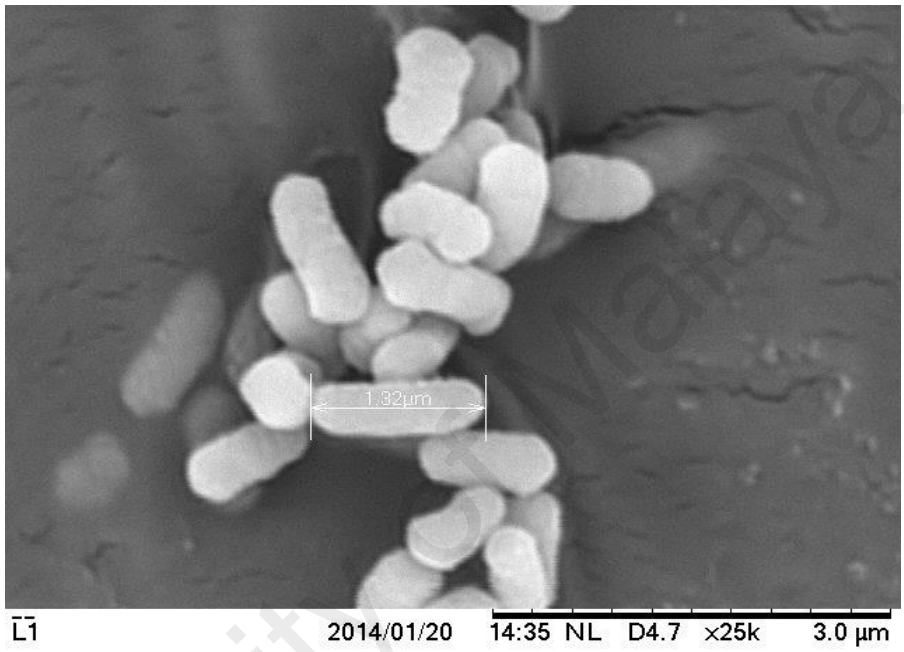

Figure 4.14: Scanning electron microscope image of *E. asburiae* L1. The size of the strain is approximately 1.32 μm (bar).

4.5.3 Phenotypic Characterization (GENIII MicroPlate)

Biolog GENIII MicroPlate analyses a microorganism in 94 phenotypic tests (71 carbon source utilization assays and 23 chemical sensitivity assays). In this research, GENIII MicroPlate was applied to confirm the identity of QS positive isolate L1 as *E. asburiae*, as well as to study the biochemical activity of isolate L1. Analysis from phenotypic characterization using GENIII Microplate identified *E. asburiae* as the closest relative of isolate L1. Biochemical profile of *E. asburiae* L1 is listed in Appendix G.

4.6 Sequencing of *E. asburiae* L1 Using PacBio SMRT Sequencer

To characterize the *luxI/R* homologues of *E. asburiae* L1, the complete genome of *E. asburiae* L1 (4.5Mbp in size) was sequenced using PacBio SMRT sequencer. The PacBio sequencing platform generated an output data with average genome coverage of 216.24×. *De novo* assembly of the insert reads was performed with the HGAP algorithm in SMRT Portal (version 2.1.1), in which the genome sequence of *E. asburiae* L1 was assembled into a GC-rich (56.1%) single contig. The complete genome sequence of *E. asburiae* L1 has been deposited in DDBJ/EMBL/GenBank under the accession number CP007546 (Lau, Yin, & Chan, 2014).

.

4.7 Whole Genome Optical Mapping of *E. asburiae* L1

The whole genome sequence accuracy of *E. asburiae* L1 was verified by optical genome mapping technology. The whole genome map of *E. asburiae* L1 generated from the single DNA molecule with the automated Argus system (OpGen Inc.) was aligned with the sequence obtained from the PacBio RS II sequencing technology to investigate the mismatch tolerance. Figure 4.15 shows that although two different sequencing technologies were applied, both sequences generated are highly aligned with each other, confirming the completeness of this genome.

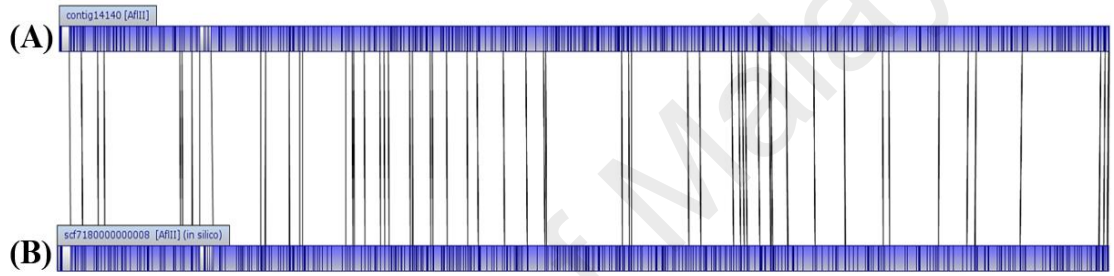

Figure 4.15: Alignment of (A) OpGen sequence with (B) PacBio sequence for *E. asburiae* L1.

4.8 Circularity Analysis of *E. asburiae* L1

Dot plot analysis was performed to confirm the circularity of the complete genome sequence of *E. asburiae* L1 with the help of Gepard (version 1.3) (Figure 4.16). Circularization of this genome was performed by trimming overlapping region in both ends of the genome manually to provide an accurate genome size.

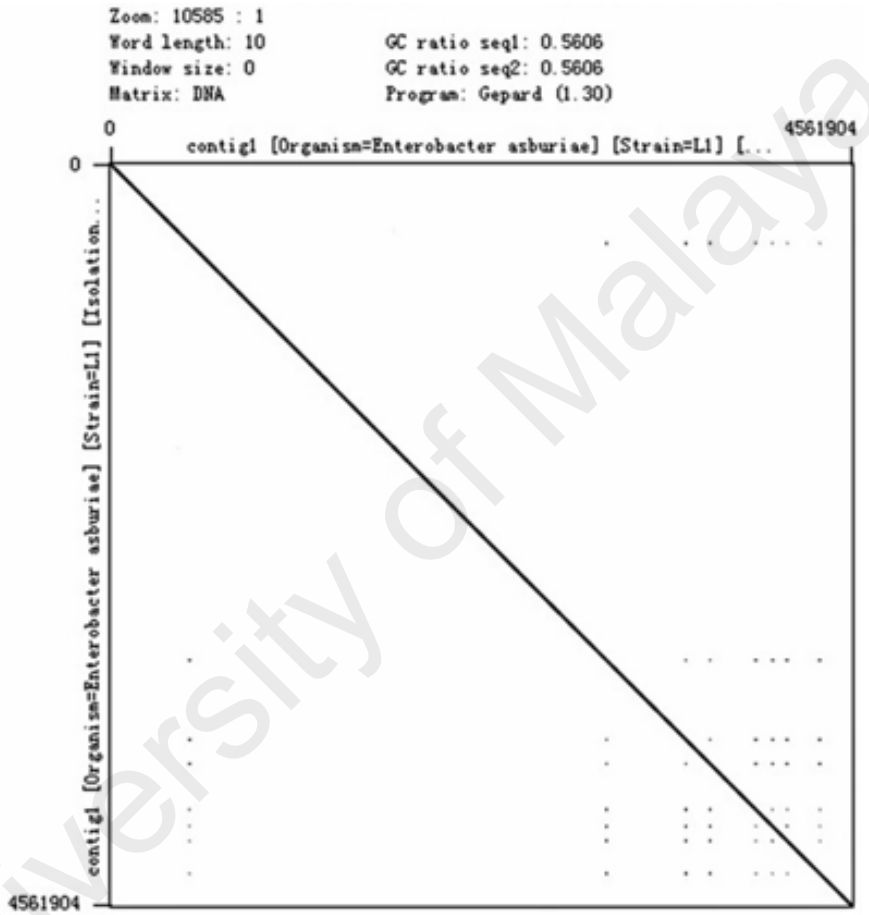

Figure 4.16: Circular representation of *E. asburiae* L1. The figure was constructed by Gepard version 1.3. The straight line of dot plot generated from Gepard supported the circular representation of this genome.

4.9 Genome Analysis of *E. asburiae* L1

4.9.1 Genome Statistic

Genome statistic of complete genome sequence of *E. asburiae* L1 is listed in Table 4.9. Digital representation of circular complete genome sequence of *E. asburiae* L1 is shown in Figure 4.17.

Table 4.9: Genome statistics of complete genome sequence of *E. asburiae* L1

Statistics	Number
DNA, total number of bases	4561905
DNA coding number of bases	4106401
DNA G+C number of bases	2557500
DNA scaffolds	1
Genes total number	4278
Protein coding genes	4168
Pseudo Genes	25
RNA genes	110
rRNA genes	25
5S rRNA	9
16S rRNA	8
23S rRNA	8
tRNA genes	84
Other RNA genes	1
Protein coding genes with function prediction	3728
without function prediction	440
Protein coding genes with enzymes	1378
w/o enzymes but with candidate KO based enzymes	1
Protein coding genes connected to Transporter Classification	766
Protein coding genes connected to KEGG pathways[3]	1548
not connected to KEGG pathways	2620

Table 4.9, continued

Statistics	Number
Protein coding genes connected to KEGG Orthology (KO)	2908
not connected to KEGG Orthology (KO)	1260
Protein coding genes connected to MetaCyc pathways	1128
not connected to MetaCyc pathways	3040
Protein coding genes with COGs[3]	3490
with KOGs[3]	868
with Pfam[3]	3925
with TIGRfam[3]	1725
with InterPro	2624
with IMG Terms	1113
with IMG Pathways	381
with IMG Parts List	364
in internal clusters	392
in Chromosomal Cassette	4238
Chromosomal Cassettes	312
Biosynthetic Clusters	14
Genes in Biosynthetic Clusters	157
Fused Protein coding genes	146
Protein coding genes coding signal peptides	443
Protein coding genes coding transmembrane proteins	1073
COG clusters	2027
KOG clusters	533
Pfam clusters	2533
TIGRfam clusters	1473
Internal clusters	170

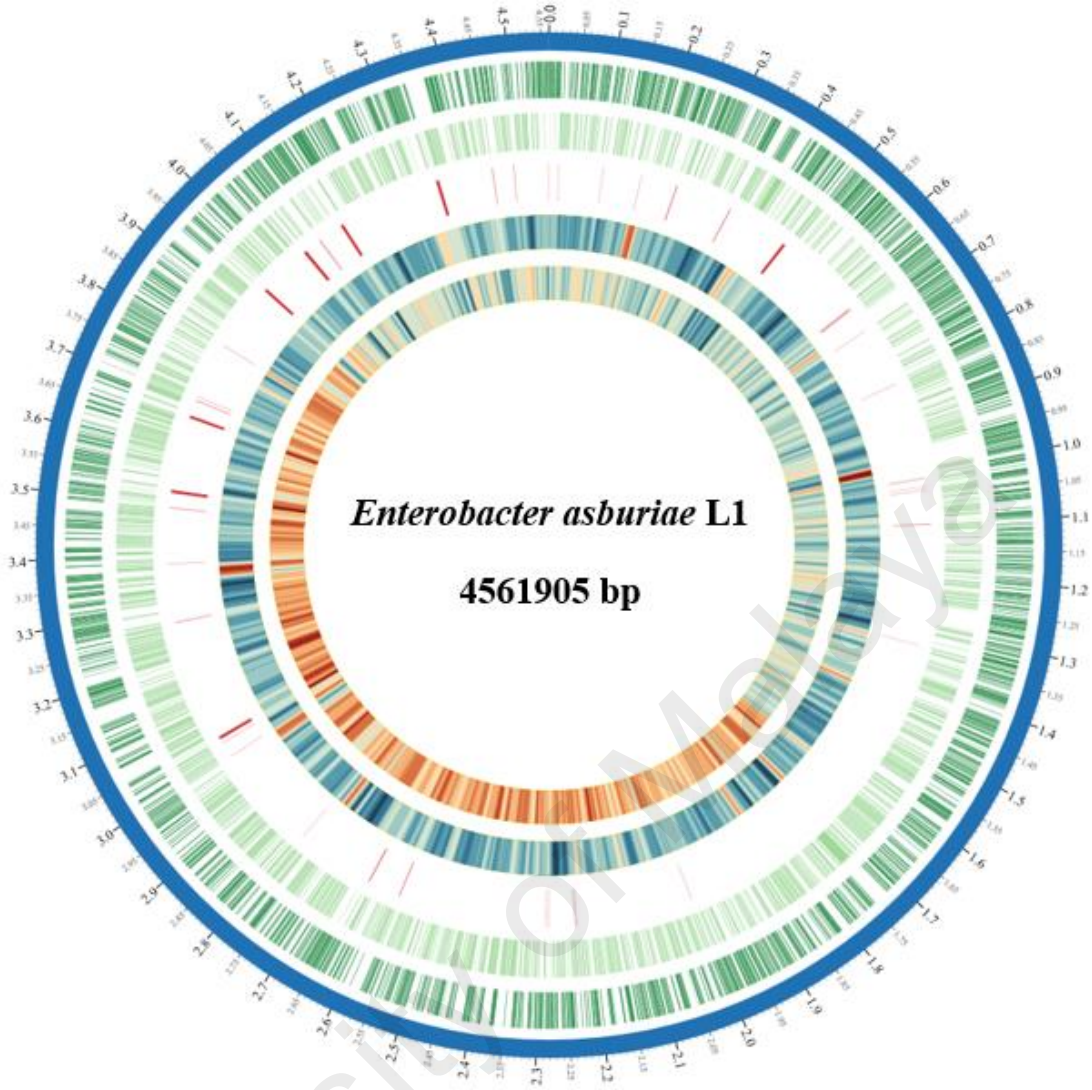

Figure 4.17: Digital representation of circular complete genome sequence of *E. asburiae* L1. List of tracks, from outside to inside: 1) Chromosome 2) CDS, forward strand, 3) CDS, reverse strand, 4) RNAs, 5) GC Content, heatmap plot, 6) GC Skew, heatmap plot.

4.9.2 KEGG Database Deposition and Pathways Statistics

The complete genome sequence of *E. asburiae* L1 has been deposited in KEGG database with details as listed in Table 4.10. KEGG pathways statistics of complete genome sequence of *E. asburiae* L1 is displayed in Figure 4.18.

Table 4.10: Details of *E. asburiae* L1 deposition in KEGG database

	***E. asburiae* L1**
T number	T03084
Org code	eau
Taxonomy	TAX: 1421338

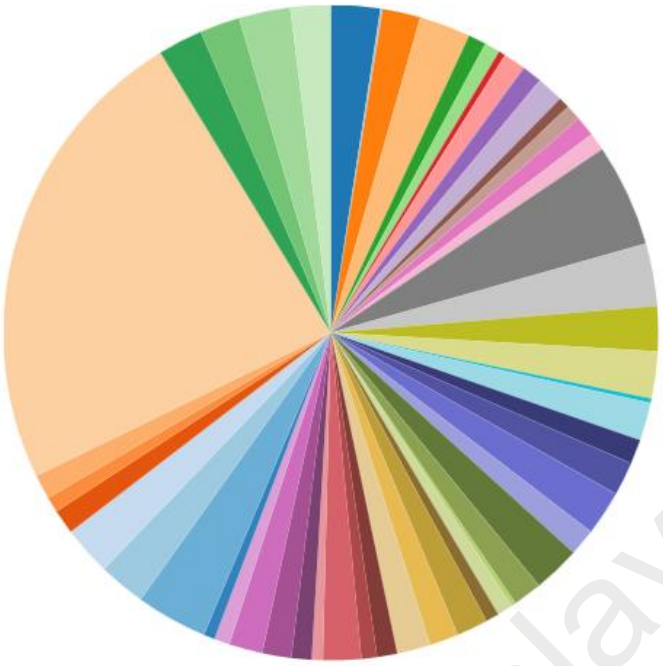

Color Code	Name	Count
	Aminoacyl-tRNA synthetases and alternate systems for amino acid activation	22
	Archael/Vacuolar-type H+ ATPase subunits	1
	Arginine biosynthesis	17
	Basal replication machinery	23
	Basal transription factors	8
	Biotin biosynthesis	7
	Cobalamin biosynthesis	3
	Coenzyme A biosynthesis	10
	DNA polymerase III subunits	9
	DNA-dependent RNA polymerase subunits	12
	Deoxyxylulose pathway of terpenoid biosynthesis	5
	Entner-Doudoroff pathway	7
	F0F1-type ATP synthase subunits	9
	FAD biosynthesis	8
	Fatty acid biosynthesis	46
	Flagellum structure and biogenesis	28
	Gluconeogenesis	20
	Glycolysis	21
	Glyoxylate bypass	2
	Heme biosynthesis	17
	Histidine biosynthesis	11
	Isoleucine biosynthesis	15
	Leucine biosyntehsis	20
	Lipid A biosynthesis	12
	Menaquinone biosynthesis	21
	Methionine biosynthesis	13

Color Code	Name	Count
	Multisubunit NA+/H+ antiporter	2
	NA+-transporting NADH:Ubiquinone oxireductase subunits	7
	NAD biosynthesis	6
	NADH:Ubiquinone oxidreductase subunits	14
	Pentose phosphate pathway	13
	Phenylalanine/tyrosine biosynthesis	15
	Preprotein translocase subunits	9
	Proline biosynthesis	7
	Purine biosynthesis	17
	Purine salvage	5
	Pyridoxal phosphate biosynthesis	9
	Pyrimidine biosynthesis	13
	Pyrimidine salvage	15
	Pyruvate decraboxylation	7
	Riboflavin biosynthesis	5
	Ribosomal proteins - large subunit	32
	Ribosomal proteins - small subunit	21
	TCA cycle	22
	Thiamine biosynthesis	11
	Threonine biosynthesis	7
	Thymidylate biosynthesis	11
	Transcriptional regulators	213
	Translation factors and enzymes involved in translation	20
	Trypotophan biosynthesis	18
	Ubiquinone biosynthesis	23
	Valine biosynthesis	18

Figure 4.18: KEGG pathways statistics of *E. asburiae* L1.

4.9.3 Gene Annotation Using RAST Server

Annotations by RAST revealed that the subsystem coverage is 62% which contributes to a total of 555 subsystems. The subsystem category distribution is shown in Figure 4.19. Similar to most Proteobacteria, majority of *E. asburiae* L1 genes (593 counts) are responsible for carbohydrate metabolism, followed by amino acids and derivatives; cofactors, vitamins, prosthetic groups and pigment production with 471 and 252 counts, respectively. Generally, these genes are responsible for the basic life-sustaining needs of the bacterial cell. Apart from the presence of the basic necessary genes in *E. asburiae* L1, there are 117 genes responsible for virulence, disease and defence. Among these 117 genes, 85 genes were found to play a role in controlling the resistance against antibiotics and toxic compounds.

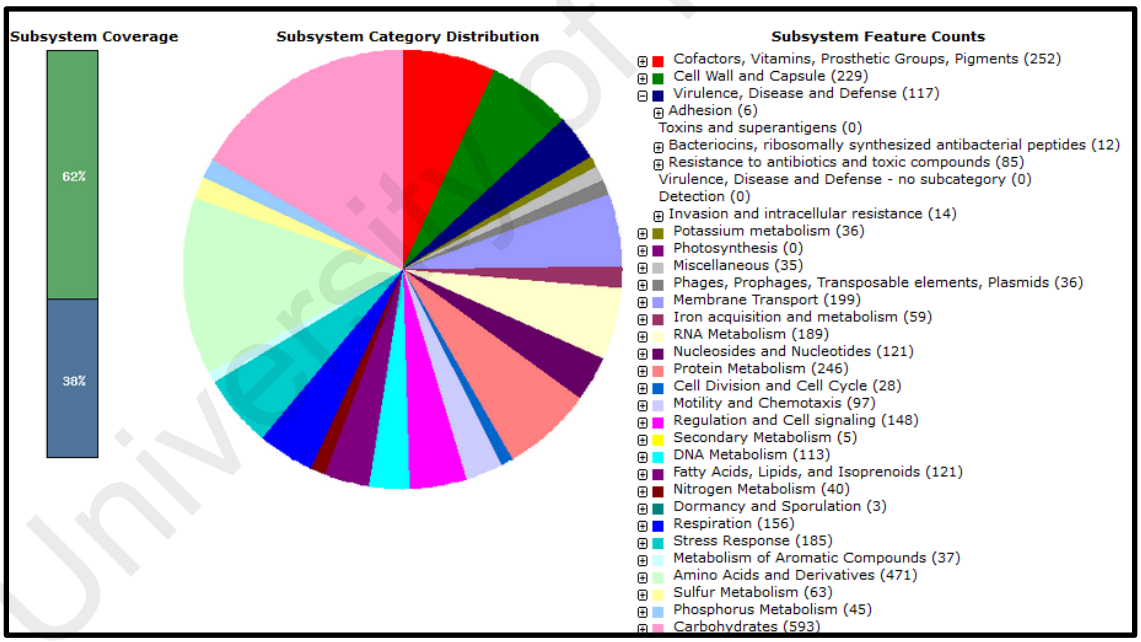

Figure 4.19: Subsystem category distribution statistics for *E. asburiae* L1. The complete genome sequence of *E. asburiae* L1 was annotated using the RAST server. The pie chart showed the count of each subsystem feature and the subsystem coverage. The green bar of the subsystem coverage corresponds to the percentage of the proteins included in the subsystems while the blue bar corresponds to the percentage of the proteins that are not included in the subsystems.

4.9.4 Comparative Genome Analysis of *E. asburiae* L1

4.9.4.1 RAST and Mauve analysis

To the best of my knowledge, *E. asburiae* L1 is the first *E. asburiae* species that showed QS activity. By this, a comparison genome analysis was performed to examine the relatedness among these different *E. asburiae* strains. Sequence-based comparative analysis of *E. asburiae* L1 was performed with other closely related strains that are available from NCBI database using RAST server. After analysis, it was found that *E. asburiae* strains ATCC 35953 (type strain), GN02073, GN02127, 33838 and PDN3 showed high similarities with *E. asburiae* L1, with at least 90% similarities (Figure 4.20). This strongly indicates that these *E. asburiae* strains were found to have very close genotypic features with *E. asburiae* L1. From the analysis, strains ATCC 35953 and PDN3 were found to be the closest species of *E. asburiae* L1, with at least 98% similarities. Analysis by MAUVE (Figure 4.21) indeed showed a high degree of synteny between *E. asburiae* L1, ATCC 35953 and PDN3. The coloured blocks of *E. asburiae* L1 are connected by lines to the collinear and homologous regions in the coloured blocks of strains ATCC 35953 and PDN3. The white areas within a coloured block of the genome are not aligned with each other and most likely contain sequence elements specific to the respective genome. Since there are not many 'white spaces' which denote sequences not in homology blocks, therefore, these three strains basically share high similarities in their genome sequences.

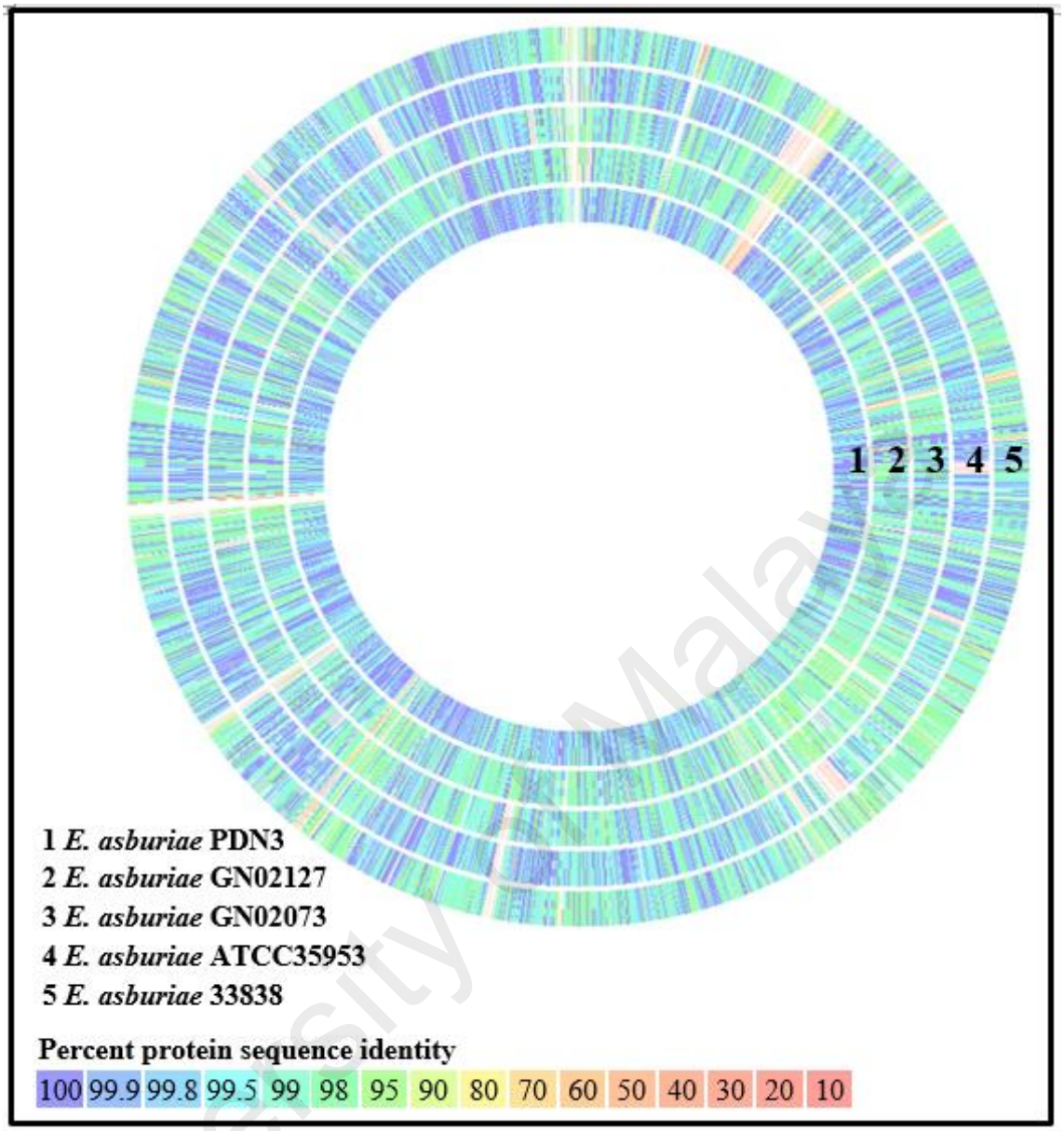

Figure 4.20: Genome comparison of *E. asburiae* L1 (reference) and five closely related species, PDN3 (JUGH00000000.1), GN02127 (LDCH00000000.1), GN02073 (LDCE01000001.1), ATCC 35953 (CP011863.1) and 33838 (LAAP00000000.1) using RAST server. The genome of the reference strain is not displayed in the figure.

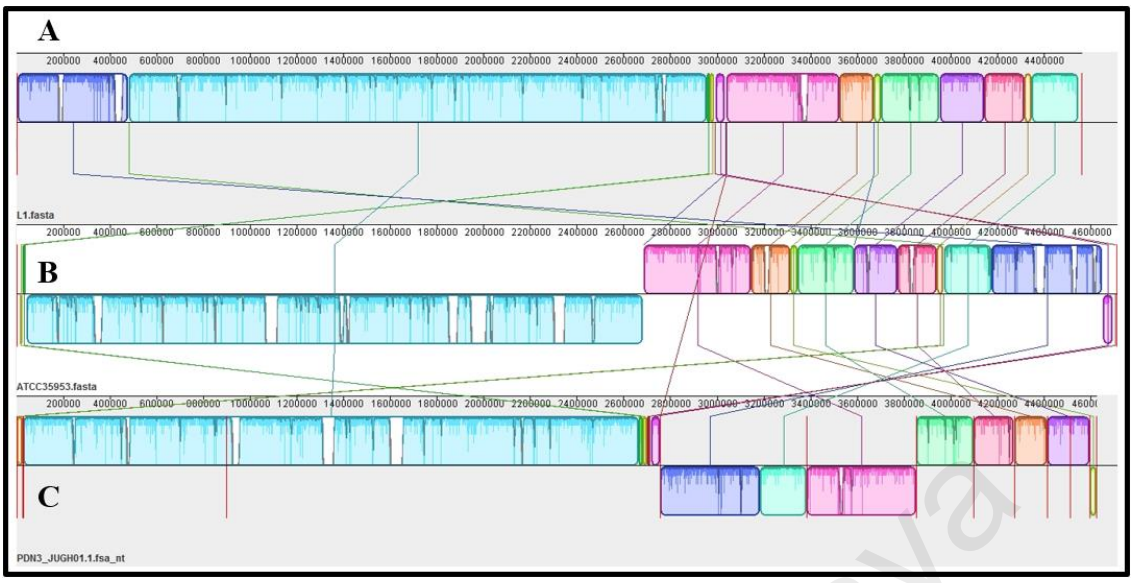

Figure 4.21: Genome alignments performed using Mauve software between A) *E. asburiae* L1 with its closely related species, B) ATCC 35953 (CP011863.1) and C) *E. asburiae* PDN3 (JUGH00000000.1). In this alignment process, a total of 18 locally collinear blocks (LCBs) were generated. Boxes with identical colours represent LCB, indicating homologous DNA regions shared between the two chromosomes without sequence rearrangement. Sequences outside coloured blocks do not have homologues in the other genome. Red lines indicate contig boundaries within the assembly.

4.9.4.2 OrthoANI (Average Nucleotide Identity) Analysis of *E. asburiae* L1

OrthoANI analysis was performed to confirm the genetic relatedness among *E. asburiae* L1 with the closely related *E. asburiae* strains as analysed by RAST. Cut-off value for species delineation in OrthoANI analysis is 95% which is correlated with 70% of DNA-DNA hybridization analysis (Goris et al., 2007;). OrthoANI analysis confirmed the relatedness of *E. asburiae* ATCC 35953, GN02073, GN02127, 33838 and PDN3 with *E. asburiae* L1.

In addition to this, this analysis was performed to confirm the identity of *E. asburiae* L1. OrthoANI value of *E. asburiae* L1 against the type strain, *E. asburiae* ATCC 35953 is 98.7%, hence reconfirmed L1 identity as *E. asburiae* (Figure 4.22).

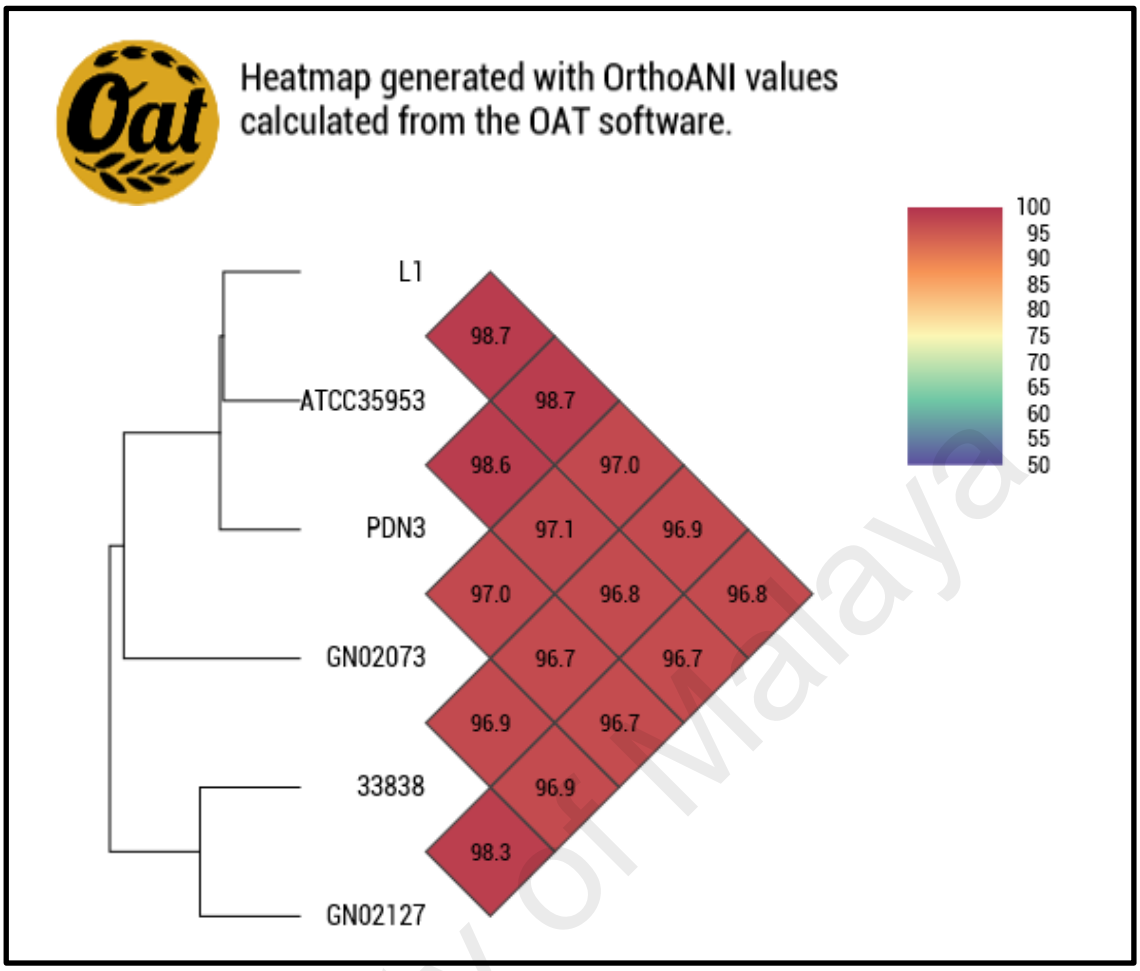

Figure 4.22: OrthoANI analysis between genome of *E. asburiae* L1 and other closely related species. GenBank accession numbers in parentheses: ATCC 35953 (CP011863.1), PDN3 (JUGH00000000.1), GN02073 (LDCE01000001.1), GN02127 (LDCH00000000.1), and 33838 (LAAP00000000.1). (Lee, Kim, Park, & Chun, 2015)

4.10 Nucleotide Sequence and Bioinformatics Analysis of *E. asburiae* L1

4.10.1 QS Genes of *E. asburiae* L1

Further analysis of *E. asburiae* L1 genome was emphasized on CDS responsible for cell-to-cell communication system in *Enterobacter* spp. *In silico* analysis of the *E. asburiae* L1 genome revealed the presence of a pair of *luxI/R* homologues which were 14 bp apart with opposite orientation (Figure 4.23). The putative *luxR* gene, designated *easR* (GenBank accession number AHW94256.1) with the size of 693 bp was identified at the location in between 1,633,036 and 1,633,728 of the *E. asburiae* L1 complete genome. Besides, an AHL synthase gene, designated *easI* (GenBank accession numbers AHW94257.1) of *E. asburiae* L1 with a size of 639 bp was found located in the region in between 1,633,743 and 1,634,381 of this genome. Phylogeny of EasI revealed that the AHL synthase found in *E. asburiae* L1 formed a separate cluster as compared with others *E. asburiae* and closely related enterobacteria (Figure 4.24). Phylogeny of EasR demonstrated that EasR was clustered within LuxR of *Enterobacter* sp. (Figure 4.25). The nucleotide sequence of *easI* and *easR* genes of *E. asburiae* L1 are displayed in Appendix H and I, respectively.

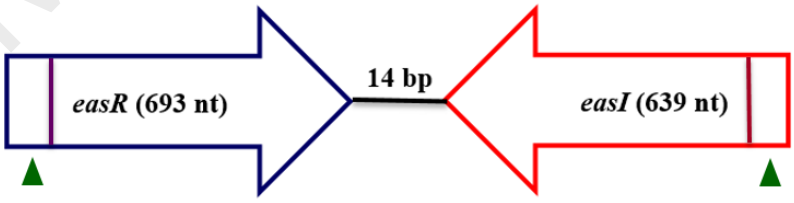

Figure 4.23: Orientation of *N*-acyl homoserine lactone synthase EasI and transcriptional regulator EasR of *E. asburiae* L1. The alignment of *easI* and *easR* genes showed that they were 14 bp apart. The green triangle indicated the site for start codons. The direction of the arrows indicates the orientation of both genes where *easI* is in the 5′–3′ direction while *easR* is in the 3′–5′ direction. The *easI* and *easR* genes sequences have been deposited in GenBank database with GenBank accession numbers AHW94257.1 and AHW94256.1, respectively.

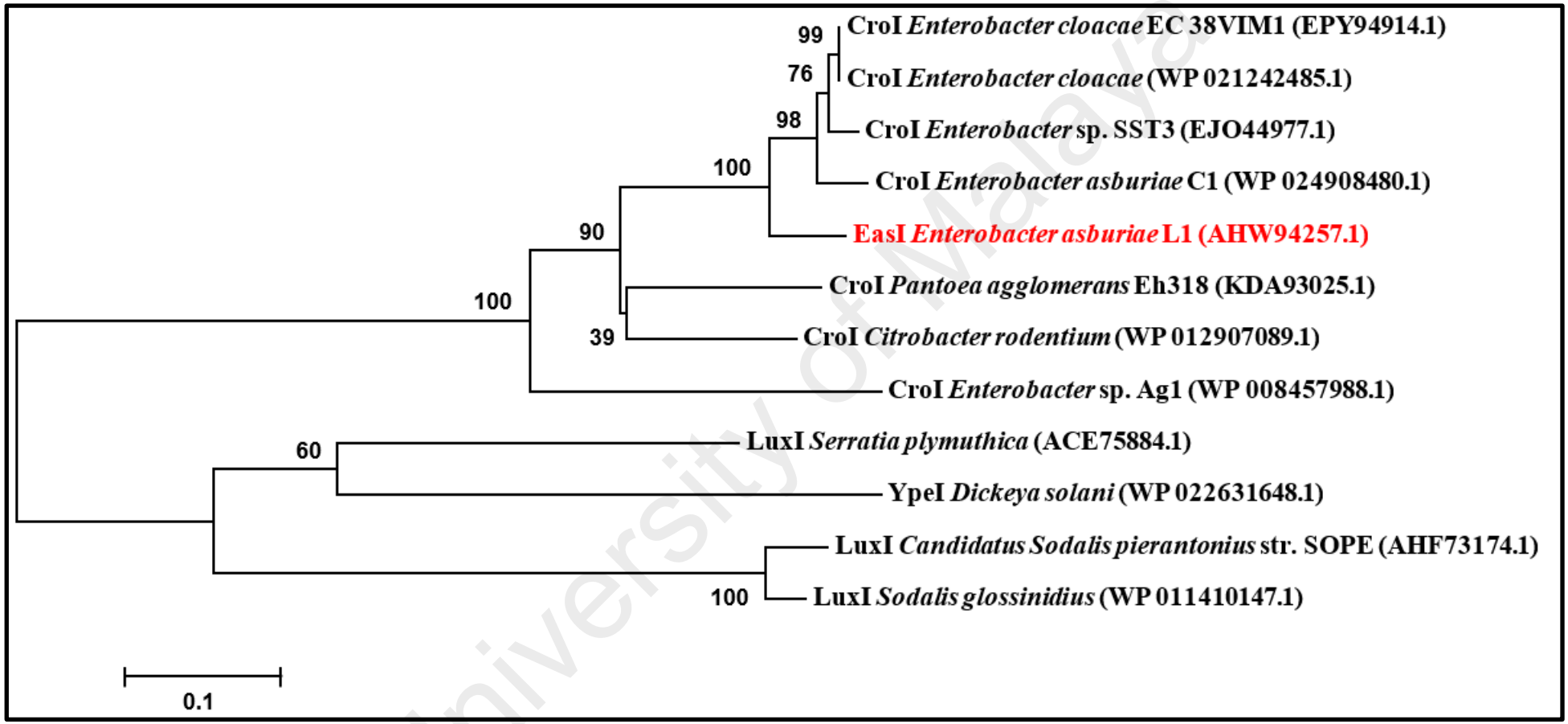

Figure 4.24: Phylogenetic analysis of *E. asburiae* L1 *easI* gene. The tree was constructed based on the similar LuxI protein sequences by Neighbour-Joining algorithm with bootstraps value of 1000 replicates. The horizontal bar at the bottom represents evolutionary distance as 0.1 change per nucleotide position.

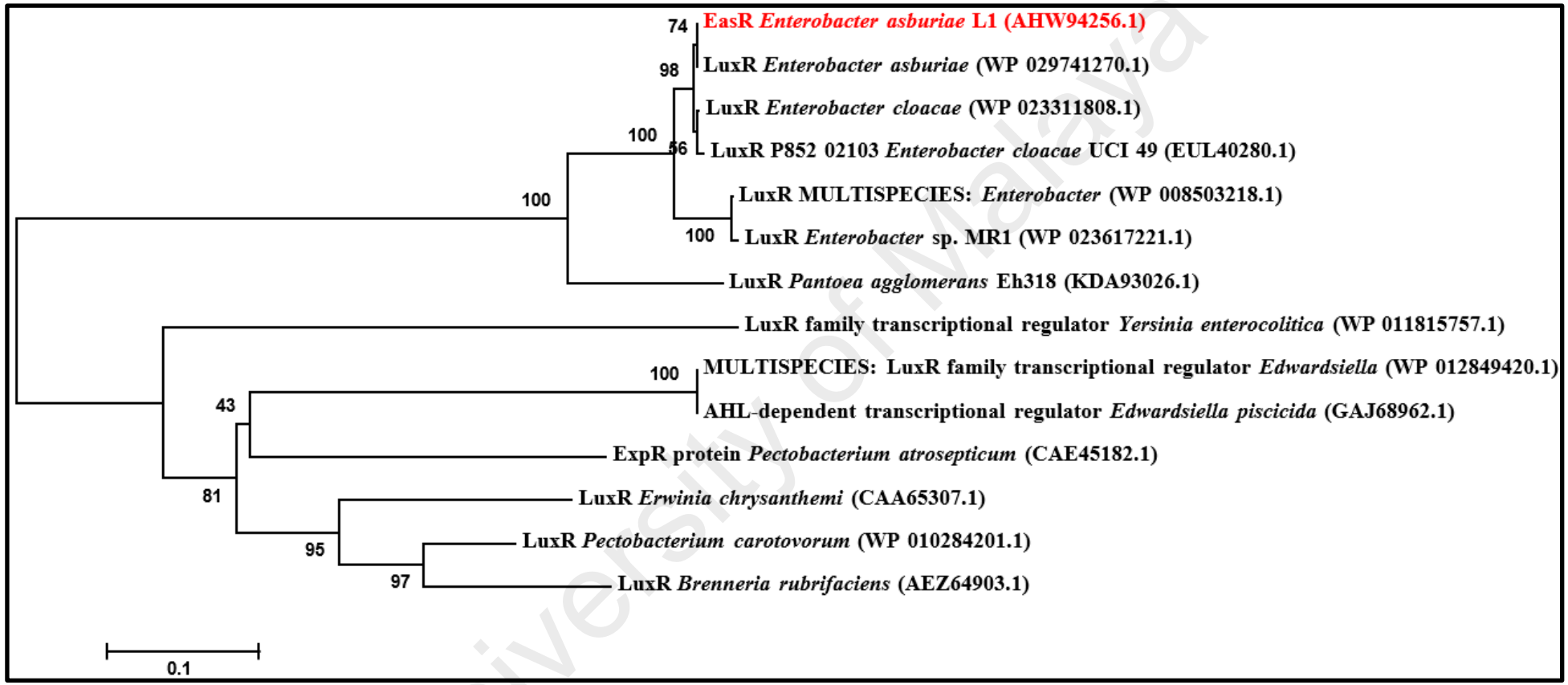

Figure 4.25: Phylogenetic analysis of *E. asburiae* L1 *easR* gene. The tree was constructed based on the similar LuxR protein sequences by Neighbour-Joining algorithm with bootstraps value of 1000 replicates. The horizontal bar at the bottom represents evolutionary distance as 0.1 change per nucleotide position.

4.10.2 EasI Gene Clusters Analysis

Analysis of the LuxI gene clusters showed a conserved variation among *E. asburiae* L1 with other closely related *E. asburiae* strains. As shown in Figure 4.26, all the *E. asburiae* strains possess LuxI homologues (ORF2) and the convergently-transcribed transcriptional regulator LuxR homologues (ORF1), except for strains C1 and GN1, which possess truncated LuxR homologues. In the vicinity of the LuxI/R homologues are GCN5-related N-acetyltransferase (ORF 11) and acetyltransferase GNAT family (ORF12). Apart from that, a signal-recognition protein, sensor histidine kinase (ORF8) is found at the downstream of LuxI homologues.

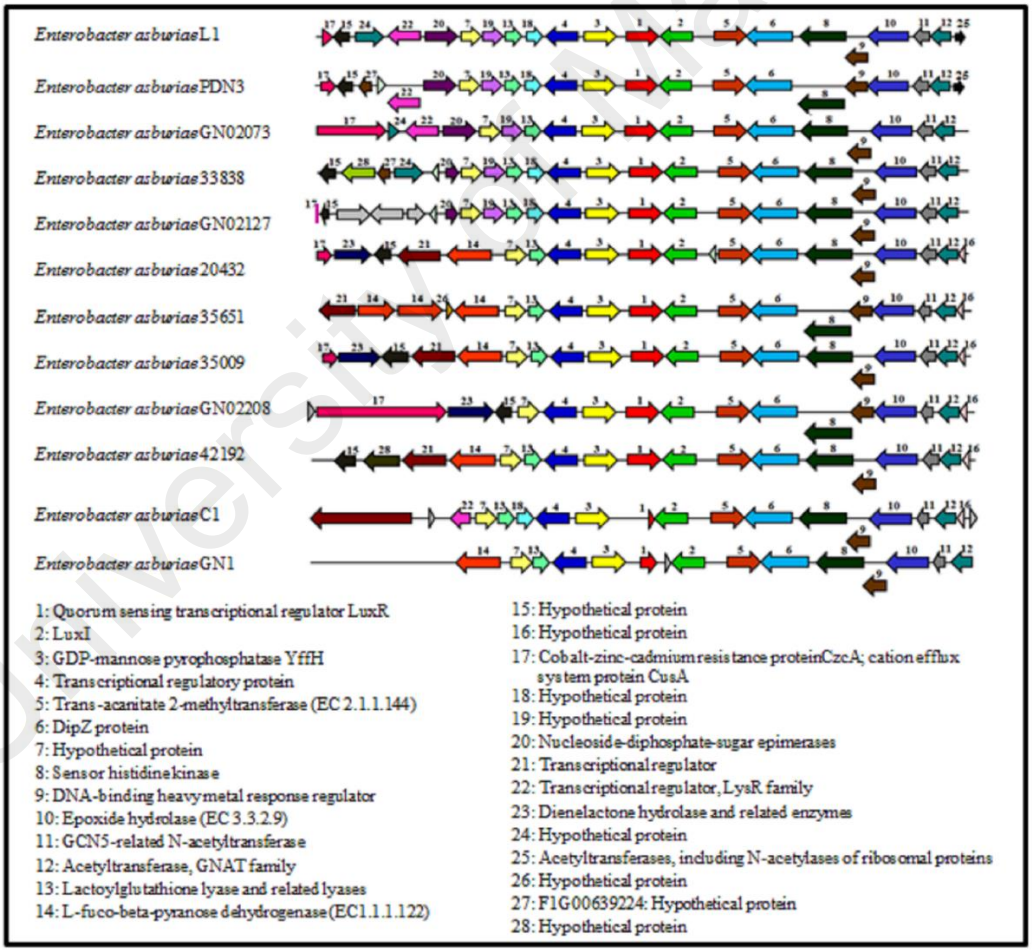

Figure 4.26: Comparison of LuxI/R homologues gene cluster and their flanking genes in *E. asburiae* L1 in comparison with closely related species, *E. asburiae* PDN3, GN02073, 33838, GN02127, 20432, 35651, 35009, GN02208, 42192, C1 and GN1. Arrows indicate the relative orientations of the genes while genes which are located outside of the line indicate overlapping genes. Homologous proteins are shown as the same colour. All autoinducer synthesis proteins, together with transcriptional regulator LuxR homologue, were found on each strain.

4.10.3 Nucleotide Sequence of the QS Genes

Based on NCBI database, *easR* encodes for a protein which consists of 230 amino acids. Figure 4.27 outlines the nucleotide sequence of the *easR* gene and its flanking sequences. On the other hand, *easI* encodes for a protein which consists of 212 amino acids. Figure 4.28 outlines the nucleotide sequence of the *easI* gene and its flanking sequences. *In silico* analysis revealed that in *easI* nucleotide sequence, the TAGTTT sequence, located at 27 nucleotides upstream of the start codon and the sequence, CTGTCC, located at 50 nucleotides upstream correspond to the potential -10 and -35 transcriptional elements, respectively. In agreement to the optimum spacing suggested by Hawley and McClure (1983) on *E. coli* RNA polymerase σ^{70} consensus promoter analysis, the two consensus regions in *E. asburiae* L1 are separated by 17 nucleotides. A putative Shine-Dalgarno site (AGGA) is located 8 bp upstream of the start codon. In addition, a putative *lux*-box (TACTTTTTAAGTA) was found 81 bp upstream of the start codon. This palindromic sequence of putative *lux* box suggests that the putative transcriptional activator, EasR, may bind to the *easI* promoter to activate *easI* expression. However, this hypothesis is yet to be validated.

The phylogenetic analysis based on amino acid sequences of LuxI homologues (Figure 4.29) showed the evolutionary distances between EasI and its counterparts from other *E. asburiae* strains, generated using Neighbour-Joining algorithm. Apart from that, CLUSTAL O (1.2.0) multiple sequence alignment of AHL autoinducer protein sequences of *E. asburiae* L1 with other *E. asburiae* strains are illustrated in Figure 4.30. The alignment shows that EasI protein shares high similarities and conserved amino acids with other AHL synthase of *E. asburiae* strains. It was found that EasI and all the LuxI family members contain the conserved 10 amino acid residues, characteristic of LuxI homologues (Parsek, Schaefer, & Greenberg, 1997).

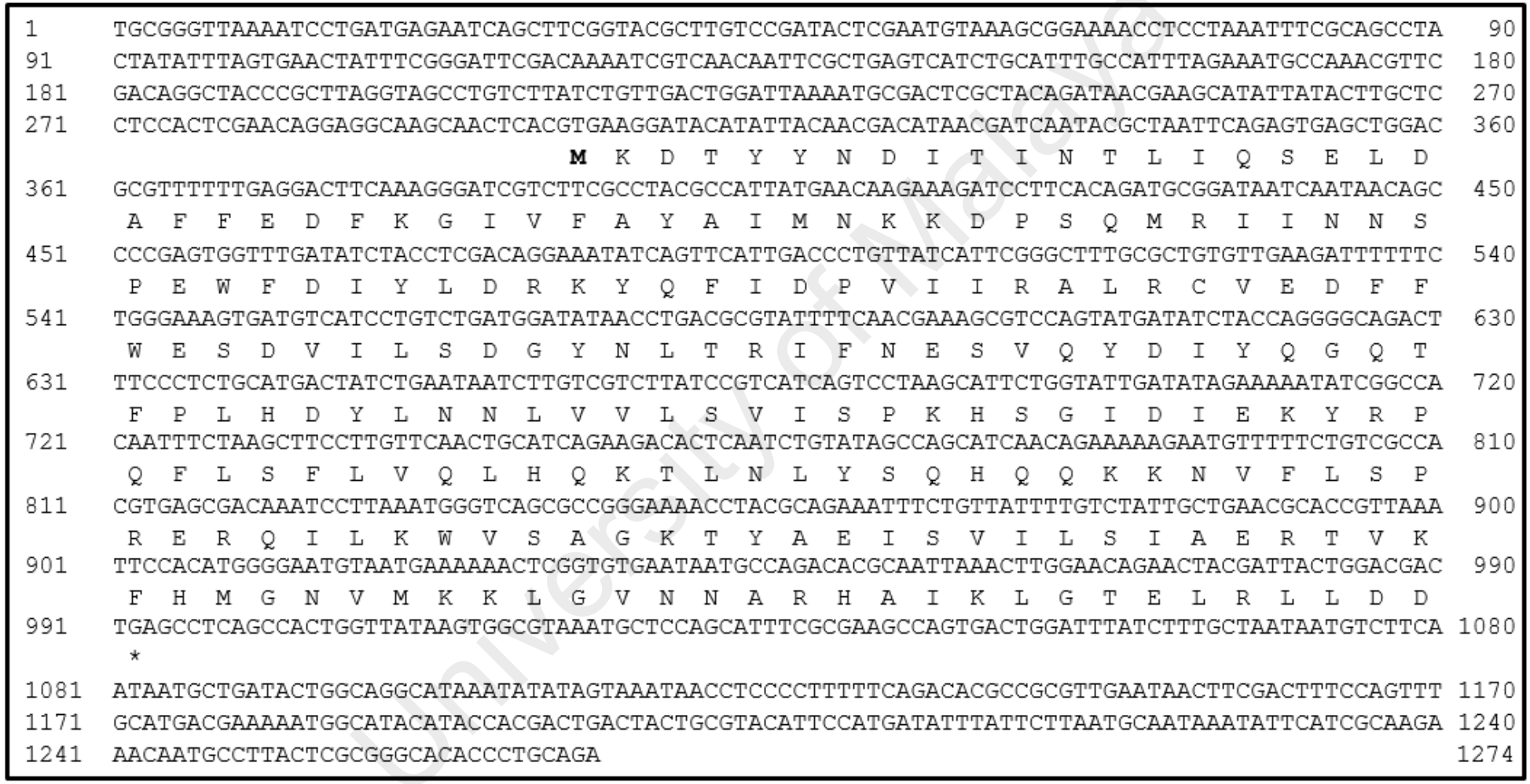

Figure 4.27: The nucleotide sequence of *easR* gene of *E. asburiae* L1 and its flanking sequences. Single letters which code for deduced amino acid sequence are shown below the nucleotide sequence. The stop codon (TGA) is marked by an asterisk. The translational start site (M) is in bold.

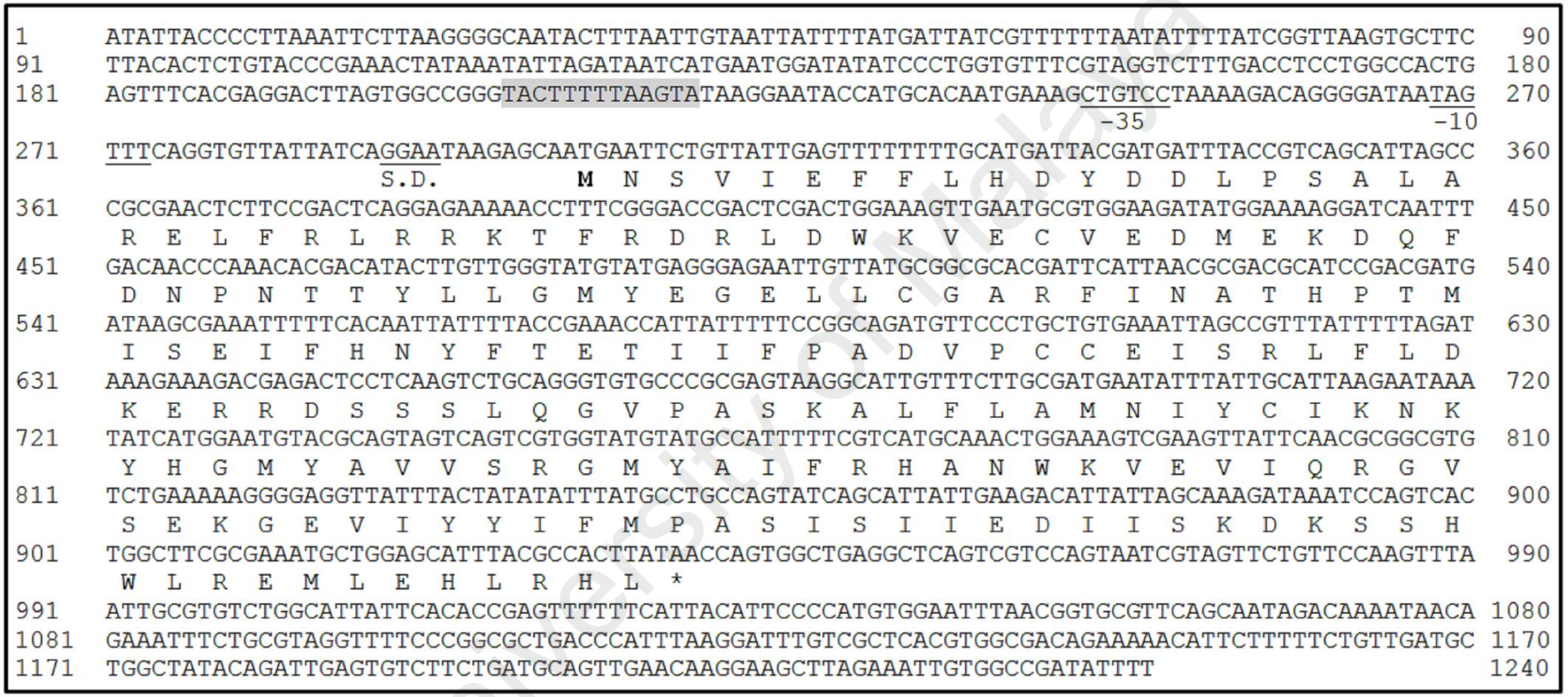

Figure 4.28: The nucleotide sequence of *easI* gene of *E. asburiae* L1 and its flanking sequences. Single letters which code for deduced amino acid sequence are shown below the nucleotide sequence. The stop codon (TAA) is marked by an asterisk. The translational start site (M) is in bold and S.D. denotes the putative Shine-Dalgarno site. The proposed core promoter elements, -10 and -35 boxes, are underlined. A putative *lux* box is highlighted in grey.

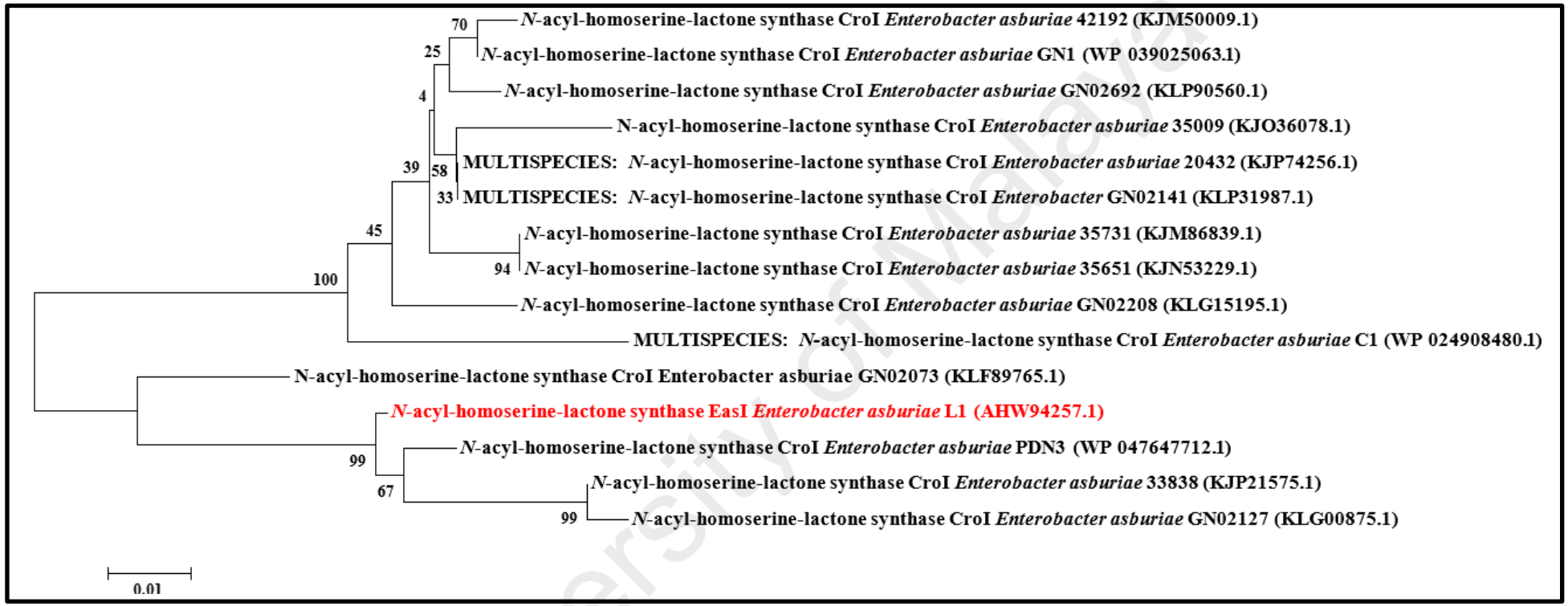

Figure 4.29: Phylogenetic tree showing the evolutionary distances between the putative AHL synthase of *E. asburiae* L1 with the other *E. asburiae* strains, generated using Neighbour-Joining algorithm. The tree is drawn to scale, with branch lengths in the same units as those of the evolutionary distances used to infer the phylogenetic tree. The horizontal bar at the bottom represents evolutionary distance as 0.01 change per nucleotide position. The numbers at the nodes indicate the bootstrap values as percentage of 1,000 replications.

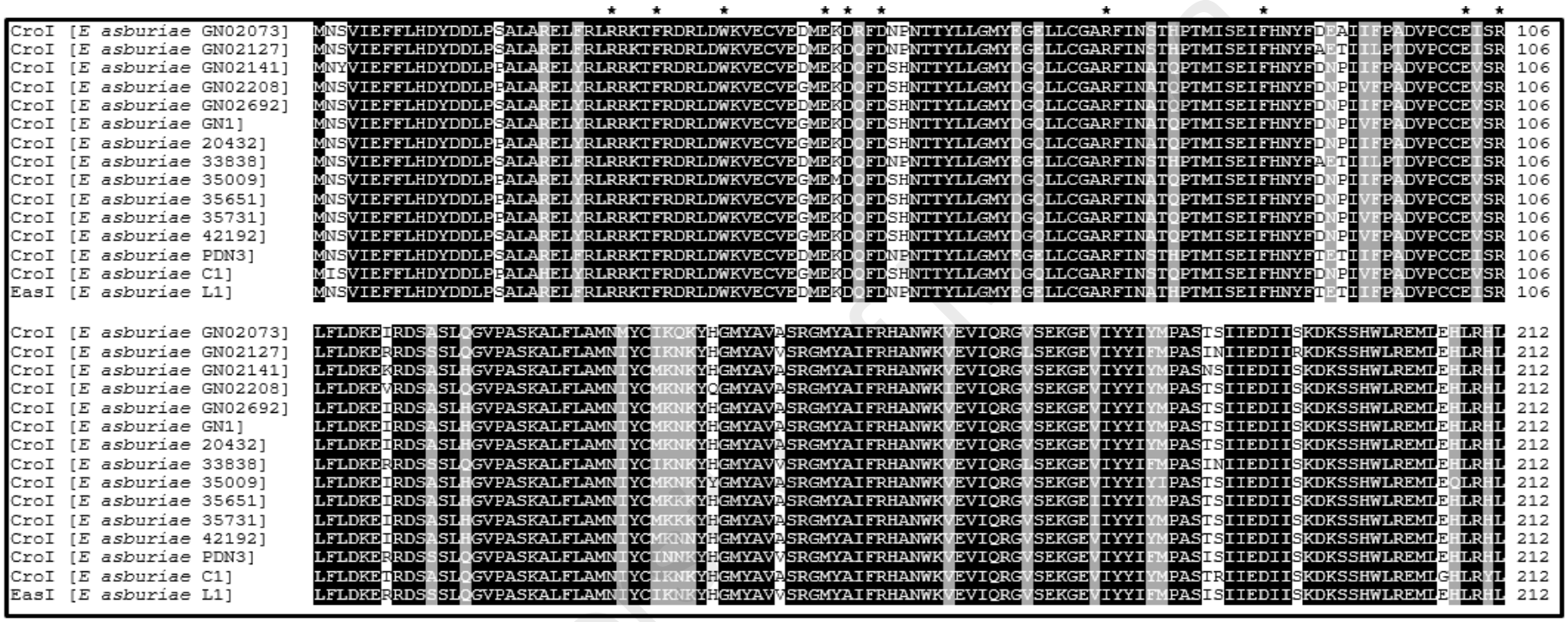

Figure 4.30: CLUSTAL O (1.2.0) multiple sequence alignment of *N*-acyl homoserine lactone autoinducer protein sequences of *E. asburiae* L1 with protein sequences from other *E. asburiae* strains. Sequences were derived from NCBI database (http://www.ncbi.nlm. nih.gov) and were aligned using CLUSTAL OMEGA software (http://www.ebi.ac.uk). The 10 invariant amino acids characteristics of LuxI homologues are denoted with asterisks. Residues that are identical among the sequences are given a black background while those that are highly similar among the sequences are given a grey background. GenBank accession numbers in parentheses: CroI *E. asburiae* GN02073 (KLF89765.1), CroI *E. asburiae* GN02127 (KLG00875.1), CroI *E. asburiae* GN02141 (KLP31987.1), CroI *E. asburiae* GN02208 (KLG15195.1), CroI *E. asburiae* GN02692 (KLP90560.1), CroI *E. asburiae* GN1 (WP_039025063.1), CroI *E. asburiae* 20432 (KJP74256.1), CroI *E. asburiae* 33838(KJP21575.1), CroI *E. asburiae* 35009 (KJO36078.1), CroI *E. asburiae* 35651 (KJN53229.1), CroI *E. asburiae* 35731 (KJM86839.1), CroI *E. asburiae* 42192 (KJM50009.1), CroI *E. asburiae* PDN3 (WP_047647712.1), CroI *E. asburiae* C1 (WP_024908480.1).

4.11 Functional Studies of QS Genes

4.11.1 Functional Studies of EasI

4.11.1.1 Purification of EasI Protein and SDS-Page Analysis

The *easI* gene which encodes the putative AHL synthase from *E. asburiae* L1 has been cloned for functional study. The *easI* gene was amplified by PCR (Figure 4.31A). This 639 bp ORF encodes an AHL synthase with a predicted molecular mass (M_r) of 24.9 kDa from ExPASy server (Wilkins et al., 1999). In addition, the theoretical isoelectric point (pI) of the recombinant protein is predicted to be 6.07. The amplicon was then cloned into pET-28a(+) overexpression vector, producing pET28a-*easI*, with a 6× His-tag driven by a T7 promoter before being transformed into *E. coli* BL21 (DE3)pLysS cells. The recombinant *easI* gene was overexpressed upon 1.0 mM IPTG induction which has been tested to be the optimum concentration for induction. The His-tagged recombinant protein was purified from cell lysate using Ni-NTA metal-affinity chromatography matrices. The estimated size of the purified protein was in agreement with the SDS-PAGE profile (Figure 4.31B).

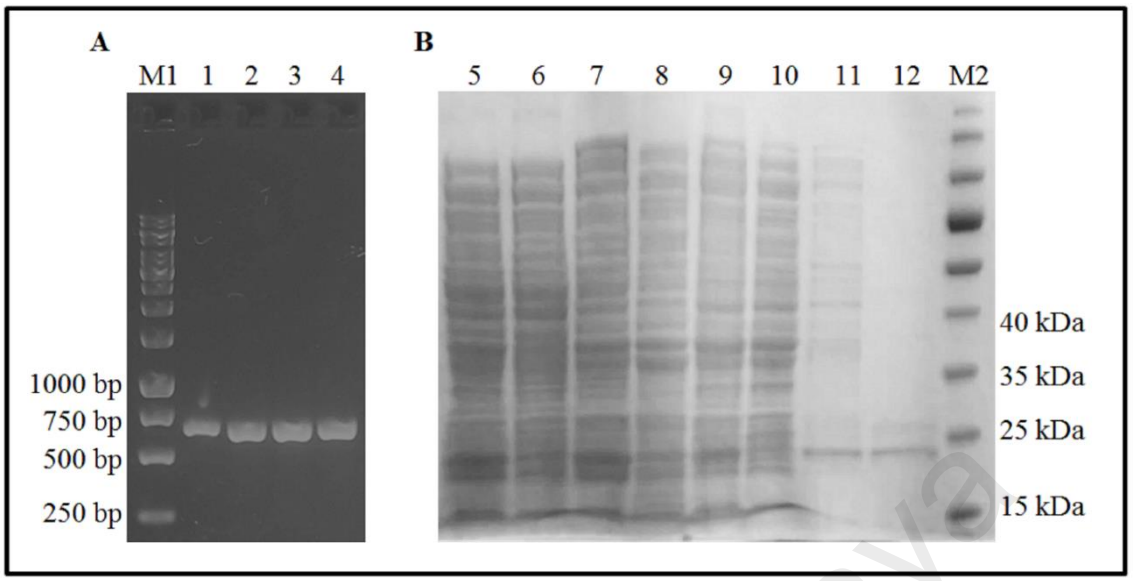

Figure 4.31: Analysis of *easI* gene and protein. (A) Fluorescent stained agarose gel containing *easI* gene amplified by PCR. Lanes 1 to 4 showed the amplified 639 bp amplicon. 10 µl of PCR products were loaded into each lane and electrophoresis was performed at 75 V for 65 min. (B) SDS-PAGE analysis of the purified recombinant EasI protein. Lane 5, cell lysates of non-induced *E. coli* BL21(DE3)pLysS; Lane 6, cell lysates of non-induced *E. coli* BL21 (DE3)pLysS harbouring pET-28a(+); Lane 7, cell lysates of induced *E. coli* BL21 (DE3)pLysS harbouring pET-28a(+); Lane 8, cell lysates of non-induced *E. coli* BL21 (DE3)pLysS harbouring pET-28a(+)-*easI*; Lane 9, cell lysates of induced *E. coli* BL21 (DE3)pLysS harbouring pET-28a(+)-*easI*, Lane 10, flow-through fraction of purification step; Lane 11, wash fraction of purification step; Lane 12, eluted fraction containing recombinant EasI protein; Lane M1, 1 kb DNA marker (Fermentas, Thermo Fisher Scientific, USA); Lane M2, molecular weight markers (Fermentas, Thermo Scientific, USA) with mass of each marker protein in kDa as indicated. The same amount of protein was loaded into each lane and subjected to electrophoresis at 150 V.

4.11.1.2 AHL Detection and Identification

The induced *E. coli* BL21 (DE3)pLysS cells harbouring pET-28a(+)-*easI* was screened using cross streaking with biosensor *C. violaceum* CV026 which produces purple pigmentation in the presence of short chain AHLs similar to the parental strain (Figure 4.32). In order to identify and confirm the AHLs produced, the extracted AHLs from the spent culture supernatant of the IPTG-induced *E. coli* BL21 (DE3)pLysS harbouring pET-28a(+)-*easI* was analysed using LC-MS/MS system. The MS analysis results of the spent culture supernatant show the presence of C4-HSL (*m/z* 172.0000) and C6-HSL (*m/z* 200.0000) (Figure 4.33). For each detected AHL, a fragment ion at *m/z* 102 was observed, which corresponds to the lactone ring moiety. The MS of the extracted AHLs were indistinguishable to the corresponding synthetic compounds at their respective retention times. No AHL was found in the *E. coli* BL21 (DE3)pLysS harbouring pET-28a(+) alone. These findings are consistent with our previous study that showed the same AHL profile (Lau, Sulaiman, Chen, Yin, & Chan, 2013).

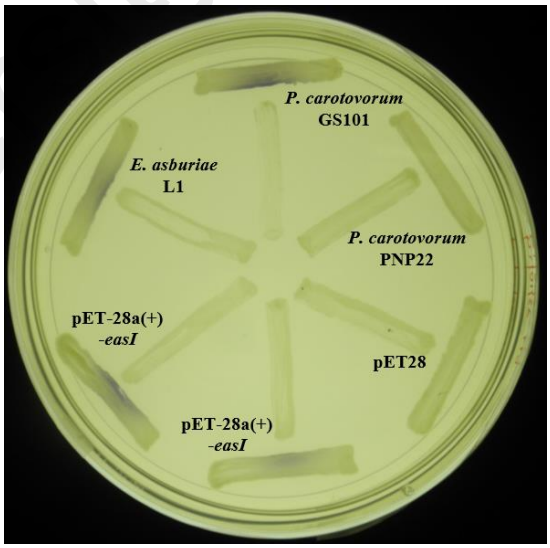

Figure 4.32: Screening for purple violacein production using *C. violaceum* CV026 cross streak. *P. carotovorum* GS101 and *E. asburiae* L1 were used as positive controls while *P. carotovorum* PNP22 and *E. coli* BL21 (DE3)pLysS harbouring pET-28a(+) were used as negative controls. Observation of purple pigment formation on the biosensor streak line indicates the production of exogenous short chain AHL molecules by the *E. coli* BL21 (λDE3)pLysS harbouring pET-28a(+)-*easI*. This indicated the *easI* gene of L1 was successfully cloned into and expressed by *E. coli* BL21 (λDE3)pLysS.

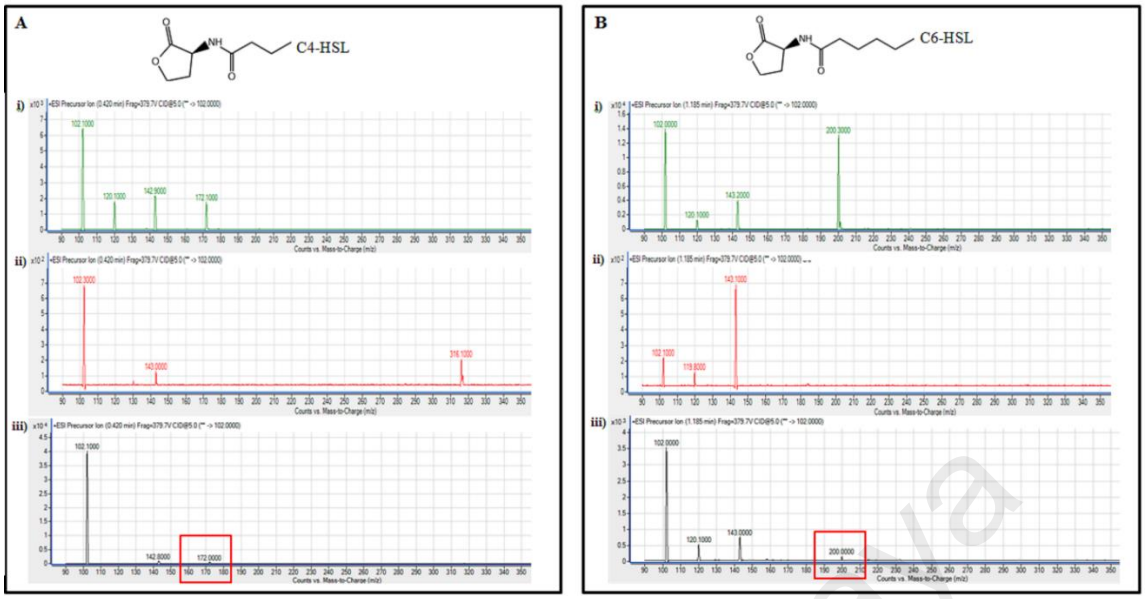

Figure 4.33: Mass spectra analyses of the extract of spent culture supernatant from IPTG-induced *E. coli* BL21 (DE3)pLysS harbouring pET-28a(+)-*easI*. By comparing with the corresponding synthetic AHL standards, the mass spectra demonstrated the presence of (A) C4-HSL (*m/z* 172.0000) and (B) C6-HSL (*m/z* 200.0000). The retention time for C4-HSL and C6-HSL are 0.420 min and 1.185 min, respectively. (i) Mass spectra of synthetic AHL standards; (ii) Mass spectra of *E. coli* BL21 (DE3)pLysS harbouring pET-28a(+) alone (control); (iii) mass spectra of induced *E. coli* BL21 (DE3)pLysS harbouring pET-28a(+)-*easI*.

4.11.2 Functional Studies of EasR

4.11.2.1 Determination of *easR*-regulated Promoter Activities Using β-galactosidase Assay

In order to test the functionality of the *easR* in respond to any AHL signals to regulate the promoters, β-galactosidase assay were carried out in *E. coli* TOP10 harbouring the pMULTIAHLPROM plasmid carrying a synthetic tandem promoter of eight different *luxI* gene promoters transcriptionally fused to a promoterless *lacZ* which respond to several different LuxR family proteins (Steindler et al., 2008). The pLNBAD empty vector as well as pLNBAD-*easR* recombinant was introduced and *lacZ* activities was determined by adding different exogenous AHLs. β-galactosidase activities were expressed in Miller units and indicated as mean values of nine separate independent experiments for each clone and the mean values were calculated. The levels of β-galactosidase expressed from these constructs were not equal. β-galactosidase activities of pLNBAD-*easR* plasmid was significantly higher in the presence of 100 µM exogenous AHLs (C4-HSL, C6-HSL, C10-HSL and C12-HSL). Among the four exogenous AHLs added, pLNBAD-*easR* construct had the highest β-galactosidase levels in the presence of C4-HSL. In addition, β-galactosidase activities of pLNBAD-*easR* plasmid was also significantly higher when compared with pLNBAD empty vector control in the presence or absence of AHLs. The β-galactosidase assay regulated by the *easR* promoter under different conditions is shown in Figure 4.34 and the Miller unit of each recombinant clones is stated in Table 4.11.

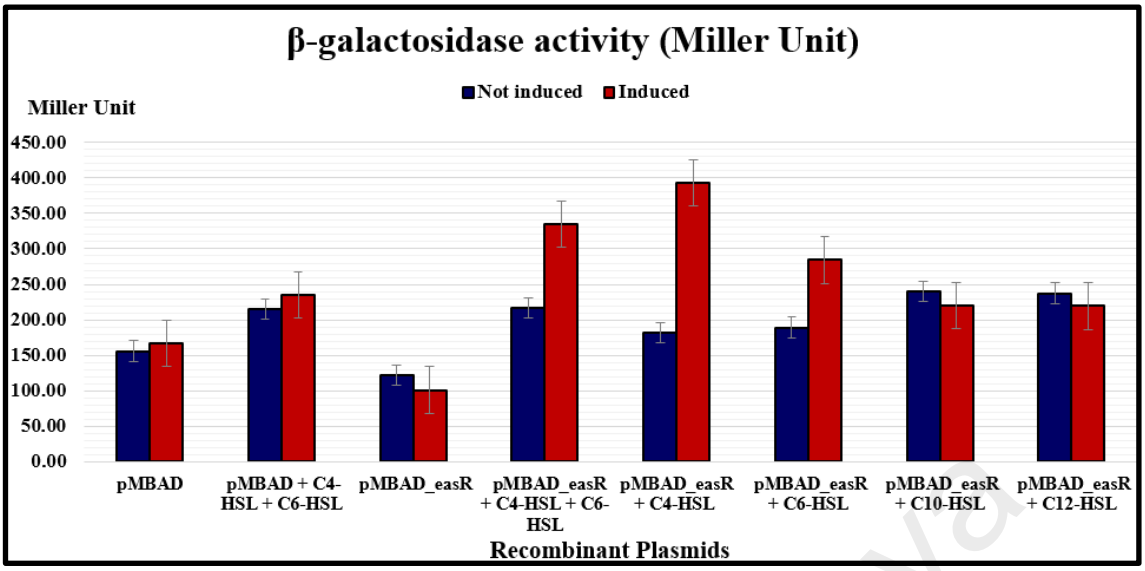

Figure 4.34: Histogram reporting *easR*-regulated promoter β-galactosidase activity of *E. coli* TOP10 harbouring pMULTIAHLPROM in the presence of either pLNBAD (pMBAD) or pLNBAD-*easR* (pMBAD-*easR*) plasmids in the presence or absence of 100 µM different AHLs (C4-HSL, C6-HSL, C10-HSL and C12-HSL). All measures were expressed in Miller units and indicated as mean values of nine separate independent experiments. Bars: Standard errors of the mean.

Table 4.11: β-galactosidase activity (Miller Unit) of pMBAD and pMBAD-*easR* under different conditions

Recombinant clones	Miller Unit
pMULTIAHLPROM- pLNBAD (pMBAD)	
Not induced	155.95
Induced	167.15
Not induced + 100 µM C4-HSL + 100 µM C6-HSL	214.72
Induced + 100 µM C4-HSL + 100 µM C6-HSL	235.12
pMULTIAHLPROM-pLNBAD-*easR* (pMBAD-*easR*)	
Not induced	122.24
Induced	100.93
Not induced + 100 µM C4-HSL + 100 µM C6-HSL	217.03
Induced + 100 µM C4-HSL + 100 µM C6-HSL	335.50
Not induced + 100 µM C4-HSL	181.52
Induced + 100 µM C4-HSL	393.36
Not induced + 100 µM C6-HSL	189.18
Induced + 100 µM C6-HSL	284.27
Not induced + 100 µM C10-HSL	240.34
Induced + 100 µM C10-HSL	220.46
Not induced + 100 µM C12-HSL	237.36
Induced + 100 µM C12-HSL	219.48

4.12 Construction of *E. asburiae* L1-Δ*easI*::Kan Mutant

4.12.1 Recombineering Mutagenesis in *E. asburiae* L1

To investigate the QS-mediated gene expression in *E. asburiae* L1, the *easI* gene of *E. asburiae* L1 was knocked-out by using recombineering technique. The linear dsDNA substrate for recombineering that containing the desired selectable marker flanked by 50 bases of homology to *E. asburiae* L1-*easI* target site was amplified. As shown in Figure 4.28, the kanamycin selectable marker from *E. coli* TKC was successfully amplified using the primers design as stated in Section 3.1.8. Following that, the λ Red recombination genes from pSIM 7 plasmid was introduced into *E. asburiae* L1 genome and sequence verification of the recombinant plasmid was performed by automated Sanger DNA sequencing (Figure 4.35). After the induction and transformation steps, the drug resistant recombinant clones were first screened with kanamycin antibiotic and then analysed with PCR to examine whether the insertion has gone to the proper location or not, followed by verification by automated Sanger DNA sequencing (Figure 4.36).

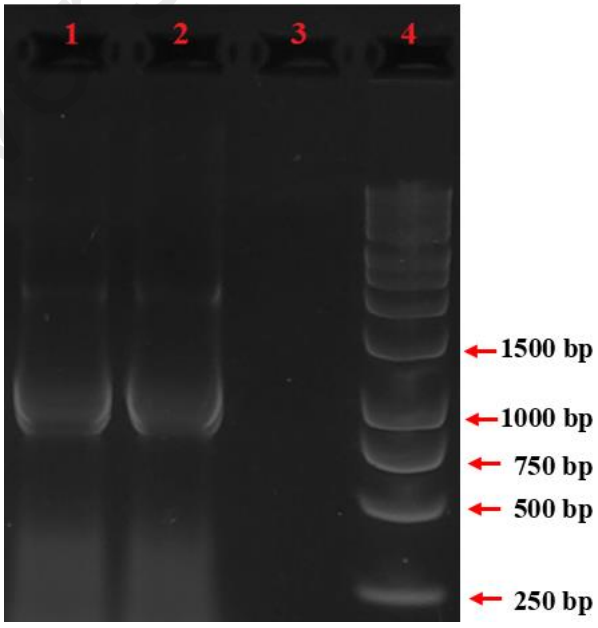

Figure 4.35: Agarose gel electrophoresis of the kanamycin resistance (Km^R) cassette amplified from *E. coli* TKC. Lane 1 and 2, kanamycin resistance cassette (~950bp); Lane 3, negative control; Lane 4, 1 kb DNA marker.

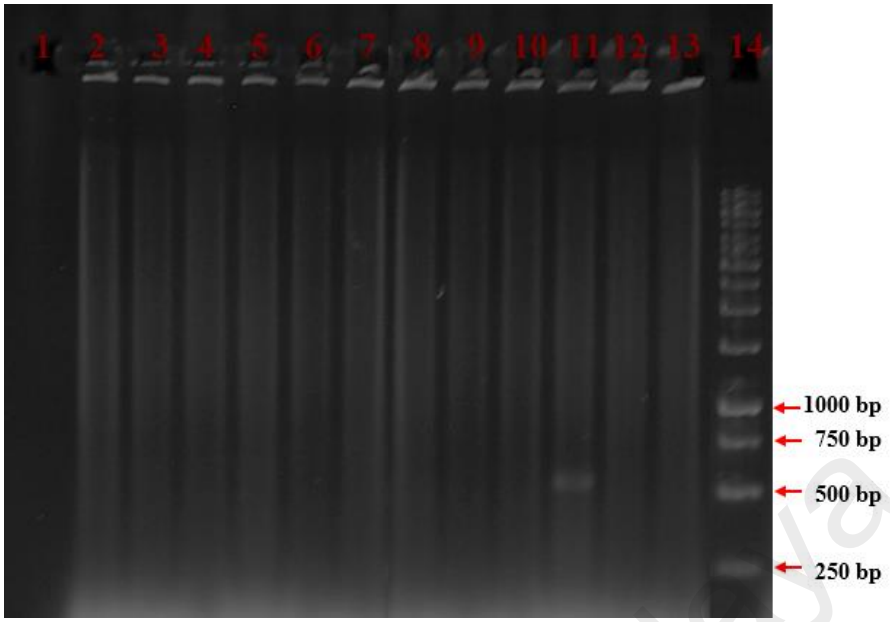

Figure 4.36: Agarose gel electrophoresis of colonies PCR that contain designed λ red recombination gene from pSIM7 plasmid. Lane 1; negative control; Lane 2 to Lane 13, clones of λ red recombination gene from pSIM7. One out of 12 clones (Lane 11) showed that λ red recombination gene from pSIM7 was transformed into *E. asburiae* L1 (~600bp); Lane 14, 1 kb DNA marker.

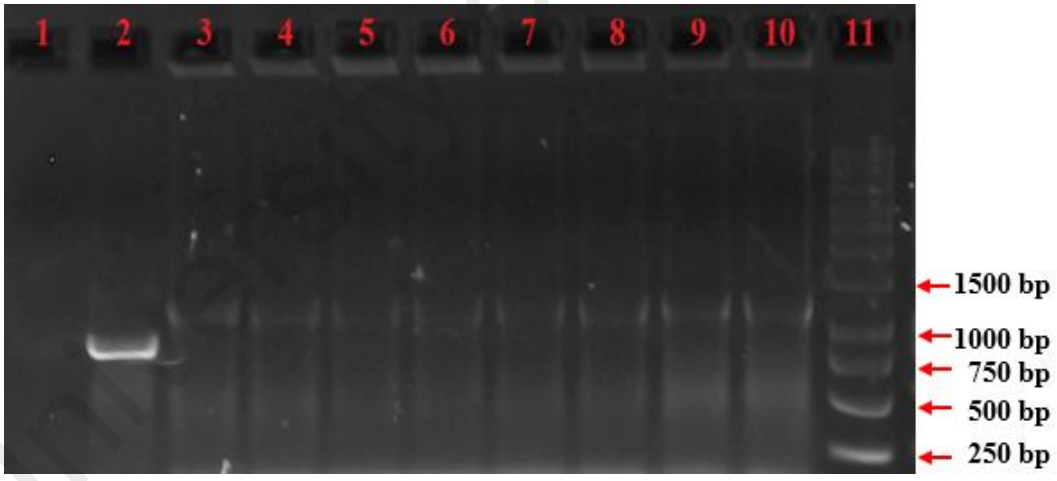

(A)

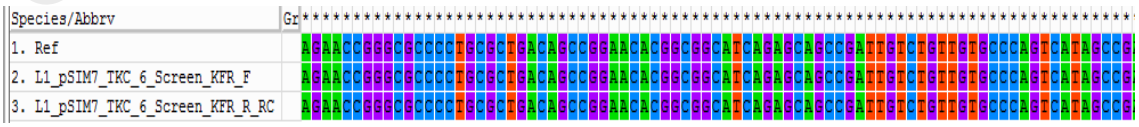

(B)

Figure 4.37: Agarose gel electrophoresis of the recombinant clones and sequence verification by automated Sanger DNA sequencing. (A) Lane 1, negative control; Lane 2, wildtype *E. asburiae* L1 *easI* (~939bp); Lane 3 to Lane 10, recombinant clones *E. asburiae* L1-Δ*easI*::Kan mutant (~1250bp); Lane 11, 1 kb DNA marker. (B) The asterisks showed that the sequence of the recombinant clones was aligned with the reference sequence, confirmed the desired mutant was successfully constructed.

4.12.2 Identification and Confirmation of *E. asburiae* L1-Δ*easI*::Kan by Biosensor *C. violaceum* CV026 and Triple Quadrupole LC-MS/MS

The constructed *E. asburiae* L1-Δ*easI*::Kan mutant cells was screened using cross streaking with biosensor *C. violaceum* CV026 to ensure the *easI* gene has been successfully knocked-out. No purple pigmentation was observed on the biosensor line streaked with *E. asburiae* L1-Δ*easI*::Kan mutant cells (Figure 4.38). In addition to this, the extracted AHLs from the spent culture supernatant of the *E. asburiae* L1-Δ*easI*::Kan mutant cells was analysed using LC-MS/MS system. The MS analysis results of the spent culture supernatant showed no detectable C4-HSL (*m/z* 172.0000) and C6-HSL (*m/z* 200.0000) under the present experimental conditions (Figure 4.39). This unequivocally confirmed that *E. asburiae* L1-Δ*easI*::Kan mutant was successfully constructed.

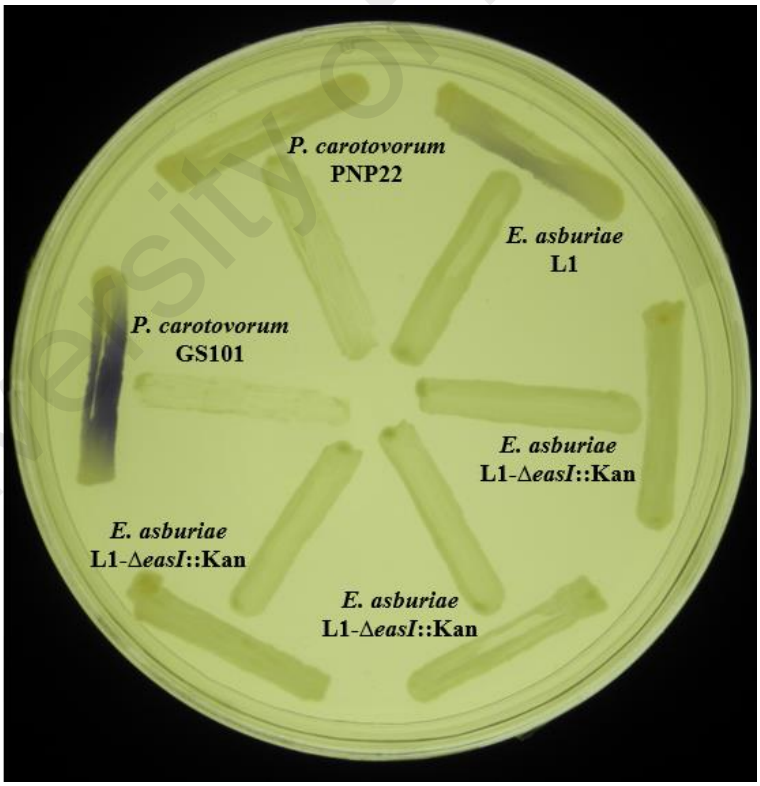

Figure 4.38: Screening for violacein production using *C. violaceum* CV026 cross streak. *P. carotovorum* GS101 and wildtype *E. asburiae* L1 were used as positive controls while *P. carotovorum* PNP22 was used as negative control. Negative purple pigmentation was observed for all *E. asburiae* L1-Δ*easI*::Kan mutant recombinant clones.

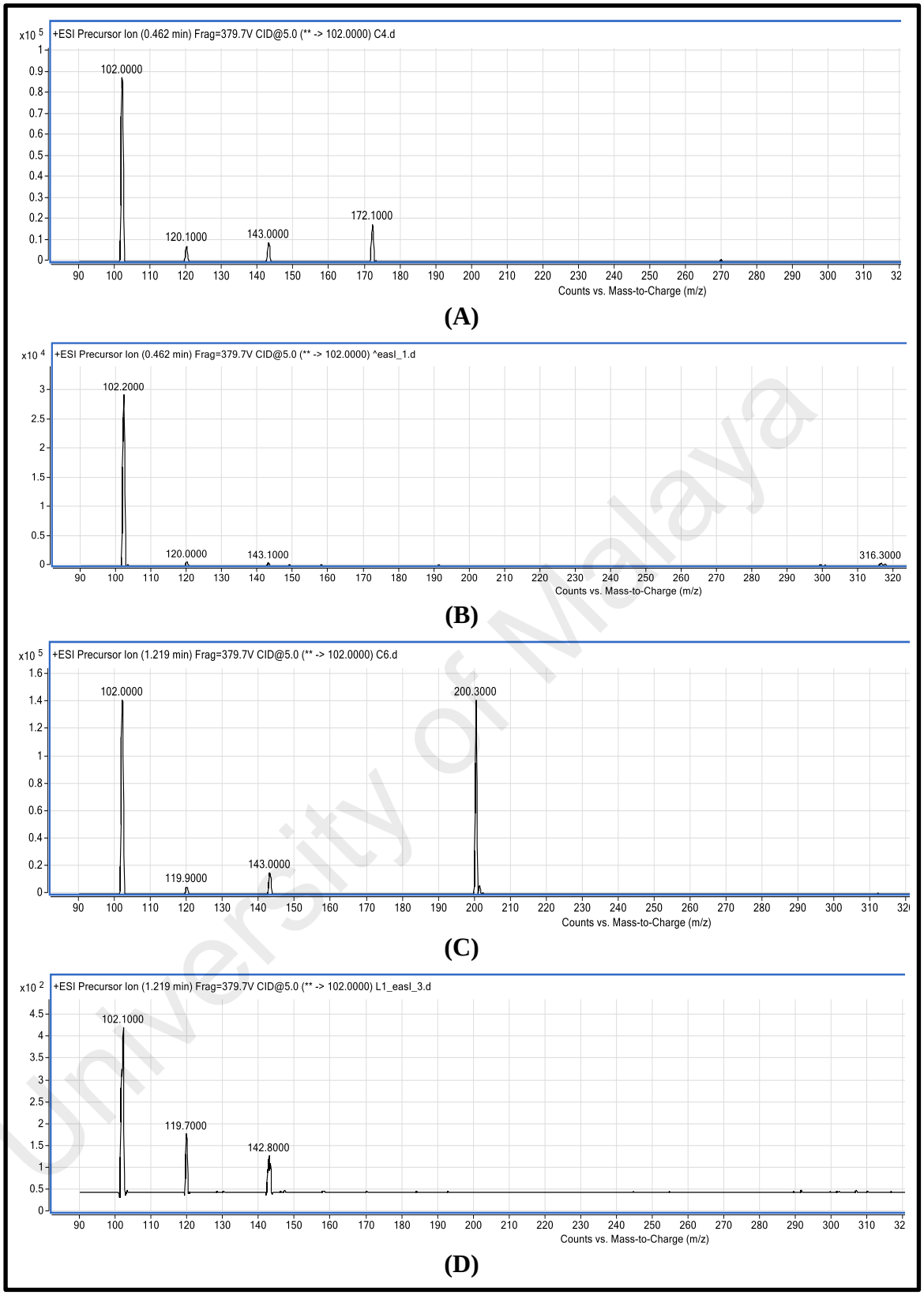

Figure 4.39: Mass spectra analyses of the extract of spent culture supernatant from *E. asburiae* L1-Δ*easI*::Kan mutant recombinant clones. By comparing with the corresponding synthetic AHL standards, the mass spectra demonstrated the absence of (B) C4-HSL (*m/z* 172.0000) and (D) C6-HSL (*m/z* 200.0000). The retention time for C4-HSL and C6-HSL are 0.462 min and 1.219 min, respectively. (A) Mass spectra of synthetic AHL standards, C4-HSL; (C) Mass spectra of synthetic AHL standards, C6-HSL.

4.13 Whole Transcriptomics Studies

4.13.1 Determination of *E. asburiae* L1 Optimal Optical Density (OD) for RNA Extraction

In order to determine the cellular response of *E. asburiae* L1 after the knocking out of QS *easI* gene, RNA-seq was applied to study the whole transcriptome changes in this bacterium. As QS is a cell density dependent mechanism, the growth curve of *E. asburiae* L1 wildtype and L1-Δ*easI*::Kan mutant strains was first determined to investigate the optimal OD for RNA extraction. The growth analysis of *E. asburiae* L1 and L1-Δ*easI*::Kan (Appendix J) showed that these strains entered mid-log phase at OD 1.5 and reached stationary phase at OD 2.5. By this, few of the ODs (1.5, 2.0, 2.5 and 3.0) in between the log and stationary phase were chosen for further analysis.

In order to ensure the QS mechanism has been activated at the desired OD for RNA extraction, the spent culture supernatant of *E. asburiae* L1 was analysed using LC-MS/MS system to detect the presence of AHLs. The MS analysis (Appendix K) showed that the AHLs was detected starting at OD 2.0. Therefore, OD 1.5 was eliminated. Following that, qPCR analysis was performed and found that OD 2.0 was the optimal OD for RNA extraction.

4.13.2 RNA-seq

RNA-seq data of *E. asburiae* L1 wildtype and L1-Δ*easI*::Kan mutant were trimmed with CLC Bio version 7 according to the manufacturer's protocol. The trimmed data were then analysed with Partek software. *E. asburiae* L1 wildtype genome was annotated using Prokka software to generate gene-finding format (gff). This file was used as a reference for genes mapping in Partek software. Based on the RNA-seq data analysis, a total of 240 genes were significantly differentially expressed after the QS *easI* gene was knocked-out

from *E. asburiae* L1 genome. Of the 240 differentially expressed genes identified ($p \leq 0.01$ fixed as the cut-off values), 128 genes and 112 genes were downregulated and upregulated, respectively in L1-Δ*easI*::Kan strain. Table 4.12 and 4.13 lists the genes that have been downregulated and upregulated with fold change ≥ 2.0 in *easI* null mutant.

Table 4.12: Genes that were significantly downregulated in L1-Δ*easI*::Kan mutant

Gene name	Product	p-value (Attribute)	FoldChange (MT vs. WT)
easI	Acyl-homoserine-lactone synthase	0.000149188	-1812.86
bsmA	Biofilm stress and motility protein	2.20E-05	-7.37356
yghA	Putative oxidoreductase YghA	3.41E-06	-5.96463
	Hypothetical protein	9.48E-05	-5.29291
lsrA	Autoinducer 2 import ATP-binding protein LsrA	6.58E-08	-4.78171
lsrR	Transcriptional regulator LsrR	0.000436882	-4.67020
ychH	Putative membrane protein YchH	7.06E-05	-4.51846
	Hypothetical protein	0.000174352	-4.49439
lsrD	Autoinducer 2 import system permease protein LsrD	0.00257074	-4.10176
osmB	Osmotically-inducible lipoprotein B precursor	0.000154684	-4.07690
lsrB	Autoinducer 2-binding protein LsrB precursor	0.000544645	-4.00351
	Putative cytoplasmic protein	0.00670757	-3.96544
	Hypothetical protein	2.42E-05	-3.96095
	Bacteriophage replication gene A protein (GPA)	0.416048	-3.85655
	Stress-induced bacterial acidophilic repeat motif	0.000884438	-3.79777
	Small integral membrane protein	0.00067389	-3.78388
potF1	Putrescine-binding periplasmic protein precursor	0.00010611	-3.65571
	Putative secreted protein	4.06E-05	-3.62286

Table 4.12, continued

Gene name	Product	p-value (Attribute)	FoldChange (MT vs. WT)
	Probable secreted protein	5.62E-06	-3.61262
uspB	Universal stress protein B	5.29E-05	-3.60942
	Hypothetical protein	2.11E-05	-3.56169
	HTH XRE-family like protein	2.34E-05	-3.48701
clpS	ATP-dependent Clp protease adapter protein ClpS	2.89E-05	-3.47774
	Hypothetical protein	0.000231181	-3.45740
	Putative biofilm stress and motility protein	0.00048915	-3.39984
	Hypothetical protein	1.15E-05	-3.36829
	Hypothetical protein	0.000134961	-3.33982
dppA4	Dipeptide-binding protein	6.19E-05	-3.24597
lsrK	Autoinducer 2 kinase LsrK	0.000227418	-3.12982
	Transglycosylase associated protein	0.00123476	-3.12005
uxaC	Uronate isomerase	2.17E-05	-3.11208
lamB1	Maltose-inducible porin	4.02E-05	-3.03245
bglA4	Aryl-phospho-beta-D-glucosidase BglA	7.65E-05	-3.02893
lsrF	Putative aldolase LsrF	0.0045203	-2.98404
uspF	Universal stress protein	4.48E-05	-2.91978
sra	30S ribosomal protein S22	0.00466006	-2.91075
ecnB	Entericidin B membrane lipoprotein	0.000154575	-2.89192
bssS	Biofilm regulator BssS	1.53E-05	-2.88861
	Hypothetical protein	4.86E-05	-2.78433
	SpoVR family protein	0.000787357	-2.76593
	CsbD-like protein	0.000936455	-2.75116
ecpD	Putative chaperone protein EcpD	0.000544603	-2.74589
	Epimerase family protein	6.76E-05	-2.74109
	Putative small protein	0.00428633	-2.71847
	Putative Fe-S protein	0.0206133	-2.71341
gbpR2	Galactose-binding protein regulator	3.73E-05	-2.70368

Table 4.12, continued

Gene name	Product	p-value (Attribute)	FoldChange (MT vs. WT)
ydcV1	Inner membrane ABC transporter permease protein YdcV	0.000328865	-2.69882
cimH1	Citrate/malate-proton symporter	1.06E-05	-2.69813
	Hypothetical protein	0.00107751	-2.69493
yhbH	Stress response UPF0229 protein YhbH;product=hypothetical protein	0.000224583	-2.65053
sodC	Superoxide dismutase [Cu-Zn] precursor	0.00124975	-2.64364
bglA2	6-phospho-beta-glucosidase BglA	0.00838437	-2.62900
	PrkA family serine protein kinase	5.19E-05	-2.62478
yohC	Inner membrane protein YohC	7.36E-05	-2.61376
fadI	3-ketoacyl-CoA thiolase	0.000170524	-2.59236
licC2	PTS system lichenan-specific EIIC component	0.0001126	-2.59028
	Hypothetical protein	0.000112471	-2.56455
rsmH	Ribosomal RNA small subunit methyltransferase H	0.000236464	-2.51408
cdhR6	Carnitine catabolism transcriptional activator	4.73E-05	-2.50719
uspC	Universal stress protein C	0.00109952	-2.49280
bssR	Biofilm formation regulatory protein BssR	0.00195232	-2.46863
lsrC	Autoinducer 2 import system permease protein LsrC	0.000849721	-2.44582
hpdA	4-hydroxyphenylacetate decarboxylase activating enzyme	0.00362137	-2.43964
yjgA	x96 protein	0.000216699	-2.4277
	Putative exported protein	0.0020417	-2.39519
	Putative cytoplasmic protein	0.00104578	-2.38409
hydN2	Electron transport protein HydN	0.00517922	-2.38121
	hemolysin	0.000148527	-2.37946

Table 4.12, continued

Gene name	Product	p-value (Attribute)	FoldChange (MT vs. WT)
gmuB1	Oligo-beta-mannoside-specific phosphotransferase enzyme IIB component	0.0079791	-2.37564
	Hypothetical protein	0.000998203	-2.36373
	Putative transcriptional regulator	0.000224758	-2.36227
	Integration host factor subunit beta	0.00327419	-2.34673
aidB	Putative acyl-CoA dehydrogenase AidB	0.000344706	-2.33638
sfsA	Sugar fermentation stimulation protein A	0.000280358	-2.33329
ygaU	LysM domain/BON superfamily protein	0.000849238	-2.32927
	Barstar (barnase inhibitor)	0.00103687	-2.29613
ftsQ	Cell division protein FtsQ	0.0001027	-2.27510
	Fructosamine-3-kinase	1.73E-05	-2.26012
potA2	Spermidine/putrescine import ATP-binding protein PotA	0.0268306	-2.25198
lip-1	Lipase 1 precursor	0.00753076	-2.23570
	Putative dehydrogenase	0.00086048	-2.23399
aspT2	Aspartate/alanine antiporter	3.93E-05	-2.22592
iscA2	Iron-sulfur cluster assembly protein	0.00242662	-2.21581
benM2	Ben and cat operon transcriptional regulator	0.00106618	-2.20486
ftnA2	Ferritin-1	0.000185694	-2.18541
osmC	Peroxiredoxin OsmC	9.23E-05	-2.18236
fdhF2	Formate dehydrogenase H	0.00333826	-2.17890
cstA	Carbon starvation protein	5.67E-05	-2.17530
rppH	RNA pyrophosphohydrolase	0.00135365	-2.16921
malE	Maltodextrin-binding protein	0.00146734	-2.16707
	Hypothetical protein	0.000208049	-2.16184

Table 4.12, continued

Gene name	Product	p-value (Attribute)	FoldChange (MT vs. WT)
fadJ	Fatty acid oxidation complex subunit alpha	3.66E-05	-2.15569
queA	S-adenosylmethionine:tRNA ribosyltransferase-isomerase	0.000803013	-2.14919
ygdR2	Putative lipoprotein YgdR precursor	0.000580406	-2.14872
	Type I secretion C-terminal target domain (VC_A0849 subclass)	0.00453116	-2.14641
yphA	Inner membrane protein YphA	2.26E-05	-2.14130
lsrG	Autoinducer 2-degrading protein LsrG	0.0241328	-2.13824
cpdA	3',5'-cyclic adenosine monophosphate phosphodiesterase CpdA	0.000467156	-2.13676
grcA	Autonomous glycyl radical cofactor	9.29E-06	-2.13585
clpA	ATP-dependent Clp protease ATP-binding subunit ClpA	0.000676961	-2.13465
csiE	Stationary phase inducible protein CsiE	0.00071734	-2.12753
oppB	Oligopeptide transport system permease protein OppB	5.30E-05	-2.10847
	V8-like Glu-specific endopeptidase	0.0186203	-2.09410
	Hypothetical protein	0.000175988	-2.07293
	Hypothetical protein	0.000350293	-2.06946
bhsA3	Copper-induced outer membrane component	6.86E-05	-2.06794
bssA	Benzylsuccinate synthase alpha subunit	0.000103006	-2.06523
nupG	Nucleoside-transport system protein NupG	5.64E-05	-2.06082
katE	Catalase HPII	8.73E-05	-2.05532
ygiD	LigB family dioxygenase	7.85E-05	-2.05129

Table 4.12, continued

Gene name	Product	p-value (Attribute)	FoldChange (MT vs. WT)
ipdC	Indole-3-pyruvate decarboxylase	0.000215701	-2.05100
ada	Regulatory protein of adaptative response	0.00121754	-2.04648
ycgZ	Putative two-component-system connector protein YcgZ	0.0142395	-2.04222
	Hypothetical protein	0.01212	-2.04019
yebV	Putative cytoplasmic protein YebV	0.000692099	-2.03621
chaB	Cation transport regulator ChaB	0.0112726	-2.03001
pabA	Para-aminobenzoate synthase glutamine amidotransferase component II	0.00376001	-2.02832
hspQ	Heat shock protein HspQ	0.000562807	-2.02228
cytR2	HTH-type transcriptional repressor CytR	0.0085511	-2.02221
uxaA	Altronate dehydratase	0.000483911	-2.00912
aroM	AroM protein	0.00072411	-2.00653
sadH1	Putative oxidoreductase SadH	0.020397	-2.00531
cpo	Non-heme chloroperoxidase	0.000896061	-2.00198
	hypothetical protein	0.677847	-2.00012
citC	[Citrate [pro-3S]-lyase] ligase	0.00363694	-2.00000

Tabel 4.13: Genes that were significantly upregulated in L1-Δ*easI*::Kan mutant

Gene name	Product	p-value (Attribute)	FoldChange (MT vs. WT)
ribB	3,4-dihydroxy-2-butanone 4-phosphate synthase	0.000347585	5.8914
ompD	Outer membrane porin protein OmpD precursor	1.10E-05	5.13161
fimD	Uter membrane usher protein FimD precursor	0.00670853	3.93877
	26 kDa periplasmic immunogenic protein precursor	8.07E-07	3.83027
sdaB	L-serine dehydratase 2	1.58E-07	3.72022
fimC	Chaperone protein FimC precursor	0.014881	3.60766
rplW	50S ribosomal protein L23	0.00089889	3.44969
kdsA	2-dehydro-3-deoxyphosphooctonate aldolase	0.0025688	3.37743
prs	Ribose-phosphate pyrophosphokinase	0.000115503	3.37438
nanE	Putative N-acetylmannosamine-6-phosphate 2-epimerase	0.0846967	3.35852
rpmC	50S ribosomal protein L29	0.00411646	3.33477
glyA	Serine hydroxymethyltransferase	1.67E-05	3.31601
fimA	Type-1A pilin	0.0327859	3.04969
fimA	Type-1A pilin	0.011507	2.958
rplB	50S ribosomal protein L2	0.00128504	2.92948
yniC	2-deoxyglucose-6-phosphate phosphatase	0.000309431	2.88073
rplD	50S ribosomal protein L4	0.00117909	2.80033
rpsS	30S ribosomal protein S19	0.00121216	2.79005
tuf1	Elongation factor Tu 1	0.00103697	2.77757
flgB	Putative proximal rod protein	0.0018078	2.77031
rpsG	30S ribosomal protein S7	0.000294748	2.69434
ppa	Inorganic pyrophosphatase	0.000745475	2.66566
aspC	Aspartate aminotransferase	0.000127796	2.66179

Table 4.13, continued

Gene name	Product	p-value (Attribute)	FoldChange (MT vs. WT)
eco	Ecotin precursor	0.000153804	2.6393
rplV	50S ribosomal protein L22	0.00402201	2.61823
fbp	Fructose-1,6-bisphosphatase class 1	0.000147712	2.60143
azr	NADPH azoreductase	0.000112804	2.59966
elfG	Putative fimbrial-like protein ElfG precursor	0.000429344	2.58668
rplC	50S ribosomal protein L3	0.0022218	2.58194
ridA	Enamine/imine deaminase	0.000720744	2.57148
	Biofilm formation regulator HmsP	0.000152071	2.53504
	Hypothetical protein	2.58E-05	2.52752
fimA	Type-1A pilin	1.95E-05	2.50826
mipA	MltA-interacting protein precursor	0.000208136	2.50786
panD	Aspartate decarboxylase	0.000467374	2.50063
flgL	Hook-filament junction protein	8.91E-05	2.47916
sucD	Succinyl-CoA ligase [ADP-forming] subunit alpha	0.0063878	2.47345
pyrB	Aspartate carbamoyltransferase catalytic chain	0.000248519	2.43833
aer	Aerotaxis receptor	0.00451986	2.43685
guaA	GMP synthase [glutamine-hydrolyzing]	0.000613661	2.41581
rpsJ	30S ribosomal protein S10	0.00610198	2.41132
fliD	Flagellar cap protein	0.00105461	2.4013
rplR	50S ribosomal protein L18	0.00861856	2.39035
osmY	Osmotically-inducible protein Y precursor	2.87E-05	2.38134
pyrE	Orotate phosphoribosyltransferase	0.000146027	2.36181
minD	Cell division inhibitor	5.66E-06	2.34459
rpsF	30S ribosomal protein S6	0.0228246	2.33638
tig	Trigger factor	2.47E-05	2.33482

Table 4.13, continued

Gene name	Product	p-value (Attribute)	FoldChange (MT vs. WT)
tktA	Transketolase 1	8.77E-05	2.32206
rpsL	30S ribosomal protein S12	0.00342954	2.32088
panC	Pantothenate synthetase	0.000490092	2.3204
priB	Primosomal replication protein n	0.00729511	2.31904
rpsC	30S ribosomal protein S3	0.00477995	2.31591
gstA	Glutathione S-transferase GstA	0.000835141	2.306
ppsA	Phosphoenolpyruvate synthase	5.18E-05	2.2853
tyrS	Tyrosine--tRNA ligase	5.43E-05	2.28431
cysP	Thiosulfate-binding protein precursor	0.0373708	2.28209
	Hypothetical protein	0.00617315	2.27523
	Putative biofilm stress and motility protein A	0.00077172	2.26972
adk	Adenylate kinase	0.000996654	2.25099
ddc	L-2,4-diaminobutyrate decarboxylase	0.00755597	2.23887
glyS	Glycine--tRNA ligase beta subunit	3.61E-05	2.23049
dsbA	Thiol:disulfide interchange protein DsbA precursor	0.00145893	2.22454
	C4-dicarboxylate anaerobic carrier	0.0545626	2.22211
pyrI	Aspartate carbamoyltransferase regulatory chain	0.000108622	2.21956
rplP	50S ribosomal protein L16	0.00253998	2.21709
	Alpha-galactosidase	0.00175128	2.2069
rpsQ	30S ribosomal protein S17	0.000878289	2.20009
tdcE	Ketobutyrate formate-lyase	0.0195958	2.19945
cysK	Cysteine synthase A	0.0190759	2.19943
rplA	50S ribosomal protein L1	0.000241401	2.1955
dctA	Aerobic C4-dicarboxylate transport protein	0.00197307	2.18693
lysS	Lysine--tRNA ligase	9.04E-05	2.18415

Table 4.13, continued

Gene name	Product	p-value (Attribute)	FoldChange (MT vs. WT)
fusA	Elongation factor G	0.00152964	2.18341
sucC	Succinyl-CoA ligase [ADP-forming] subunit beta	0.0156926	2.17844
	6-N-hydroxylaminopurine resistance protein	0.00279472	2.17319
ftnA	Ferritin-1	0.00144892	2.16638
selD	Selenide, water dikinase	0.000969254	2.16526
rplI	50S ribosomal protein L9	0.0111099	2.16093
eno1	Enolase	1.98E-05	2.15513
rplX	50S ribosomal protein L24	0.00151914	2.15497
tisB	LexA-regulated protein TisB	0.316865	2.14257
cah	Carbonic anhydrase precursor	0.000139644	2.14182
argF	Ornithine carbamoyltransferase	0.0462385	2.11891
arcC12	Carbamate kinase 1	0.0368903	2.11004
flgD	Basal-body rod modification protein FlgD	0.00117221	2.09574
rcnB	Nickel/cobalt homeostasis protein RcnB precursor	0.000831335	2.08917
yabJ	Enamine/imine deaminase	0.00244521	2.08825
rplF	50S ribosomal protein L6	0.0121911	2.08753
	UDP-glucose 4-epimerase	0.000777371	2.0834
nuoC	NADH-quinone oxidoreductase subunit C/D	0.0049416	2.07517
recA	Recombinase	2.40E-05	2.07459
accC	Biotin carboxylase	0.000282036	2.07239
icd	Isocitrate dehydrogenase [NADP]	0.000208105	2.07127
gstB	Glutathione S-transferase GstB	0.000642433	2.06838
upp	Uracil phosphoribosyltransferase	0.00309382	2.06742
rplQ	50S ribosomal protein L17	0.00279652	2.06465
ydgA	Putative GTP-binding protein YdgA	8.48E-05	2.06299

Table 4.13, continued

Gene name	Product	p-value (Attribute)	FoldChange (MT vs. WT)
cysG1	Siroheme synthase	0.0413005	2.05358
moeA	Molybdopterin molybdenumtransferase	0.000673292	2.04713
tsf	Elongation factor Ts	0.000280918	2.0458
nadE	NH(3)-dependent NAD(+) synthetase	3.13E-05	2.04122
gmhA	Phosphoheptose isomerase	9.73E-05	2.03904
fabH	3-oxoacyl-[acyl-carrier-protein] synthase 3	0.00379531	2.03891
ppiD	Peptidyl-prolyl cis-trans isomerase D	0.00146601	2.02752
moeB	Molybdopterin-synthase adenylyltransferase	0.00781338	2.02694
asnS	Asparagine--tRNA ligase	0.000203156	2.02524
flgG	Distal rod protein	0.0279279	2.02105
rplO	50S ribosomal protein L15	0.0109305	2.02094
fklB	FKBP-type 22 kDa peptidyl-prolyl cis-trans isomerase	0.00319133	2.01925
sdhD	Succinate dehydrogenase hydrophobic membrane anchor subunit	0.00243547	2.01611
dapA1	4-hydroxy-tetrahydrodipicolinate synthase	0.00012026	2.00925

4.13.3 Validation of RNA-seq Results

4.13.3.1 qPCR Analysis

In order to validate the RNA-seq results, downregulated and upregulated genes in the L1-Δ*easI*::Kan mutant were randomly selected for verification. The selected downregulated genes were *bsmA*, *lsrD* and *lsrB* while the upregulated *ompD*, *sdaB* genes and 26 kDa periplasmic immunogenic protein precursor. Reference genes *gapA*, *pyrG* and *recG* were included for analysis. The primers sequence for each selected and reference genes are stated in Table 3.3 (Section 3.1.8). Figure 4.40 (downregulated genes) and Figure 4.41 (upregulated genes) illustrate the expression of selected genes quantified using qPCR. Notably, the expression of all these selected genes were closely correlated with the RNA-seq data. These results confirmed the reliability of the RNA-seq data.

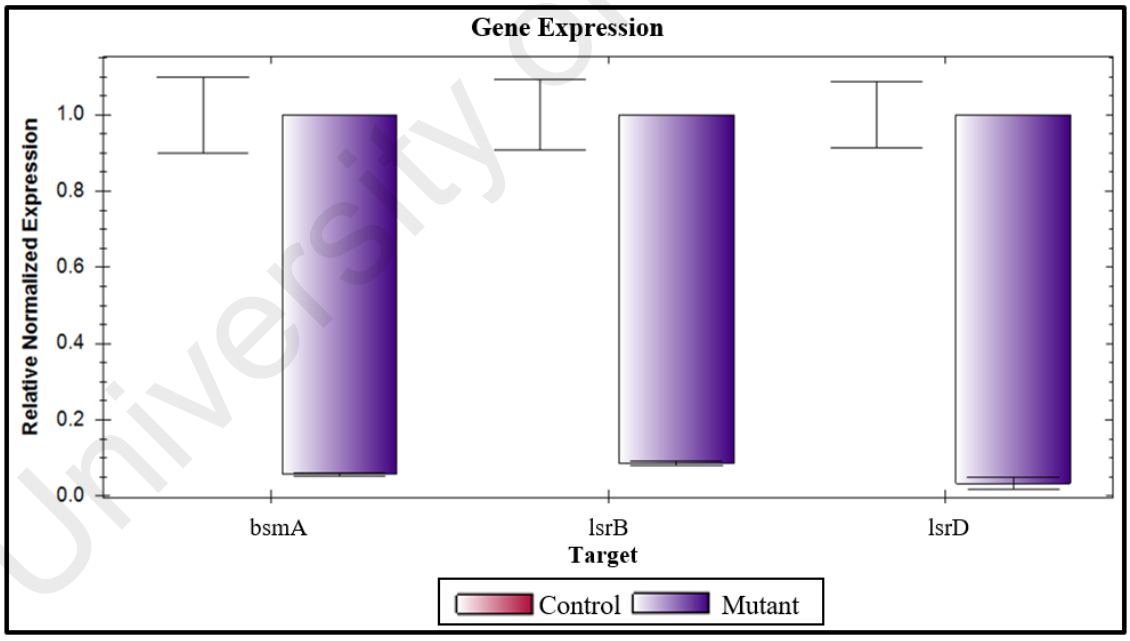

Figure 4.40: Gene expression analysis of *E. asburiae* L1 downregulated genes using qPCR. The selected downregulated genes for validation of RNA-seq data were *bsmA*, *lsrD* and *lsrB*. Bar chart shows the relative normalized expression levels of the downregulated genes. Reference genes *gapA*, *pyrG* and *recG* with the M value of less than 1.0 were selected. Each sample was performed in triplicate with three technical replicates. Bars: Standard errors of the mean.

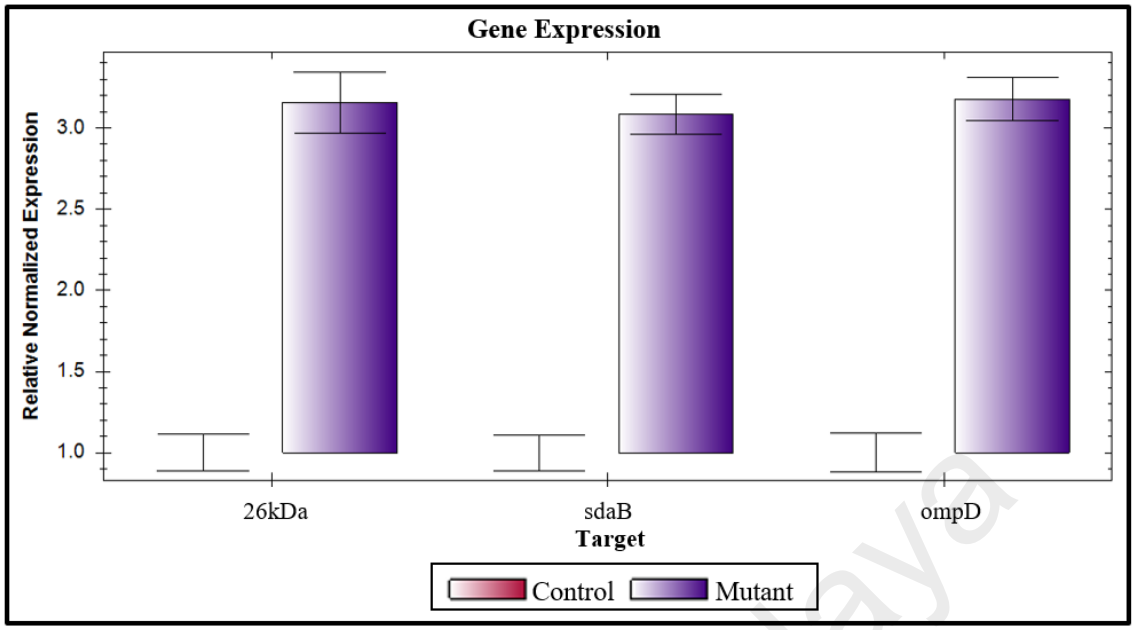

Figure 4.41: Gene expression analysis of *E. asburiae* L1 upregulated genes using qPCR. The selected upregulated genes for validation of RNA-seq data were 26 kDa periplasmic immunogenic protein precursor, *sdaB* and *ompD* genes. Bar chart shows the relative normalized expression levels of the downregulated genes. Reference genes *gapA*, *pyrG* and *recG* with the M value of less than 1.0 were selected. Each sample was performed in triplicate with three technical replicates. Bars: Standard errors of the mean.

4.13.3.2 Biofilm Formation and Quantification

Based on the RNA-seq data, out of the 128 downregulated genes, the *bsmA* gene that responsible for the biofilm stress and motility was the top gene being downregulated, with approximately sevenfold in *E. asburiae* L1-Δ*easI*::Kan mutant. In addition, it was found that there were three others biofilm-related genes being significantly downregulated after knocked-out of *easI* gene. Since biofilm development and QS are closely interconnected processes (Solano, Echeverz, & Lasa, 2014), biofilm formation was quantified by a standard crystal violet binding assay. After 72 h of growth at 37°C, quantification of biofilm in *E. asburiae* L1 wildtype and mutant strains was performed by comparison with a well-known biofilm-forming bacterium, *P. aeruginosa* PAO1. A detectable basal biofilm formation was found in *E. asburiae* L1 wildtype strain, similar to *P. aeruginosa* PAO1. The biofilm formation in *E. asburiae* L1-Δ*easI*::Kan mutant has decreased approximately half if compared to *E. asburiae* L1 wildtype strain. Based on this finding,

it was proven that the QS regulated *easI* gene in *E. asburiae* L1 indeed plays an important role in the biofilm formation.

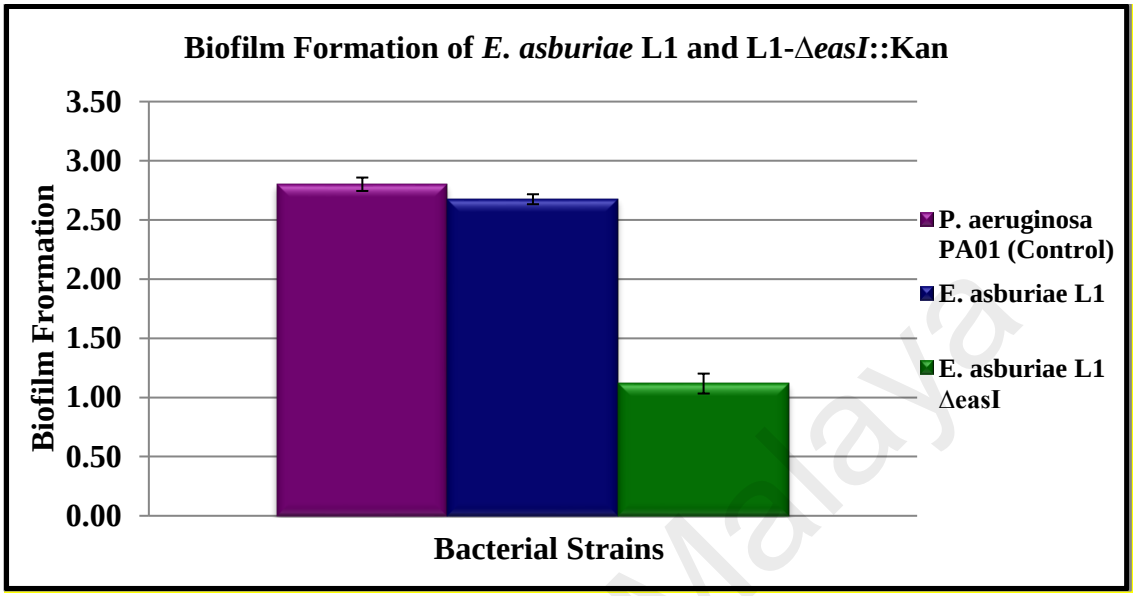

Figure 4.42: Qualitative analyses of biofilm formation in *E. asburiae* L1 wildtype and L1-Δ*easI*::Kan mutant strains. *P. aeruginosa* PAO1 was used as positive control. Bars: Standard errors of the mean. Statistical significance was determined using unpaired t-test (P <0.001).

4.13.4 Phenotypic Analysis--Biolog Omnilog® PM Assay

The phenotypic analysis of *E. asburiae* L1 wildtype and L1-Δ*easI*::Kan mutant strains was performed using Biolog Omnilog® PM assay. Thousands of phenotypes were tested after inoculation with a standardized cell suspension. The list of substrates used in PM assay (PM1-20) is listed in Appendix M. Areas of overlap (i.e. no change) are coloured green, whereas differences are highlighted as patches of red or blue. The parameter was set as min hour, 0 h; Max hour, 24 h (PM1-2, PM9-20); 48 h (PM3-8); Max value, 500 OmniLog units and Area, sum of all OmniLog values over all timepoints (area under the curve). The overall phenotypes utilized by *E. asburiae* L1 and L1-Δ*easI*::Kan wildtype and mutant strains were described in the form of heatmap shown in Figure 4.43 and 4.44. The significant differences noted between the *E. asburiae* L1 and *easI* null mutant was listed in Tables 4.14 and 4.15 with the numerical data shown. Phenotypic differences based on the bacteria's ability to utilize carbon, nitrogen, phosphorous and sulphur as well as peptide nitrogen sources were noted. An important point worth noting is the *easI* null mutant was found metabolically less active than wildtype strain when the peptide nitrogen source was utilized. In addition to this, growth responses to some of the different pH growth environments, as measured by the array were also observed for both strains. Besides, antibiotic resistance patterns and the ability to respire in the presence of toxic compounds for both of the strains showed differences. It was found that *E. asburiae* L1-Δ*easI*::Kan strain has gained more resistance towards several antimicrobial substances.

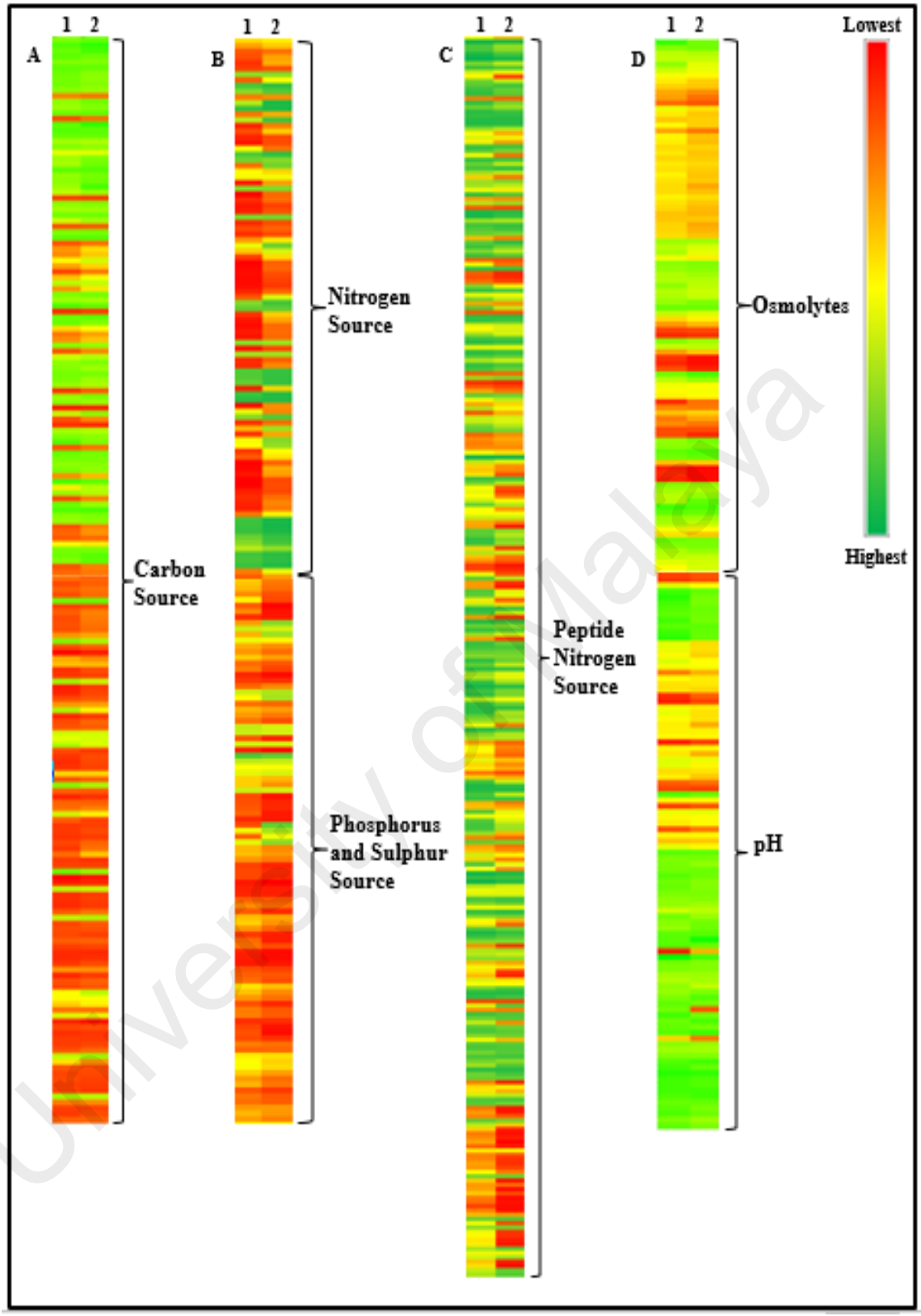

Figure 4.43: Heatmap of phenotype microarray (Carbon; phosphorus and sulphur; peptide nitrogen source; osmolytes and pH). 1: *E. asburiae* L1; 2: *E. asburiae* L1-Δ*easI*::Kan.

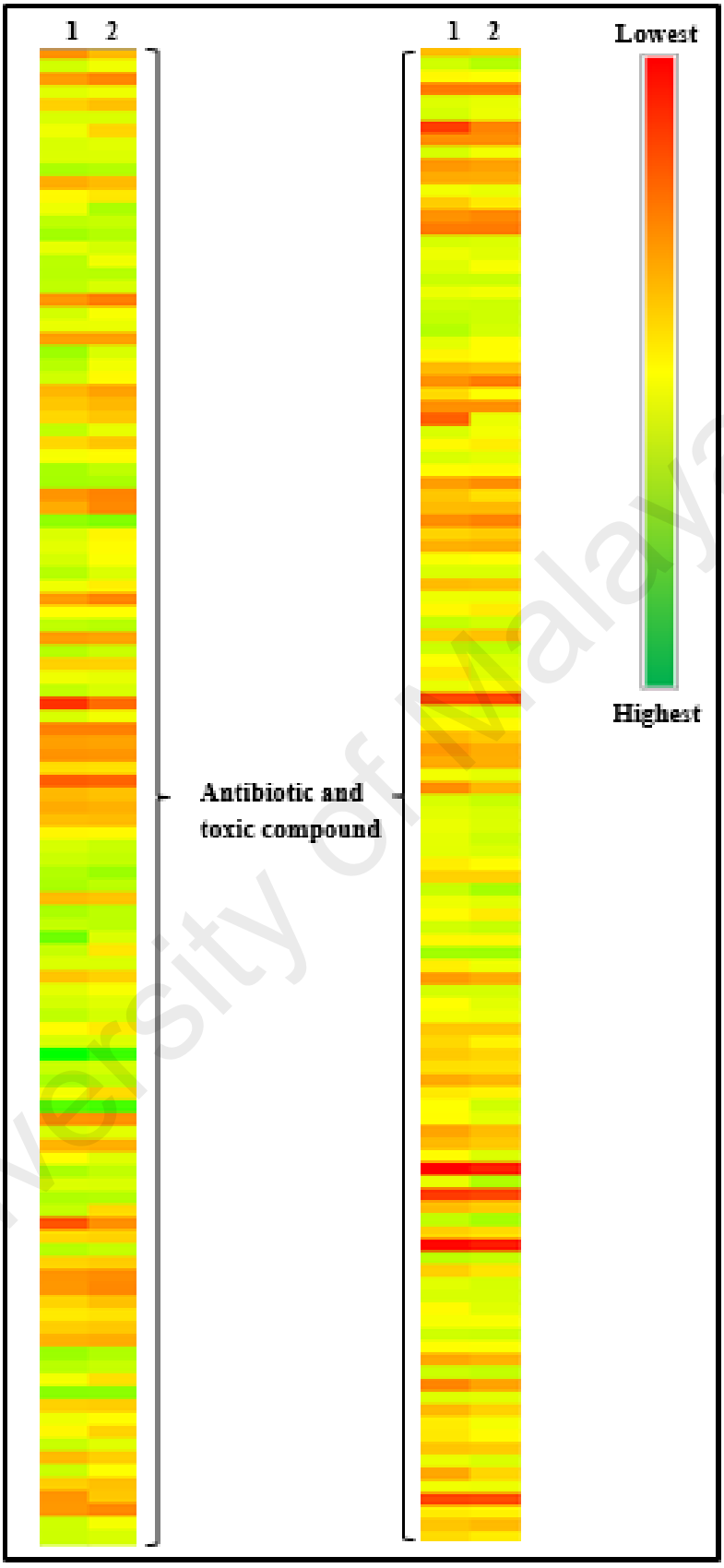

Figure 4.44: Heatmap of phenotype microarray (antibiotic and toxic compound). 1: *E. asburiae* L1; 2: *E. asburiae* L1-Δ*easI*::Kan

Table 4.14: Phenotypes lost by *E. asburiae* L1-Δ*easI*::Kan mutant relative to *E. asburiae* L1 wildtype strain

Test compound	Difference (Area)	Mode of action
D-Glucosaminic acid	-5125.00	C-source, carbohydrate
Lactulose	-5821.00	C-source, carbohydrate
L-Phenylalanine	-5618.00	C-Source, amino acid
Gly-Phe	-21614.00	Peptide nitrogen source
Gly-Tyr	-17965.00	Peptide nitrogen source
Met-Asp	-15580.00	Peptide nitrogen source
Met-Pro	-15889.00	Peptide nitrogen source
Phe-Ala	-25468.00	Peptide nitrogen source
Phe-Gly	-22645.00	Peptide nitrogen source
Phe-Ser	-23470.00	Peptide nitrogen source
Ser-Gly	-16125.00	Peptide nitrogen source
Ser-Phe	-16834.00	Peptide nitrogen source
Thr-Glu	-20460.00	Peptide nitrogen source
Tyr-Ala	-22165.00	Peptide nitrogen source
Tyr-Gly	-21263.00	Peptide nitrogen source
Tyr-Gly	-21263.00	Peptide nitrogen source
Tyr-Phe	-25435.00	Peptide nitrogen source
Tyr-Tyr	-22871.00	Peptide nitrogen source
Val-Arg	-17296.00	Peptide nitrogen source
Val-Arg	-20176.00	Peptide nitrogen source
γ-Glu-Gly	-25235.00	Peptide nitrogen source
Phe-Tyr	-22878.00	Peptide nitrogen source
Phe-Gly-Gly	-16487.00	Peptide nitrogen source
pH 9.5 + Agmatine	-17220.00	pH, deaminase
pH 9.5 + Tyramine	-6754.00	pH, deaminase
Ceftriaxone	-5158.00	Cell wall synthesis
Novobiocin	-6669.00	DNA topoisomerase
Cinoxacin	-13434.00	Protein synthesis
D,L-Methionine Hydroxamate	-8215.00	tRNA synthetase
Poly-L-lysine	-5035.00	Membrane, detergent, cationic

Table 4.14, Continued

Test	Difference (Area)	Mode of action
Gallic Acid	-12619.00	Antimicrobial, from plants
Coumarin	-16519.00	DNA intercalator
D,L-Thioctic Acid	-6494.00	Oxidizing agent
Thioglycerol	-16580.00	Reducing agent, thiol, adenosyl methionine antagonist
Iodonitro Tetrazolium Violet	-6394.00	Respiration
4-Hydroxycoumarin	-7304.00	DNA intercalator
18-Crown-6-Ether	-8988.00	Respiration, ionophore

Table 4.15: Phenotypes gained by *E. asburiae* L1-Δ*easI*::Kan mutant relative to *E. asburiae* L1 wildtype strain

Test	Difference (Area)	Mode of action
Caproic acid	6895.00	Carbon source
Inosine	18226.00	Nitrogen source
Thymidine	19174.00	Nitrogen source
Uridine	19394.00	Nitrogen source
L-Histidine	19548.00	Nitrogen source
N-Acetyl-L-Glutamic Acid	21548.00	Nitrogen source
L-Glutamic Acid	25644.00	Nitrogen source
L-Threonine	28451.00	Nitrogen source
Guanosine- 5'-monophosphate	15648.00	Phosphorus and sulphur source
Uridine- 2',3'- cyclic monophosphate	15757.00	Phosphorus and sulphur source
Adenosine- 2',3'-cyclic monophosphate	19022.00	Phosphorus and sulphur source
Adenosine- 3'-monophosphate	23292.00	Phosphorus and sulphur source
Uridine- 2'- monophosphate	32327.00	Phosphorus and sulfur source
Sodium lactate 6%	5098.00	Osmotic sensitivity, sodium formate
pH 9.5 + L-Tryptophan	10714.00	pH, deaminase
Enoxacin	7704.00	DNA topoisomerase, quinolone
Colistin	20805.00	Membrane, cyclic peptide
Tetracycline	5261.00	Protein synthesis, tetracycline
2,4-Diamino-6,7-Diisopropylpteridine	6801.00	Folate antagonist, vibriostatic agent
Penimepicycline	10747.00	Protein synthesis, tetracycline
Paromomycin	53369.00	Protein synthesis, aminoglycoside
Nickel chloride	7263.00	Toxic cation

Table 4.15, continued

Test	Difference (Area)	Mode of action
Rolitetracycline	9621.00	Protein synthesis, 30S ribosomal subunit, tetracycline
Alexidine	5150.00	Membrane, biguanide, electron transport
Domiphen bromide	6538.00	Membrane, detergent, cationic, fungiside
Hydroxyurea	8081.00	Ribonucleotide DP reductase, antifolate (inhibits thymine and methionine synthesis)
Puromycin	11846.00	Protein synthesis, 30S ribosomal subunit, premature chanin termination
Trimethoprim	12903.00	Folate antagonist, dihyldrofolate reductase
Salicylate	5219.00	Anti-capsule, anti-inflammatory, mar inducer
Sulfisoxazole	12537.00	Folate synthesis, PABA analog
Polymyxin B	17935.00	Membrane, outer
Pridinol	7127.00	Cholinergic antagonist
8-Hydroxyquinoline	16994.00	Chelator, lipophilic

CHAPTER 5: DISCUSSION

5.1 Isolation and Identification of Enterobacteriaceae From Fresh Salad Vegetables

From the past decade, outbreaks of human diseases associated with the consumption of raw vegetables have been increasing due to the lifestyle changing of consumers' eating habit towards convenient, ready-to-eat food products (such as salad vegetables). In Malaysia, salad vegetables are commonly served raw (Lund, 1992) as a side dishes during the meals. Consequently, consumption of contaminated vegetables may contribute to outbreak of food-borne diseases and cause public health at a serious risk due to the fact that most of these vegetables are consumed with minimal washing or cooking. Therefore, there is a need to study the factors contributing to the transmission of microbiological hazards on vegetables and the epidemiology of food-borne diseases, in the hope to prevent or minimize outbreaks cases due to consumption of contaminated fresh vegetables. Extensive studies have shown that microbiological contamination of food products is largely due to the naturally occurring phenomenon of biofilm formation. It has been reported that biofilm-forming characteristic is mediated by QS. This mechanism is achieved via small diffusible chemical signalling molecules, known as autoinducers (Chen et al., 2002), to mediate group-coordinated behaviours (Miller & Bassler, 2001).

Six different types of fresh vegetables (Lettuces, bitter gourds, cabbages, long beans, tomatoes, and chili) that are popular among Malaysian population were selected as isolation sources to assess the QS abilities of bacteria inhabiting phyllosphere environment. In this study, MacConkey agar plates as the selective media was used for growing Gram-negative bacteria particularly Enterobacteriaceae while inhibiting any growth of Gram positive bacteria.

Subsequent isolation procedure resulted in twenty Enterobacteriaceae bacterial colonies. Nineteen Enterobacteriaceae bacterial colonies were successfully identified by MALDI-TOF-MS up to genus level and one at probable genus level. Eight genera namely, *Enterobacter*, *Klebsiella*, *Morganella*, *Rahnella*, *Citrobacte*r, *Kluyvera*, *Raoultella* and *Salmonella* were identified in this work. Some of the species from these genera have been reported to contaminate vegetables. For instance, *Enterobacter cloacae*, *Klebsiella pneumoniae*, *Kluyvera cryocrescens* and *Rahnella aquatilis* have been isolated from fresh vegetables, such as iceberg lettuce and carrot. (Blaak et al., 2014; Falomir, Rico, & Gozalbo, 2013; Ingham et al., 2004; Ruimy et al., 2010). In addition to this, most of the species from these genera are well-known as human opportunistic pathogens which are often associated with nosocomial infection (Seng et al., 2016; Singla, Kaistha, Gulati, & Chander, 2010; Tash, 2005).

5.2 AHLs Detection of Bacterial Isolates

To date, no work has been reported on QS bacteria isolates from fresh vegetables. Since the major QS signalling molecules produced and utilized by Proteobacteria are AHLs (Case et al., 2008), hence the AHL characterization was focused in this study. All isolates were subjected to the screening for the AHL production. Preliminary screening of AHL production among the isolates was performed using two different biosensors, a violacein-based *C. violaceum* CV026 and bioluminescence-based *E. coli* [pSB401]. *C. violaceum* CV026 is a transposon mutant strain of *C. violaceum* that is unable to synthesize C6-HSL. Therefore, violacein production in *C. violaceum* CV026 is only inducible by AHLs evaluated with *N*-acyl side chains range from C4 to C8, with varying degree of sensitivity (Choo, Rukayadi, & Hwang, 2006; McClean et al., 1997). On the other hand, *E. coli* [pSB401] is a biosensor that responds well to 3-OC6-HSL. It was initially constructed to ease the identification of the AHLs signal produced by bacteria through cross streaking or conditioned medium assays. Its construction involves the fusion of *luxI/R* region of *Vibrio fischeri* with the *Photorhabdus luminescens luxCDABE* region (Winson et al., 1998). Among the tested isolates, only strain L1 (identified as *E. asburiae*) that was isolated from Batavia lettuce leaves mange to induce the violacein production of biosensor, suggesting the biosynthesis of short chain AHL molecules. The MS analysis results of the spent culture supernatant of *E. asburiae* provided evidence for the presence of C4-HSL and C6-HSL, which have never been reported in any of the *Enterobacter* spp.

5.3 Bacterial Characterization of AHL-Producing Bacterium *E. asburiae* L1

Enterobacter spp. have gained more attention as important and challenging pathogens (Sanders & Sanders, 1997). This is mainly due to their resistance towards a wide range of antimicrobial agents, such as cefoxitin, a third-generation cephalosporin, colistin, and aminoglycosides (Bouza & Cercenado, 2002; Paterson, 2006). Recently, a more concerned public health crisis is the emergence of Enterobacteria that produce *Klebsiella pneumoniae* carbapenemase (KPC-type carbapenemases), (Kitchel et al., 2009; Nordmann, Naas, & Poirel, 2011; Tzouvelekis, Markogiannakis, Psichogiou, Tassios, & Daikos, 2012), which are highly resistant to different classes of antimicrobial agents and predominantly involved in nosocomial and systemic infections (Arnold et al., 2011).

Although knowledge of the genus *Enterobacter* and its roles in human disease has expanded exponentially, the underlying complex mechanisms of pathogenicity of different *Enterobacter* spp. is yet to be discovered. Moreover, little is known about the AHL-type QS mechanism in *Enterobacter* spp. In fact, whether this cell-to-cell communication system mediates the regulation of virulence factors of *Enterobacter* spp. remains an unsolved mystery. Nonetheless, in previous studies, AHL-type QS activity has been proven to regulate virulence factors in other species such as *Burkholderia cepacia*, *Agrobacterium tumefaciens* and *P. carotovorum* (de Kievit & Iglewski, 2000). Therefore, there is a compelling need to further characterize and expand the studies towards the QS properties of this firstly reported AHL-producing *E. asburiae* L1.

E. asburiae is a Gram-negative bacillus belonging to the *Enterobacter* genus that has been isolated from soil, water and a variety of human sources including urine, respiratory tracts, stools, wounds and blood (Bi, Rice, & Preston, 2009; Brenner, McWhorter, Kai, Steigerwalt, & Farmer, 1986; Koth, Boniface, Chance, & Hanes, 2012; Paterson et al., 2005). This organism also has been found from a wide variety of crops

such as rice, cucumber, and cotton (Asis & Adachi, 2004; Elbeltagy et al., 2001; McInroy & Kloepper, 1995).

Previous work has identified some of the *E. asburiae* isolates as human pathogens while most of the *E asburiae* were identified as an opportunistic pathogen that causes different human diseases such as wound infection, community-acquired pneumonia and soft tissue infections (Brenner et al., 1986; Cha, Heo, Park, Choi, & Jeon, 2013; Koth, Boniface, Chance, & Hanes, 2012; Stewart & Quirk, 2001). Besides, *E. asburiae* also has been found to produce the Bush group 1 β-lactamase enzyme constitutively at high levels which causes this bacterium be resistant to most β-lactam antibiotics (Pitout, Moland, Sanders, Thomson, & Fitzsimmons, 1997). Recently, cases of colistin-resistant *E. asburiae* have been reported (Kadar, Kocsis, Kristof, Toth, & Szabo, 2015). Although *E. asburiae* has been reported to possess AI-2 receptors (Rezzonico, Smits, & Duffy, 2012), there are no reports on the production of AHLs by this bacterial species. Therefore, this AHL-producing bacterium (*E. asburiae* L1) was characterized in this work. Generally, the species (i.e. *E. asburiae* and *E. cloacae*) of *Enterobacter* genus share high similarity in their characteristics, hence their identification by MALDI-TOF-MS sometime could be mismatched. Hence, biochemical tests (API 20E, IMViC, decarboxylation, nitrate reduction and carbohydrate fermentation tests) that are commonly applied for characterization of Enterobacteriaceae and phenotypic characterization (GENIII MicroPlate) were conducted, in order to confirm the identity of the AHL-producing bacterium strain L1. For the biochemical tests, *E. asburiae* ATCC 35953 type strain was included for comparison. Phenotypic characterization of strain L1 by GENIII MicroPlate confirmed its identity as *E. asburiae*. Findings from the biochemical tests also showed that strain L1 generally shared the same characteristics as the ATCC 35953 type strain. This confirmed the identity of strain L1 as *E. asburiae*.

Interestingly, it was found that *E. asburiae* L1 showed positive reaction for VP test while *E. asburiae* ATCC 35953 showed negative reaction. Basically, VP test detects microorganisms that utilize the butylene glycol pathway and produce acetoin. This indicated that *E. asburiae* L1 can ferment glucose and further metabolize pyruvic acid to form acetyl-methyl carbinol (acetoin) through butylene glycol pathway. Acetoin (end product) in the presence of potassium hydroxide and atmospheric oxygen is converted to diacetyl. Diacetyl, under the catalytic action of alpha-naphthol and creatine, is converted into a red complex. Besides, carbohydrate fermentation test indicated that *E. asburiae* L1 did not use lactose as the carbon source. Lactose is a disaccharide consisting of the glucose and galactose connected by glycosidic bond. Since *E. asburiae* L1 has failed to produce the enzyme lactase, it cannot break the covalent bond and release free glucose that can be easily utilized by the organism.

As *E. asburiae* L1 and *E. asburiae* ATCC 35953 were isolated from different environments (phyllosphere and human source), it is expected to observe biochemical deviations between these strains. It is a normal situation for bacterial to utilize different pathways in order to increase their survival advantage in the environments that they inhabit. In this study, although differences were observed between *E. asburiae* L1 and *E. asburiae* ATCC 35953, these deviations did not challenge the certainty of the phylogenetic assignment of these two strains (Appendix L).

5.4 Genome Sequencing oF *E. asburiae* L1

In the effort to identify *luxI/R*, genomes sequencing was first performed using HiSeq 2000 next generation sequencer platform as this technology is more cost effective. Unfortunately, this technology only managed to assemble *E. asburiae* L1 genome into 195 contigs with many gaps in between. This caused the failure to obtain a complete blueprint for *E. asburiae* L1 as there might be a lot of crucial and valuable genes that fall in between the gaps, hence missed out during analysis.

Hence, another sequencing technology, PacBio SMRT which employed parental long-read of 10- to 20- kb of amplification free insert template library was applied (Roberts, Carneiro, & Schatz, 2013). One of the advantage of the long-read set is to span many more repeats and missing bases, thereby closing many of the gaps automatically. This increase the possibility of complete genome closure. In addition to this, PacBio SMRT sequencing also manage to differentiate the bacterial chromosome from plasmids and recognized the bacteria methylation profile from SMRT sequencing data because of the change in DNA polymerase kinetics. In this study, the complete genome of *E. asburiae* L1 (4.5Mbp in size) was successfully generated using PacBio SMRT sequencer.

In order to verify the whole genome sequence accuracy of *E. asburiae* L1, another independent sequencing technology (optical genome mapping technology) was used. This is a technology that gathers genomic long-range information similar to ordered restriction digest maps. As the maps are constructed directly from genomic DNA molecules, cloning, DNA amplification, probe-selection for hybridization or sequencing bias are avoided. Since optical consensus maps can be generated without a reference, optical mapping can detect insertions and deletions easily, whilst at the same time providing sizing and restriction maps of the missing sequence (Howe & Wood, 2015). The completeness of *E. asburiae* L1 was confirmed by this technology.

5.5 Comparative Genome Analysis of *E. asburiae* L1

Within this framework, the complete genome of *E. asburiae* L1 and comparative genomic analysis was performed with its closest sequenced relatives. Among the strains analysed, ATCC 35953 (type strain) is a multidrug resistance pathogen that was isolated from human source (Brenner et al., 1986). Besides, GN02073, GN02127 and 33838 are KPC-producing strains that were isolated from human source as well while PDN3 was available from Populus root. As shown by RAST and OrthoANI analysis, although *E. asburiae* L1 and PDN3 were isolated from phyllosphere environment, their genomes share high similarities with *E. asburiae* clinical strains. This strongly indicates a close relationship among these bacterial strains and suggested *E. asburiae* L1 might possess some virulence factors that are similar to the clinical strains. OrthoANI analysis revealed that *E. asburiae* L1 share highest similarities with the type strain (98.7%) and PDN3 (98.6%), in agreement with Mauve analysis. Since *E. asburiae* ATCC 35953 and PDN3 were isolated from different environments, this postulated that *E. asburiae* L1 might possess some unique genes that enable it to survive in both phyllosphere and clinical environments. However, this hypothesis is yet to be proven.

Besides, RAST analysis revealed the absence of heme, hemin uptake and utilization subsystems in *E. asburiae* L1, ATCC 35953 and PDN3 but not in the KPC-producing strains. This possibly suggests that these three closest strains depend on the high-affinity iron-binding molecules namely siderophore to scavenge iron from its environment. Although previous studies did mention that siderophore in *Enterobacter* spp. is involved in promoting plant growth (Ahemad and Khan 2010; Taghavi *et al*. 2010), correlation between QS and siderophore in *Enterobacter* spp. has never been explored. A study by Wen et al. (2012) suggests that siderophore production is regulated by cell density. Indeed, numerous studies have shown that QS regulation of siderophores will regulate the production of virulence factors and biofilm formation activity of *P. aeruginosa*

(Lamont, Beare, Ochsner, Vasil, & Vasil, 2002; Patriquin et al., 2008; Rutherford & Bassler, 2012). Therefore, current finding of siderophore in this QS producing strain might be a stepping stone to unravel the exact roles of QS and siderophore especially in *E*. asburiae.

5.6 Nucleotide Sequence and Bioinformatics Analysis of *E. asburiae* L1

In a complete AHL-based QS system, the *luxI/R* homologues interact with each other whereby AHLs synthesized by LuxI bind to and activate the LuxR-type protein (Subramoni & Venturi, 2009). This AHL-protein complex in turn regulates the expression of certain genes, leading to the collective behaviours of the bacteria (Bassler, 2002). Although the *luxI/R* pairs are often genetically linked, there are examples where the *luxI/R* functional pairs are distantly located in the bacterial chromosome or plasmid. *In silico* analysis of the *E. asburiae* L1 genome revealed the presence of a pair of *luxI/R* homologues. Initial analysis of the *luxI* homologue of *E. asburiae* L1 was annotated as '*croI*' found in *Citrobacter rodentium*. The phylogenetic analysis based on amino acid sequences showed that the AHL synthase found in *E. asburiae* L1 formed a separate cluster as compared with others *E. asburiae* and closely related enterobacteria. By this, the *luxI/R* homologues of *E. asburiae* L1 was renamed to *easI/R* based on the genetic nomenclature guideline.

Sequence alignment of AHL autoinducer protein in *E. asburiae* strains revealed the presence of highly conserved AHL synthase among them. This indicated that AHL synthase is commonly found among *E. asburiae*. However, to date, no work has been reported on the AHL synthase in *E. asburiae.* Reports on the presence of LuxI in other *Enterobacter* spp. are also very limited. This is because most of the current studies focused on the pathogenicity of *Enterobacter* spp. Therefore, later stage of this study focused on the CDS that are responsible for cell-to-cell communication system in *Enterobacter* spp. in order to understand its QS roles. *In silico* analysis of the *luxI* gene cluster among *E. asburiae* L1 and its closely related species showed conserved *luxI/R* QS-related genes. In the vicinity of the *luxI/R* genes are GCN5-related N-acetyltransferase and acetyltransferase GNAT family, which play a role in fatty acid synthesis (Williams, Winzer, Chan, & Cámara, 2007; Xie, Zeng, Luo, Pan, & Xie, 2014).

Apart from that, a signal-recognition protein, sensor histidine kinase is found at downstream of *luxI* homologue. Studies have shown that this protein is essential in many aspects of bacterial physiology, including bacterial infections, by facilitating the bacteria to sense environmental or cellular stimuli and alter its cytoplasmic autokinase activity in response to these signals (Bader et al., 2005). One study showed the RcsC sensor histidine kinase is required for normal biofilm development in *E. coli* (Ferrieres & Clarke, 2003).

Biofilm formation on food surfaces and food processing equipment is a persistent problem in the food industry, leading to serious health problems and causing great economic loss (Bai & Rai, 2011; Kumar & Anand, 1998). Biofilms are important environmental reservoirs for pathogens, and the biofilm growth mode may provide organisms with survival advantages in natural environments and increase their virulence (Parsek & Singh, 2003). In addition to this, the ability of bacteria to form biofilms is often linked to pathogenic traits during chronic infection (Bjarnsholt, 2013; Wolcott & Ehrlich, 2008). Biofilm development and QS have been reported as a closely interconnected processes (Solano et al., 2014). For instance, in a study by Viana et al. (2009), a common bacterial food contaminant, *Hafnia alvei* 071, synthesizes AHL molecules under the direction of the *halI* gene. The AHLs were found to be important in biofilm formation. However, biofilm formation was found to be impaired in *H. alvei* 071 *halI* mutant (Bai & Rai, 2011; Viana, Campos, Ponce, Mantovani, & Vanetti, 2009). By this, it is hypothesized that *E. asburiae* L1 might possess and utilize biofilms as its survival advantages in different environments to increase its virulence.

5.7 Functional Studies of QS Genes

5.7.1 Functional Studies of EasI

The *easI* gene which encoding the putative AHL synthase from *E. asburiae* L1 has been cloned and characterized in this work. Heterologously expressed EasI protein activated AHL biosensor *C. violaceum* CV026, indicating this EasI is a functional AHL synthase. LC-MS/MS analysis confirmed the production of C4-HSL and C6-HSL from spent culture supernatant of induced *E. coli* BL21 (DE3)pLysS harbouring the recombinant EasI, suggesting that EasI is indeed the AHL synthase of *E. asburiae* L1. Interestingly, the production of C4-HSL was present in a higher amount than C6-HSL by *E. coli* harbouring *easI*, possibly indicating the former AHL may possess a more important role in executing the physiological functions of the cells or expression of virulence factors.

Since the role of AHL synthase in *E. asburiae* has never been explored, the EasI protein homologue was compared to other bacteria possessing similar QS protein. Analysis showed that the EasI protein is most similar to the AHL synthase, CroI from *C. rodentium* (77% identity), followed by AHL synthase, SmaI from *Serratia* sp. ATCC 39006 (46% identity). Several studies have shown that both of these closest homologues, CroI and SmaI, also produce C4-HSL as the major AHL and C6-HSL as the minor AHL (Barnard et al., 2007; Coulthurst et al., 2007). In *C. rodentium*, the *croI* mutant was observed to attach less well to an abiotic surface than the wild-type strain (Coulthurst et al., 2007). Barnard et al. (2007) have proven that SmaI was found to regulate the carbapenem production, prodigiosin and virulence factor production in strain ATCC 39006. Research by Favre-Bonte et al. (2003) further demonstrated that biofilm formation in a well-known opportunistic pathogen *P. aeruginosa* is controlled by a cell-to-cell signalling circuit relying on the secretion of C4-HSL (Favre-Bonte, Kohler, & Van Delden, 2003). According to the previous studies, it is postulated that EasI homologue

may play an important role in the biofilm formation as well as controlling the expression of virulence factors. Nevertheless, the mechanism of QS in contributing to the virulence and pathogenic potential in this bacterium requires further validation.

5.7.2 Functional Studies of EasR

In QS, transcriptional regulator LuxR is a key player in QS that are involved in gene regulation. The function of LuxR homologues as quorum sensors is mediated by the binding of AHL signal molecules to the N-terminal receptor site of the proteins. In this study, the *easR* gene of *E. asburiae* L1 was cloned to the downstream of a P_{BAD} promoter in pLNBAD vector, and co-transformed into *E. coli* TOP10 together with pMULTIAHLPROM vector. The pLNBAD vector harbours an inducible P_{BAD} promoter which is positively and also negatively regulated by the products of the *araC* gene (Schleif, 2010). In the presence of L-arabinose, AraC will form a complex with L-arabinose, allowing transcription to begin. On the other hand, the pMULTIAHLPROM is a pMP220-derived plasmid which carries a synthetic tandem promoter of eight different *luxI* gene promoters (*luxI, cviI, ahlI, rhlI, cepI, phzI, traI* and *ppuI*) transcriptionally fused to a promoterless *lacZ* gene. All these promoters are known to contain *lux*-boxes which are positively regulated by the cognate LuxR-family protein in the presence of the cognate AHL thus representing a wide range of LuxR-family regulated promoters (Steindler et al., 2008). In this assay, *E. coli* TOP10 was chosen over *E. coli* DH5α due to its capability of transporting L-arabinose, but not metabolizing it, and thus ensure the level of L-arabinose will be constant inside the cell and not decrease over time.

In order to test the functionality of *easR* in *E. asburiae* L1, the recombinants were subjected to β-galactosidase assay either in the presence or absence of exogenous AHLs. β-galactosidase, encoded by *lacZ*, hydrolyses β-D-galactosides, allowing the bacteria to grow on carbon sources such as lactose by cleaving it into glucose and galactose for the

cells to utilize as both carbon and energy sources. The β-galactosidase assay carried out in this work utilized o-NPG in place of lactose as the substrate. Cleavage of o-NPG by β-galactosidase releases *o*-nitrophenol which has a yellow colour and absorbs at 420 nm (Miller, 1972). The reading at 420 nm is a combination of absorbance by o-nitrophenol and light scattering by cell debris. The increase in absorbance at 420 nm would be a reflection of β-galactosidase activity. It was postulated that if *easR* is a functional transcriptional regulator, it could bind to any of the exogenous AHLs and then possibly initiate transcription from one or more of the *luxI*-family gene promoters present in pMULTIAHLPROM. Since the production of AHLs by *E. asburiae* L1 was reported as C4-HSL and C6-HSL, both of these short chain AHLs were included to evaluate the β-galactosidase activities of cells harbouring pMBAD-*easR*. In addition to this, another two long-chain AHLs (C10-HSL and C12-HSL) were included to test whether *easR* is able to initiate transcription from any of the *luxI*-family gene promoters present in pMULTIAHLPROM apart from the AHLs produced by *E. asburiae* L1.

The functionality of the *easR* was validated when higher β-galactosidase activities were detected for cells harbouring pMBAD-*easR* with the presence of exogenous AHLs, when compared with the cells harbouring pMBAD-*easR* with the absence of exogenous AHLs. Interestingly, β-galactosidase activities of cells harbouring pMBAD-*easR* with addition of C4-HSL was present in higher amount than C6-HSL. This was in agreement with the previous hypothesis that the former AHL may possess a more important role in executing the physiological functions of the cells or expression of virulence factors. Furthermore, β-galactosidase activity was also detected for cells harbouring pMBAD-*easR* with addition of long-chain AHLs. However, the β-galactosidase activity in these cells is much lower if compared with the cells harbouring pMBAD-*easR* with addition of short chain AHLs.

5.8 Whole Transcriptomics Studies

To investigate the QS-mediated gene expression in *E. asburiae* L1, a global transcriptional analysis of gene expression after the deficit of QS *easI* gene. Analysis revealed that the gene most downregulated was *bsmA* that responsible for the biofilm stress and motility. It has previously been documented that BsmA is able to influence *E. coli* biofilm maturation and stress response (Weber, French, Barnes, Siegele, & McLean, 2010). In addition to this, it is noteworthy that another putative biofilm stress and motility protein as well as two others biofilm-related genes, *bssR* and *bssS* were also significantly being downregulated after knocked-out of *easI* gene. Study by Domka et al. (2006) indicated that BssR and BssS play a role in regulating the biofilm formation of *E. coli* K-12 (Domka, Lee, & Wood, 2006).

Generally, biofilm formation is a cooperative group behaviour that involves bacterial populations living embedded in a self-produced extracellular matrix. A typical development of biofilm includes several stages: 1) attachment to a surface, 2) formation of micro colonies, 3) development of young biofilm, 4) differentiation of structured mature biofilm, and 5) dispersal of mature biofilm. During chronic infection, the ability of bacteria to form biofilms is often linked to pathogenic traits (Bjarnsholt, 2013; Wolcott & Ehrlich, 2008). Bacterial biofilms are particularly problematic as they can become resistant to most available antibiotics. In addition, biofilms are also important as environmental reservoirs for pathogens, and the biofilm growth mode may provide organisms with survival advantages in natural environments and increase their virulence (Parsek & Singh, 2003).

To date, no studies has been conducted to evaluate and quantify the biofilm formation in *E. asburiae*. The transcriptomic analysis of the current study and the previous *in silico* analysis of *E. asburiae* L1 genome both also discerned the importance

of biofilm in this bacterial strain. To address this, biofilm formation of this strain was further quantified and validated by a standard crystal violet binding assay. After 72 h of growth at 37°C, quantification of biofilm in *E. asburiae* L1 was performed by comparison with a well-known biofilm-forming bacterium, *P. aeruginosa* PAO1. A detectable basal biofilm formation was found in *E. asburiae* L1, similar to strain PAO1 (Figure 4.42). On the other hand, the biofilm formation in *easI* null mutant has decreased approximately half if compared to its wildtype strain. This work has proven that the QS regulated *easI* gene in *E. asburiae* L1 indeed plays an important role in the biofilm formation.

On the other hand, the gene that most upregulated was *ribB* encodes the DHBP synthetase. RibB is believed to be a key enzyme that catalyses the conversion of D-ribulose 5-phosphate to formate and 3,4-dihydroxy-2- butanone 4-phosphate, a precursor for the xylene ring of riboflavin (Callahan & Dunlap, 2000; Gupta et al., 2014; Pedrolli et al., 2015). Besides, with respect to luminescence, the involvement of RibB in synthesis of riboflavin could possibly contribute to light production (Callahan & Dunlap, 2000). Studies revealed that in the marine bioluminescent bacterium, *V. fischeri*, *ribB* gene was identified at downstream of the *lux* operon without linkage to the *lux* operon; nevertheless, its expression is controlled co-ordinately with the *lux* operon (Callahan & Dunlap, 2000). Current study revealed that the expression level of *ribB* gene was upregulated in the *E. asburiae* L1-Δ*easI*::Kan mutant strain.

According to previous findings, it leads to a speculation that the presence of *easI* gene in *E. asburiae* L1 will repress the expression of *ribB* gene. Absence of LuxI protein will cause insufficient AHL synthesis. By this, the binding process of the AHL to the cognate receptor (LuxR homologue) which is essential for the regulation of the *lux* operon (*luxICDABEG*) will be inhibited. Under this situation, the *ribB* gene in *E. asburiae* L1 will be derepressed with regard to riboflavin biosynthesis (i.e. an increase of *ribB*

expression occurred in the absence of the regulatory element). Nonetheless, additional studies will be necessary to ascertain this prediction.

The second most highly upregulated gene was *ompD* that responsible for the outer membrane porin protein OmpD precursor. Study by Ipinza et al. (2014) indicated that *Salmonella* Typhimurium has the ability to downregulate the expression of *ompD* in order to improve its survival inside the host, thus allowing spreading and the establishment of a systemic infection (Ipinza et al., 2014). If higher level of *ompD* is expressed in a bacterium, it will bring more benefit to the host by reducing the bacteria survival in the host. Within this framework, *ompD* gene was upregulated at $\log_2$ fold change of 5.13161 after the deficit of QS *easI* gene. This postulates that *E. asburiae* L1 which possesses QS gene might be more pathogenic and can cause infection when reside a host.

5.9 Phenotypic Analysis--PM Assay

Generally, a sufficient supply of various biomolecules is necessary for bacteria to support their metabolic activity. However, in natural environments, bacteria are often found to survive under limited nutrients supply. Hence, bacteria will normally evolve redundant metabolic systems in order to support efficient adaptation and to ensure their growth in different conditions through their capability to utilize broad range of different substrates (Yan et al., 2013). The PM array data give an insight into how these features differ, between the *E. asburiae* L1 wildtype and mutant strains.

Based on the PM analysis, it was found that *E. asburiae* L1-Δ*easI*::Kan mutant was metabolically less active than parental strain when the peptide nitrogen source was utilized. Besides, the mutant strain was found metabolically more active than parental strain when nitrogen source as well as phosphorus and sulphur source were utilized. These findings suggested that peptide nitrogen source might be an essential energy source required to involve in the AHL-based QS mechanism in *E. asburiae* L1. In contrast, the *easI* null mutant might require a balance of the nitrogen source as well as phosphorus and sulphur source for maintaining their growth and metabolic. However, these hypotheses require further metabolomics analysis to prove them.

The phenotypic study of *E. asburiae* L1 indicated that the utilization of agmatine by *E. asburiae* L1-Δ*easI*::Kan was significantly reduced. Previous studies showed that biofilm formation involved the utilization of agmatine (Gilbertsen & Williams 2014; Jones et al. 2010). It seems that when the biofilm formation by a bacteria strain is reduced, the utilization of agmatine will reduce as well. In addition, the *easI* null mutant was found to exhibit less activity in the presence of poly-L-lysine (Colville, Tompkins, Rutenberg, & Jericho, 2010). It is widely known that poly-L-lysine functions as an enhancer for microbial adhesion. With the presence of poly-L-lysine, microorganisms has the ability

to form thicker biofilms (Cowan, Liepmann, & Keasling, 2001). In this study, since the *easI* gene that controls the regulation of biofilm formation has been knocked-out, the usage of poly-L-lysine will reduce, hence, less activity was expected to occur. Present phenotypic study once again confirmed that the biofilm formation is indeed a phenotype controlled by *easI* gene in *E. asburiae* L1.

Interestingly, L1-Δ*easI*::Kan mutant strain has gained more resistance towards several antimicrobial substances such as enoxacin, colistin and polymyxin B. However, it remains enigmatic as how L1-Δ*easI*::Kan mutant show higher resistance towards these antimicrobial substances. Preliminary, it was hypothesized that the antibiotic resistance changes pattern demonstrated by L1-Δ*easI*::Kan mutant might be a consequence of the *easI* gene replacement by aminoglycosides kanamycin drug cassette. Several studies have reported that aminoglycosides resistance enzyme did conferred cross-resistance to chemically unrelated drug classes through different mechanisms (Chen, He, Li, & Ryu, 2009; Kohanski, DePristo, & Collins, 2010; Maus, Plikaytis, & Shinnick, 2005; Reeves et al., 2013). For instance, study by Reeves et al. (2013) revealed that mutation has contributed to aminoglycoside cross-resistance in *Mycobacterium tuberculosis* against clinically used second-line antibiotics. Besides, aminoglycosides kanamycin was found to induce cross-resistance by promoting the development of low-level resistance to other functionally and structurally unrelated antibiotics in *E. coli* B23 (Chen et al., 2009). This hyphothesis will be validated in future by removing the entire drug cassette in L1-Δ*easI*::Kan mutant by counter selection.

The phenotypic study provides essential information regarding *E. asburiae*. Current phenotypic study postulates that *E. asburiae* L1 might be a potential food-borne pathogen that possesses multidrug resistance characteristic. For instance, this bacterium was found to be resistant towards the last resort antibiotic namely colistin. Since *E. asburiae* L1 was

isolated from lettuce leaves, there might be a great chance for this bacterium to infect and reside in human host to cause illnesses. Hence, further studies are indeed necessary to gain some insight on how the interactions between QS system and other systems in *E. asburiae* L1 can benefit or harm the hosts in the environments that they inhabit. In addition, as drug resistance continues to develop and spread, there is an urge to continue study and understand the molecular basis and mechanisms of antibiotic resistance demonstrated by L1-Δ*easI*::Kan mutant.

5.10 Future Work

The present work identified the AHL synthase and receptor for *E. asburiae* L1 AHL. Biofilm formation was proven to be one of the crucial physiological activity regulated by QS *easI* gene of *E. asburiae* L1. However, a number of the significantly downregulated genes identified from the transcriptomic study in this work are of unknown functions and hence require further analysis. In future, related studies will be carried out to identify and characterize these genes in order to help shed some light on the exact roles of these genes correlated with the *easI* gene of *E. asburiae* L1.

To obtain a complete profile of the QS system in *E. asburiae* L1, gene knock-out of the transcriptional regulator *easR* as well as double mutant of *easI/easR* will be carried out in future using the recombineering technique. Comparison studies which involved the transcriptomic and phenotypic changes among these mutants will be performed. By truly understand the QS and its role in *E. asburiae* L1, it will definitely help to find out new biomolecules targeting QS in controlling the virulence and infection that possibly caused by this bacterium.

CHAPTER 6: CONCLUSION

Eight bacterial genera were isolated, namely *Enterobacter*, *Klebsiella*, *Morganella.*, *Rahnella*, *Citrobacter*, *Kluyvera, Raoultella* and *Salmonella* were isolated in this work as confirmed by MALDI-TOF-MS. *E. asburiae* L1 was found to produce short chain AHLs. LC-MS/MS analysis of the *E. asburiae* L1 spent culture supernatant confirmed the production of C4-HSL and C6-HSL. For the first time, AHL-based QS was discovered in *E. asburiae*. The complete genome of *E. asburiae* L1 (4.5Mbp in size) was obtained using the single molecule real time sequencer and the whole genome sequence accuracy was verified by optical genome mapping technology. *In silico* analysis of the *E. asburiae* L1 genome revealed the presence of a pair of *luxR* and *luxI* homologues, designated as *easR* and *easI*. Characterization and functional studies of *easI/R* homologues of *E. asburiae* L1 were performed, indicating that EasI is indeed a functional AHL synthase in *E. asburiae* L1. Functionality of transcriptional regulator EasR in *E. asburiae* L1 was confirmed with β-galactosidase assay. With the constructed *E. asburiae* L1-Δ*easI*::Kan mutant, whole transcriptomic analysis confirmed the important role of this QS regulated *easI* gene in controlling biofilm formation in *E. asburiae* L1. Phenotypic study revealed that the *easI* null mutant was metabolically less active than wildtype strain when the peptide nitrogen source was utilized and the mutant is generally more resistance to antibiotics. Current work has laid the foundation for developing a deeper understanding in elucidating the roles of AHLs in *E. asburiae* L1. This could possibly provide a model for bacterial cell-cell communication among *E. asburiae* strains. Nonetheless, more studies need to be conducted on the AHL-based QS system in *E. asburiae* before we can fully characterize and understand the QS mechanism in this bacterium.

REFERENCES

Altekruse, S. F., & Swerdlow, D. L. (1996). The changing epidemiology of foodborne diseases. *The American Journal of the Medical Sciences*, *311*(1), 23-29.

Andersen, J. B., Sternberg, C., Poulsen, L. K., Bjørn, S. P., Givskov, M., & Molin, S. (1998). New unstable variants of green fluorescent protein for studies of transient gene expression in bacteria. *Applied and Environmental Microbiology, 64*(6), 2240-2246.

Annous, B. A., Fratamico, P. M., & Smith, J. L. (2009). Quorum sensing in biofilms: why bacteria behave the way they do. *Journal of Food Science, 74*(1), R1-R14.

Antunes, L. C., Ferreira, R. B., Lostroh, C. P., & Greenberg, E. P. (2008). A mutational analysis defines *Vibrio fischeri* LuxR binding sites. *Journal of Bacteriology, 190*(13), 4392-4397.

Arnold, R. S., Thom, K. A., Sharma, S., Phillips, M., Johnson, J. K., & Morgan, D. J. (2011). Emergence of *Klebsiella pneumoniae* Carbapenemase (KPC)-producing bacteria. *Southern Medical Journal, 104*(1), 40-45.

Asis, C. A. Jr., & Adachi, K. (2004). Isolation of endophytic diazotroph *Pantoea agglomerans* and nondiazotroph *Enterobacter asburiae* from sweetpotato stem in Japan. *Letters in Applied Microbiology, 38*(1), 19-23.

Atkinson, S., Chang, C. Y., Sockett, R. E., Camara, M., & Williams, P. (2006). Quorum sensing in *Yersinia enterocolitica* controls swimming and swarming motility. *Journal of Bacteriology, 188*(4), 1451-1461.

Atkinson, S., Throup, J. P., Stewart, G. S., & Williams, P. (1999). A hierarchical quorum-sensing system in *Yersinia pseudotuberculosis* is involved in the regulation of motility and clumping. *Molecular Microbiology, 33*(6), 1267-1277.

Atkinson, S., & Williams, P. (2009). Quorum sensing and social networking in the microbial world. *Journal of The Royal Society Interface*.

Aziz, R. K., Bartels, D., Best, A. A., DeJongh, M., Disz, T., Edwards, R. A., . . . Zagnitko, O. (2008). The RAST Server: rapid annotations using subsystems technology. *BMC Genomics, 9*, 75.

Bader, M. W., Sanowar, S., Daley, M. E., Schneider, A. R., Cho, U., Xu, W., . . . Miller, S. I. (2005). Recognition of antimicrobial peptides by a bacterial sensor kinase. *Cell, 122*(3), 461-472.

Bai, A. J., & Rai, V. R. (2011). Bacterial quorum sensing and food industry. *Comprehensive Reviews in Food Science and Food Safety, 10*(3), 183-193.

Bainton, N. J., Bycroft, B. W., Chhabra, S. R., Stead, P., Gledhill, L., Hill, P. J., . . . Williams, P. (1992). A general role for the *lux* autoinducer in bacterial cell signalling: control of antibiotic biosynthesis in *Erwinia*. *Gene, 116*(1), 87-91.

Barber, C. E., Tang, J. L., Feng, J. X., Pan, M. Q., Wilson, T. J. G., Slater, H., . . . Daniels, M. J. (1997). A novel regulatory system required for pathogenicity of *Xanthomonas campestris* is mediated by a small diffusible signal molecule. *Molecular Microbiology, 24*(3), 555-566.

Barnard, A. M., Bowden, S. D., Burr, T., Coulthurst, S. J., Monson, R. E., & Salmond, G. P. (2007). Quorum sensing, virulence and secondary metabolite production in plant soft-rotting bacteria. *Philosophical Transactions of the Royal Society B, 362*(1483), 1165-1183.

Bassler, B. L. (2002). Small talk. Cell-to-cell communication in bacteria. *Cell, 109*(4), 421-424.

Bassler, B. L., Wright, M., Showalter, R. E., & Silverman, M. R. (1993). Intercellular signalling in *Vibrio harveyi*: sequence and function of genes regulating expression of luminescence. *Molecular Microbiology, 9*(4), 773-786.

Berger, C. N., Sodha, S. V., Shaw, R. K., Griffin, P. M., Pink, D., Hand, P., & Frankel, G. (2010). Fresh fruit and vegetables as vehicles for the transmission of human pathogens. *Environmental Microbiology, 12*(9), 2385-2397.

Bi, C., Rice, J. D., & Preston, J. F. (2009). Complete fermentation of xylose and methylglucuronoxylose derived from methylglucuronoxylan by *Enterobacter asburiae* strain JDR-1. *Applied and Environmental Microbiology, 75*(2), 395-404.

Bjarnsholt, T. (2013). The role of bacterial biofilms in chronic infections. *APMIS Supplement,* (136), 1-51.

Blaak, H., van Hoek, A. H., Veenman, C., Docters van Leeuwen, A. E., Lynch, G., van Overbeek, W. M., & de Roda Husman, A. M. (2014). Extended spectrum ss-lactamase- and constitutively AmpC-producing Enterobacteriaceae on fresh produce and in the agricultural environment. *International Journal of Food Microbiology, 168-169*, 8-16.

Bochner, B. R., Gadzinski, P., & Panomitros, E. (2001). Phenotype microarrays for high-throughput phenotypic testing and assay of gene function. *Genome Research, 11*(7), 1246-1255.

Borglin, S., Joyner, D., DeAngelis, K. M., Khudyakov, J., D'haeseleer, P., Joachimiak, M. P., & Hazen, T. (2012). Application of phenotypic microarrays to environmental microbiology. *Current Opinion in Biotechnology, 23*(1), 41-48.

Bouza, E., & Cercenado, E. (2002). *Klebsiella* and *Enterobacter*: antibiotic resistance and treatment implications. *Seminars in Respiratory Infections, 17*(3), 215-230.

Brenner, D. J., McWhorter, A. C., Kai, A., Steigerwalt, A. G., & Farmer, J. J., 3rd. (1986). *Enterobacter asburiae* sp. nov., a new species found in clinical specimens, and reassignment of *Erwinia dissolvens* and *Erwinia nimipressuralis* to the genus *Enterobacter* as *Enterobacter* dissolvens comb. nov. and *Enterobacter nimipressuralis* comb. nov. *Journal of Clinical Microbiology, 23*(6), 1114-1120.

Burnett, S. L., & Beuchat, L. R. (2001). Human pathogens associated with raw produce and unpasteurized juices, and difficulties in decontamination. *Journal of Industrial Microbiology and Biotechnology, 27*(2), 104-110.

Callahan, S. M., & Dunlap, P. V. (2000). LuxR- and acyl-homoserine-lactone-controlled non-*lux* genes define a quorum-sensing regulon in *Vibrio fischeri. Journal of Bacteriology, 182*(10), 2811-2822.

Case, R. J., Labbate, M., & Kjelleberg, S. (2008). AHL-driven quorum-sensing circuits: their frequency and function among the Proteobacteria. *The ISME Journal, 2*(4), 345-349.

Cha, S. W., Heo, J. N., Park, C.-K., Choi, Y. W., & Jeon, S. C. (2013). *Enterobacter asburiae* pneumonia with cavitation. *Journal of the Korean Society of Radiology, 68*(3), 217-219.

Chalupowicz, L., Barash, I., Panijel, M., Sessa, G., & Manulis-Sasson, S. (2009). Regulatory interactions between quorum-sensing, auxin, cytokinin, and the Hrp regulon in relation to gall formation and epiphytic fitness of *Pantoea agglomerans* pv. gypsophilae. *Molecular Plant-Microbe Interactions Journal, 22*(7), 849-856.

Chapon-Herve, V., Akrim, M., Latifi, A., Williams, P., Lazdunski, A., & Bally, M. (1997). Regulation of the xcp secretion pathway by multiple quorum-sensing modulons in *Pseudomonas aeruginosa*. *Molecular Microbiology, 24*(6), 1169-1178.

Chen, L. X., He, S., Li, C., & Ryu, J. (2009). Sublethal kanamycin induced cross resistance to functionally and structurally unrelated antibiotics. *Journal of Experimental Microbiology and Immunology, 13*, 53-57.

Chen, X., Schauder, S., Potier, N., Van Dorsselaer, A., Pelczer, I., Bassler, B. L., & Hughson, F. M. (2002). Structural identification of a bacterial quorum-sensing signal containing boron. *Nature, 415*(6871), 545-549.

Choi, S. H., & Greenberg, E. P. (1991). The C-terminal region of the *Vibrio fischeri* LuxR protein contains an inducer-independent lux gene activating domain. *Proceedings of the National Academy of Sciences USA, 88*(24), 11115-11119.

Choo, J. H., Rukayadi, Y., & Hwang, J. K. (2006). Inhibition of bacterial quorum sensing by vanilla extract. *Letters in Applied Microbiology, 42*(6), 637-641.

Cobo, F. (2013). Application of MALDI-TOF mass spectrometry in clinical virology: a review. *The Open Virology Journal, 7*, 84-90.

Colville, K., Tompkins, N., Rutenberg, A. D., & Jericho, M. H. (2010). Effects of poly(L-lysine) substrates on attached *Escherichia coli* bacteria. *Langmuir, 26*(4), 2639-2644.

Cooley, M., Chhabra, S. R., & Williams, P. (2008). *N*-acylhomoserine lactone-mediated quorum sensing: a twist in the tail and a blow for host immunity. *Chemistry & Biology, 15*(11), 1141-1147.

Coulthurst, S. J., Clare, S., Evans, T. J., Foulds, I. J., Roberts, K. J., Welch, M., . . . Salmond, G. P. C. (2007). Quorum sensing has an unexpected role in virulence in the model pathogen *Citrobacter rodentium*. *EMBO Reports, 8*(7), 698-703.

Coulthurst, S. J., Williamson, N. R., Harris, A. K., Spring, D. R., & Salmond, G. P. (2006). Metabolic and regulatory engineering of *Serratia marcescens*: mimicking phage-mediated horizontal acquisition of antibiotic biosynthesis and quorum-sensing capacities. *Microbiology, 152*(Pt 7), 1899-1911.

Cowan, S. E., Liepmann, D., & Keasling, J. D. (2001). Development of engineered biofilms on poly-L-lysine patterned surfaces. *Biotechnology Letters, 23*(15), 1235-1241.

Darling, A. C. E., Mau, B., Blattner, F. R., & Perna, N. T. (2004). Mauve: multiple alignment of conserved genomic sequence with rearrangements. *Genome Research, 14*(7), 1394-1403.

de Kievit, T. R., & Iglewski, B. H. (2000). Bacterial quorum sensing in pathogenic relationships. *Infection and Immunity, 68*(9), 4839-4849.

Defoirdt, T., Boon, N., Sorgeloos, P., Verstraete, W., & Bossier, P. (2008). Quorum sensing and quorum quenching in *Vibrio harveyi*: lessons learned from in vivo work. *The ISME Journal, 2*(1), 19-26.

Devine, J. H., Shadel, G. S., & Baldwin, T. O. (1989). Identification of the operator of the *lux* regulon from the *Vibrio fischeri* strain ATCC7744. *Proceedings of the National Academy of Sciences, 86*(15), 5688-5692.

Diggle, S. P., Gardner, A., West, S. A., & Griffin, A. S. (2007). Evolutionary theory of bacterial quorum sensing: when is a signal not a signal? *Philosophical Transactions of the Royal Society B: Biological Sciences, 362*(1483), 1241-1249.

Domka, J., Lee, J., & Wood, T. K. (2006). YliH (BssR) and YceP (BssS) regulate *Escherichia coli* K-12 biofilm formation by influencing cell signaling. *Applied and Environmental Microbiology, 72*(4), 2449-2459.

Dong, Y. H., & Zhang, L. H. (2005). Quorum sensing and quorum-quenching enzymes. *Journal of Microbiology, 43 Spec No*, 101-109.

Dubern, J. F., Lugtenberg, B. J., & Bloemberg, G. V. (2006). The *ppuI-rsaL-ppuR* quorum-sensing system regulates biofilm formation of *Pseudomonas putida* PCL1445 by controlling biosynthesis of the cyclic lipopeptides putisolvins I and II. *Journal of Bacteriology, 188*(8), 2898-2906.

Duerkop, B. A., Ulrich, R. L., & Greenberg, E. P. (2007). Octanoyl-homoserine lactone is the cognate signal for *Burkholderia mallei* BmaR1-BmaI1 quorum sensing. *Journal of Bacteriology, 189*(14), 5034-5040.

Dunlap, P. V. (1999). Quorum regulation of luminescence in *Vibrio fischeri*. *Journal of Molecular Microbiology and Biotechnology, 1*(1), 5-12.

Eberhard, A., Burlingame, A. L., Eberhard, C., Kenyon, G. L., Nealson, K. H., & Oppenheimer, N. J. (1981). Structural identification of autoinducer of *Photobacterium fischeri* luciferase. *Biochemistry, 20*(9), 2444-2449.

El Said Said, D. (2012). Detection of parasites in commonly consumed raw vegetables. *Alexandria Journal of Medicine, 48*(4), 345-352.

Elbeltagy, A., Nishioka, K., Sato, T., Suzuki, H., Ye, B., Hamada, T., . . . Minamisawa, K. (2001). Endophytic colonization and in planta nitrogen fixation by a *Herbaspirillum* sp. isolated from wild rice species. *Applied and Environmental Microbiology, 67*(11), 5285-5293.

Falomir, M. P., Rico, H., & Gozalbo, D. (2013). *Enterobacter* and *Klebsiella* species isolated from fresh vegetables marketed in Valencia (Spain) and their clinically relevant resistances to chemotherapeutic agents. *Foodborne Pathogens and Disease, 10*(12), 1002-1007.

Farrand, S. K., Qin, Y., & Oger, P. (2002). Quorum-sensing system of *Agrobacterium* plasmids: analysis and utility. *Methods in Enzymology, 358*, 452-484.

Favre-Bonte, S., Kohler, T., & Van Delden, C. (2003). Biofilm formation by *Pseudomonas aeruginosa*: role of the C4-HSL cell-to-cell signal and inhibition by azithromycin. *Journal of Antimicrobial Chemotherapy, 52*(4), 598-604.

Ferrieres, L., & Clarke, D. J. (2003). The RcsC sensor kinase is required for normal biofilm formation in *Escherichia coli* K-12 and controls the expression of a regulon in response to growth on a solid surface. *Molecular Microbiology, 50*(5), 1665-1682.

Flavier, A. B., Clough, S. J., Schell, M. A., & Denny, T. P. (1997). Identification of 3-hydroxypalmitic acid methyl ester as a novel autoregulator controlling virulence in *Ralstonia solanacearum. Molecular Microbiology, 26*(2), 251-259.

Fletcher, M. P., Diggle, S. P., Camara, M., & Williams, P. (2007). Biosensor-based assays for PQS, HHQ and related 2-alkyl-4-quinolone quorum sensing signal molecules. *Nature Protocols, 2*(5), 1254-1262.

Fuqua, C., Parsek, M. R., & Greenberg, E. P. (2001). Regulation of gene expression by cell-to-cell communication: acyl-homoserine lactone quorum sensing. *Annual Review of Genetics, 35*, 439-468.

Glessner, A., Smith, R. S., Iglewski, B. H., & Robinson, J. B. (1999). Roles of *Pseudomonas aeruginosa las* and *rhl* quorum-sensing systems in control of twitching motility. *Journal of Bacteriology, 181*(5), 1623-1629.

González, J. E., & Marketon, M. M. (2003). Quorum sensing in nitrogen-fixing rhizobia. *Microbiology and Molecular Biology Reviews, 67*(4), 574-592.

Goris, J., Konstantinidis, K. T., Klappenbach, J. A., Coenye, T., Vandamme, P., & Tiedje, J. M. (2007). DNA–DNA hybridization values and their relationship to whole-genome sequence similarities. *International Journal of Systematic and Evolutionary Microbiology, 57*(1), 81-91.

Gray, K. M. (1997). Intercellular communication and group behavior in bacteria. *Trends in Microbiology, 5*(5), 184-188.

Gray, K. M., & Garey, J. R. (2001). The evolution of bacterial LuxI and LuxR quorum sensing regulators. *Microbiology, 147*(Pt 8), 2379-2387.

Guentzel, M. N. (1996). *Escherichia, Klebsiella, Enterobacter, Serratia, Citrobacter*, and *Proteus*. *Medical Microbiology. 4th edition.*

Gupta, A., Gopal, M., Thomas, G. V., Manikandan, V., Gajewski, J., Thomas, G., . . . Gupta, R. (2014). Whole genome sequencing and analysis of plant growth promoting bacteria isolated from the rhizosphere of plantation crops coconut, cocoa and arecanut. *PLoS ONE, 9*(8), e104259.

Hanzelka, B. L., & Greenberg, E. P. (1995). Evidence that the N-terminal region of the *Vibrio fischeri* LuxR protein constitutes an autoinducer-binding domain. *Journal of Bacteriology, 177*(3), 815-817.

Hanzelka, B. L., Parsek, M. R., Val, D. L., Dunlap, P. V., Cronan, J. E., Jr., & Greenberg, E. P. (1999). Acylhomoserine lactone synthase activity of the *Vibrio fischeri* AinS protein. *Journal of Bacteriology, 181*(18), 5766-5770.

Hao, G., & Burr, T. J. (2006). Regulation of long-chain *N*-acyl-homoserine lactones in *Agrobacterium vitis*. *Journal of Bacteriology*, *188*(6), 2173-2183.

Harris, L. J., Farber, J. N., Beuchat, L. R., Parish, M. E., Suslow, T. V., Garrett, E. H., & Busta, F. F. (2003). Outbreaks associated with fresh produce: incidence, growth, and survival of pathogens in fresh and fresh-cut produce. *Comprehensive Reviews in Food Science and Food Safety, 2*, 78-141.

Heaton, J. C., & Jones, K. (2008). Microbial contamination of fruit and vegetables and the behaviour of enteropathogens in the phyllosphere: a review. *Journal of Applied Microbiology, 104*(3), 613-626.

Hornick, D. B., Allen, B. L., Horn, M. A., & Clegg, S. (1991). Fimbrial types among respiratory isolates belonging to the family Enterobacteriaceae. *Journal of Clinical Microbiology*, *29*(9), 1795-1800.

How, K. Y., Hong, K.-W., Sam, C.-K., Koh, C.-L., Yin, W.-F., & Chan, K. G. (2015). Unravelling the genome of long chain *N*-acylhomoserine lactone-producing *Acinetobacter* sp. strain GG2 and identification of its quorum sensing synthase gene. *Frontiers in Microbiology, 6,* 240.

Howe, K., & Wood, J. M. D. (2015). Using optical mapping data for the improvement of vertebrate genome assemblies. *GigaScience, 4*, 10.

Huber, B., Riedel, K., Hentzer, M., Heydorn, A., Gotschlich, A., Givskov, M., . . . Eberl, L. (2001). The *cep* quorum-sensing system of *Burkholderia cepacia* H111 controls biofilm formation and swarming motility. *Microbiology, 147*(Pt 9), 2517-2528.

Iida, A., Ohnishi, Y., & Horinouchi, S. (2008). Control of acetic acid fermentation by quorum sensing via *N*-acylhomoserine lactones in *Gluconacetobacter intermedius*. *Journal of Bacteriology, 190*(7), 2546-2555.

Ingham, S. C., Losinski, J. A., Andrews, M. P., Breuer, J. E., Breuer, J. R., Wood, T. M., & Wright, T. H. (2004). *Escherichia coli* contamination of vegetables grown in soils fertilized with noncomposted bovine manure: garden-scale studies. *Applied and Environmental Microbiology, 70*(11), 6420-6427.

Ipinza, F., Collao, B., Monsalva, D., Bustamante, V. H., Luraschi, R., Alegría-Arcos, M., . . . Saavedra, C. P. (2014). Participation of the *Salmonella* OmpD porin in the infection of RAW264.7 macrophages and BALB/c mice. *PLoS ONE, 9*(10), e111062.

Kadar, B., Kocsis, B., Kristof, K., Toth, A., & Szabo, D. (2015). Effect of antimicrobial peptides on colistin-susceptible and colistin-resistant strains of *Klebsiella pneumoniae* and *Enterobacter asburiae*. *Acta Microbiologica et Immunologica Hungarica, 62*(4), 501-508.

Kahn, D., & Ditta, G. (1991). Modular structure of Fix J: homology of the transcriptional activator domain with the -35 binding domain of sigma factors. *Molecular Microbiology, 5*(4), 987-997.

Keller, L., & Surette, M. G. (2006). Communication in bacteria: an ecological and evolutionary perspective. *Nature Reviews Microbiology, 4*(4), 249-258.

Khan, S. R., Mavrodi, D. V., Jog, G. J., Suga, H., Thomashow, L. S., & Farrand, S. K. (2005). Activation of the *phz* operon of *Pseudomonas fluorescens* 2-79 requires the LuxR homolog PhzR, N-(3-OH-Hexanoyl)-L-homoserine lactone produced by the LuxI homolog PhzI, and a cis-acting *phz* box. *Journal of Bacteriology, 187*(18), 6517-6527.

Kitchel, B., Rasheed, J. K., Patel, J. B., Srinivasan, A., Navon-Venezia, S., Carmeli, Y., . . . Giske, C. G. (2009). Molecular epidemiology of KPC-producing *Klebsiella pneumoniae* isolates in the United States: clonal expansion of multilocus sequence type 258. *Antimicrobial Agents and Chemotherapy, 53*(8), 3365-3370.

Kohanski, M. A., DePristo, M. A., & Collins, J. J. (2010). Sublethal antibiotic treatment leads to multidrug resistance via radical-induced mutagenesis. *Molecular Cell, 37*(3), 311-320.

Koiv, V., & Mae, A. (2001). Quorum sensing controls the synthesis of virulence factors by modulating *rsmA* gene expression in *Erwinia carotovora* subsp. carotovora. *Molecular Genetics and Genomics, 265*(2), 287-292.

Koth, K., Boniface, J., Chance, E. A., & Hanes, M. C. (2012). *Enterobacter asburiae* and *Aeromonas hydrophila*: soft tissue infection requiring debridement. *Orthopedics, 35*(6), e996-999.

Koutsoudis, M. D., Tsaltas, D., Minogue, T. D., & von Bodman, S. B. (2006). Quorum-sensing regulation governs bacterial adhesion, biofilm development, and host colonization in *Pantoea stewartii* subspecies stewartii. *Proceedings of the National Academy of Sciences, 103*(15), 5983-5988.

Krick, A., Kehraus, S., Eberl, L., Riedel, K., Anke, H., Kaesler, I., . . . Konig, G. M. (2007). A marine *Mesorhizobium* sp. produces structurally novel long-chain *N*-acyl-L-homoserine lactones. *Applied and Environmental Microbiology, 73*(11), 3587-3594.

Krumsiek, J., Arnold, R., & Rattei, T. (2007). Gepard: a rapid and sensitive tool for creating dotplots on genome scale. *Bioinformatics, 23*(8), 1026-1028.

Kumar, C. G., & Anand, S. K. (1998). Significance of microbial biofilms in food industry: a review. *International Journal of Food Microbiology, 42*(1-2), 9-27.

Labbate, M., Queck, S. Y., Koh, K. S., Rice, S. A., Givskov, M., & Kjelleberg, S. (2004). Quorum sensing-controlled biofilm development in *Serratia liquefaciens* MG1. *Journal of Bacteriology, 186*(3), 692-698.

Lamont, I. L., Beare, P. A., Ochsner, U., Vasil, A. I., & Vasil, M. L. (2002). Siderophore-mediated signaling regulates virulence factor production in *Pseudomonas aeruginosa*. *Proceedings of the National Academy of Sciences, 99*(10), 7072-7077.

Lau, Y., Yin, W.-F., & Chan, K.-G. (2014). *Enterobacter asburiae* strain L1: complete genome and whole genome optical mapping analysis of a quorum sensing bacterium. *Sensors, 14*(8), 13913.

Lau, Y., Sulaiman, J., Chen, J., Yin, W.-F., & Chan, K.-G. (2013). Quorum sensing activity of *Enterobacter asburiae* isolated from lettuce leaves. *Sensors, 13*(10), 14189.

Lee, I., Kim, Y. O., Park, S. C., & Chun, J. (2015). OrthoANI: An improved algorithm and software for calculating average nucleotide identity. *International Journal of Systematic and Evolutionary Microbiology*.

Lemonnier, M., Ziegelin, G., Reick, T., Gómez, A. M., Díaz-Orejas, R., & Lanka, E. (2003). Bacteriophage P1 Ban protein is a hexameric DNA helicase that interacts with and substitutes for *Escherichia coli* DnaB. *Nucleic Acids Research, 31*(14), 3918-3928.

Lewenza, S., Conway, B., Greenberg, E. P., & Sokol, P. A. (1999). Quorum sensing in *Burkholderia cepacia*: identification of the LuxRI homologs CepRI. *Journal of Bacteriology, 181*(3), 748-756.

Li, X. Z., Mehrotra, M., Ghimire, S., & Adewoye, L. (2007). Beta-lactam resistance and beta-lactamases in bacteria of animal origin. *Veterinary Microbiology, 121*(3-4), 197-214.

Lindsay, A., & Ahmer, B. M. (2005). Effect of *sdiA* on biosensors of *N*-acylhomoserine lactones. *Journal of Bacteriology, 187*(14), 5054-5058.

Llamas, I., Keshavan, N., & Gonzalez, J. E. (2004). Use of *Sinorhizobium meliloti* as an indicator for specific detection of long-chain *N*-acyl homoserine lactones. *Applied and Environmental Microbiology, 70*(6), 3715-3723.

Loh, J., Carlson, R. W., York, W. S., & Stacey, G. (2002). Bradyoxetin, a unique chemical signal involved in symbiotic gene regulation. *Proceedings of the National Academy of Sciences USA, 99*(22), 14446-14451.

Lund, B. M. (1992). Ecosystems in vegetable foods. *The Society for Applied Bacteriology Symposium, 21,* 115s-126s.

Lynch, M. J., Swift, S., Kirke, D. F., Keevil, C. W., Dodd, C. E., & Williams, P. (2002). The regulation of biofilm development by quorum sensing in *Aeromonas hydrophila*. *Environmental Microbiology, 4*(1), 18-28.

Malott, R. J., Baldwin, A., Mahenthiralingam, E., & Sokol, P. A. (2005). Characterization of the *cciIR* quorum-sensing system in *Burkholderia cenocepacia*. *Infection and Immunity, 73*(8), 4982-4992.

Mandrell, R. E. (2009). Enteric human pathogens associated with fresh produce: sources, transport, and ecology. *Microbial Safety of Fresh Produce* (pp. 1-41). Wiley-Blackwell.

Marvin, L. F., Roberts, M. A., & Fay, L. B. (2003). Matrix-assisted laser desorption/ionization time-of-flight mass spectrometry in clinical chemistry. *Clinica Chimica Acta, 337*(1-2), 11-21.

Maus, C. E., Plikaytis, B. B., & Shinnick, T. M. (2005). Molecular analysis of cross-resistance to capreomycin, kanamycin, amikacin, and viomycin in *Mycobacterium tuberculosis*. *Antimicrobial Agents and Chemotherapy, 49*(8), 3192-3197.

McClean, K. H., Winson, M. K., Fish, L., Taylor, A., Chhabra, S. R., Camara, M., . . . Williams, P. (1997). Quorum sensing and *Chromobacterium violaceum*: exploitation of violacein production and inhibition for the detection of *N*-acylhomoserine lactones. *Microbiology, 143 (Pt 12),* 3703-3711.

McGowan, S., Sebaihia, M., Jones, S., Yu, B., Bainton, N., Chan, P. F., . . . Salmond, G. P. (1995). Carbapenem antibiotic production in *Erwinia carotovora* is regulated by CarR, a homologue of the LuxR transcriptional activator. *Microbiology, 141 (Pt 3),* 541-550.

McInroy, J. A., & Kloepper, J. W. (1995). Survey of indigenous bacterial endophytes from cotton and sweet corn. *Plant and Soil, 173*(2), 337-342.

Miller, J. H. (1972). Assays of lac operon enzymes: β-galactosidase permease, repressor, transacetylase, a complementation. *Experiments in Molecular Genetics* (pp. 352-355). New York, NY: *Cold Spring Harbor Laboratory Press*.

Miller, M. B., & Bassler, B. L. (2001). Quorum sensing in bacteria. *Annual Review of Microbiology, 55,* 165-199.

Milton, D. L., Chalker, V. J., Kirke, D., Hardman, A., Camara, M., & Williams, P. (2001). The LuxM homologue VanM from *Vibrio anguillarum* directs the synthesis of *N*-(3-hydroxyhexanoyl)homoserine lactone and *N*-hexanoylhomoserine lactone. *Journal of Bacteriology, 183*(12), 3537-3547.

More, M. I., Finger, L. D., Stryker, J. L., Fuqua, C., Eberhard, A., & Winans, S. C. (1996). Enzymatic synthesis of a quorum-sensing autoinducer through use of defined substrates. *Science, 272*(5268), 1655-1658.

Niu, C., Clemmer, K. M., Bonomo, R. A., & Rather, P. N. (2008). Isolation and characterization of an autoinducer synthase from *Acinetobacter baumannii*. *Journal of Bacteriology, 190*(9), 3386-3392.

Nordmann, P., Naas, T., & Poirel, L. (2011). Global spread of carbapenemase-producing Enterobacteriaceae. *Emerging Infectious Diseases, 17*(10), 1791-1798.

Parish, M. E., Beuchat, L. R., Suslow, T. V., Harris, L. J., Garrett, E. H., Farber, J. N., & Busta, F. F. (2003). Methods to reduce/eliminate pathogens from fresh and fresh-cut produce. *Comprehensive Reviews in Food Science and Food Safety, 2*, 161-173.

Park, S., Szonyi, B., Gautam, R., Nightingale, K., Anciso, J., & Ivanek, R. (2012). Risk factors for microbial contamination in fruits and vegetables at the preharvest level: a systematic review. *Journal of Food Protection, 75*(11), 2055-2081.

Parsek, M. R., & Greenberg, E. P. (2000). Acyl-homoserine lactone quorum sensing in gram-negative bacteria: a signaling mechanism involved in associations with higher organisms. *Proceedings of the National Academy of Sciences USA, 97*(16), 8789-8793.

Parsek, M. R., Schaefer, A. L., & Greenberg, E. (1997). Analysis of random and site-directed mutations in *rhlI*, a *Pseudomonas aeruginosa* gene encoding an acylhomoserine lactone synthase. *Molecular Microbiology, 26*(2), 301-310.

Parsek, M. R., & Singh, P. K. (2003). Bacterial biofilms: an emerging link to disease pathogenesis. *Annual Review of Microbiology, 57*, 677-701.

Passador, L., Cook, J. M., Gambello, M. J., Rust, L., & Iglewski, B. H. (1993). Expression of *Pseudomonas aeruginosa* virulence genes requires cell-to-cell communication. *Science, 260*(5111), 1127-1130.

Paterson, D. L. (2006). Resistance in gram-negative bacteria: Enterobacteriaceae. *American Journal of Infection Control, 34*(5 Suppl 1), S20-28; discussion S64-73.

Paterson, D. L., Rossi, F., Baquero, F., Hsueh, P. R., Woods, G. L., Satishchandran, V., . . . Chow, J. W. (2005). In vitro susceptibilities of aerobic and facultative Gram-negative bacilli isolated from patients with intra-abdominal infections worldwide: the 2003 Study for Monitoring Antimicrobial Resistance Trends (SMART). *Journal of Antimicrobial Chemotherapy, 55*(6), 965-973.

Patriquin, G. M., Banin, E., Gilmour, C., Tuchman, R., Greenberg, E. P., & Poole, K. (2008). Influence of quorum sensing and iron on twitching motility and biofilm formation in *Pseudomonas aeruginosa*. *Journal of Bacteriology, 190*(2), 662-671.

Pearson, J. P., Gray, K. M., Passador, L., Tucker, K. D., Eberhard, A., Iglewski, B. H., & Greenberg, E. P. (1994). Structure of the autoinducer required for expression of *Pseudomonas aeruginosa* virulence genes. *Proceedings of the National Academy of Sciences USA, 91*(1), 197-201.

Pearson, J. P., Van Delden, C., & Iglewski, B. H. (1999). Active efflux and diffusion are involved in transport of *Pseudomonas aeruginosa* cell-to-cell signals. *Journal of Bacteriology, 181*(4), 1203-1210.

Pedrolli, D., Langer, S., Hobl, B., Schwarz, J., Hashimoto, M., & Mack, M. (2015). The *ribB* FMN riboswitch from *Escherichia coli* operates at the transcriptional and translational level and regulates riboflavin biosynthesis. *The FEBS Journal, 282*(16), 3230-3242.

Penalver, C. G., Cantet, F., Morin, D., Haras, D., & Vorholt, J. A. (2006). A plasmid-borne truncated *luxI* homolog controls quorum-sensing systems and extracellular carbohydrate production in *Methylobacterium extorquens* AM1. *Journal of Bacteriology, 188*(20), 7321-7324.

Pesci, E. C., Milbank, J. B., Pearson, J. P., McKnight, S., Kende, A. S., Greenberg, E. P., & Iglewski, B. H. (1999). Quinolone signaling in the cell-to-cell communication system of *Pseudomonas aeruginosa*. *Proceedings of the National Academy of Sciences USA, 96*(20), 11229-11234.

Pierson, L. S., Gaffney, T., Lam, S., & Gong, F. (1995). Molecular analysis of genes encoding phenazine biosynthesis in the biological control bacterium. *Pseudomonas aureofaciens* 30-84. *FEMS Microbiology Letters, 134*(2-3), 299-307.

Piper, K. R., Beck Von Bodman, S., Hwang, I., & Farrand, S. K. (1999). Hierarchical gene regulatory systems arising from fortuitous gene associations: controlling quorum sensing by the opine regulon in *Agrobacterium*. *Molecular Microbiology, 32*(5), 1077-1089.

Pitout, J. D., Moland, E. S., Sanders, C. C., Thomson, K. S., & Fitzsimmons, S. R. (1997). Beta-lactamases and detection of beta-lactam resistance in *Enterobacter* spp. *Antimicrobial Agents and Chemotherapy, 41*(1), 35-39.

Puskas, A., Greenberg, E. P., Kaplan, S., & Schaefer, A. L. (1997). A quorum-sensing system in the free-living photosynthetic bacterium *Rhodobacter sphaeroides*. *Journal of Bacteriology, 179*(23), 7530-7537.

Reeves, A. Z., Campbell, P. J., Sultana, R., Malik, S., Murray, M., Plikaytis, B. B., . . . Posey, J. E. (2013). Aminoglycoside cross-resistance in *Mycobacterium tuberculosis* due to mutations in the 5' untranslated region of *whiB7*. *Antimicrobial Agents and Chemotherapy, 57*(4), 1857-1865.

Rezzonico, F., Smits, T. H. M., & Duffy, B. (2012). Detection of AI-2 receptors in genomes of Enterobacteriaceae suggests a role of type-2 quorum sensing in closed ecosystems. *Sensors, 12*(5), 6645-6665.

Riedel, K., Hentzer, M., Geisenberger, O., Huber, B., Steidle, A., Wu, H., . . . Eberl, L. (2001). *N*-acylhomoserine-lactone-mediated communication between *Pseudomonas aeruginosa* and *Burkholderia cepacia* in mixed biofilms. *Microbiology, 147*(Pt 12), 3249-3262.

Rivas, M., Seeger, M., Jedlicki, E., & Holmes, D. S. (2007). Second acyl homoserine lactone production system in the extreme acidophile *Acidithiobacillus ferrooxidans*. *Applied and Environmental Microbiology, 73*(10), 3225-3231.

Roberts, R. J., Carneiro, M. O., & Schatz, M. C. (2013). The advantages of SMRT sequencing. *Genome Biology, 14*(7), 1-4.

Rodelas, B., Lithgow, J. K., Wisniewski-Dye, F., Hardman, A., Wilkinson, A., Economou, A., . . . Downie, J. A. (1999). Analysis of quorum-sensing-dependent control of rhizosphere-expressed (*rhi*) genes in *Rhizobium leguminosarum* bv. viciae. *Journal of Bacteriology, 181*(12), 3816-3823.

Ruimy, R., Meziane-Cherif, D., Momcilovic, S., Arlet, G., Andremont, A., & Courvalin, P. (2010). RAHN-2, a chromosomal extended-spectrum class A β-lactamase from *Rahnella aquatilis. Journal of Antimicrobial Chemotherapy, 65*(8), 1619-1623.

Rutherford, S. T., & Bassler, B. L. (2012). Bacterial quorum sensing: its role in virulence and possibilities for its control. *Cold Spring Harbor Perspectives in Medicine, 2*(11), a012427.

Sambrook, & Russel. (2001). *Molecular cloning: A laboratory manual* (3rd ed.). New York: Cold Spring Harbor Laboratory Press.

Sanders, W. E., & Sanders, C. C. (1997). *Enterobacter* spp.: pathogens poised to flourish at the turn of the century. *Clinical Microbiology Reviews, 10*(2), 220-241.

Schaefer, A. L., Greenberg, E. P., Oliver, C. M., Oda, Y., Huang, J. J., Bittan-Banin, G., . . . Harwood, C. S. (2008). A new class of homoserine lactone quorum-sensing signals. *Nature, 454*(7204), 595-599.

Schaefer, A. L., Val, D. L., Hanzelka, B. L., Cronan, J. E., & Greenberg, E. P. (1996). Generation of cell-to-cell signals in quorum sensing: acyl homoserine lactone synthase activity of a purified *Vibrio fischeri* LuxI protein. *Proceedings of the National Academy of Sciences USA, 93*(18), 9505-9509.

Schauder, S., & Bassler, B. L. (2001). The languages of bacteria. *Genes & Development, 15*(12), 1468-1480.

Schleif, R. (2010). AraC protein, regulation of the L-arabinose operon in *Escherichia coli*, and the light switch mechanism of AraC action. *FEMS Microbiology Reviews, 34*(5), 779-796.

Seng, P., Drancourt, M., Gouriet, F., La Scola, B., Fournier, P. E., Rolain, J. M., & Raoult, D. (2009). Ongoing revolution in bacteriology: routine identification of bacteria by matrix-assisted laser desorption ionization time-of-flight mass spectrometry. *Clinical Infectious Diseases, 49*(4), 543-551.

Seng, P., Theron, F., Honnorat, E., Prost, D., Fournier, P.-E., & Stein, A. (2016). *Raoultella ornithinolytica*: An unusual pathogen for prosthetic joint infection. *IDCases, 5*, 46-48.

Sharan, S. K., Thomason, L. C., Kuznetsov, S. G., & Court, D. L. (2009). Recombineering: A homologous recombination-based method of genetic engineering. *Nature Protocols, 4*(2), 206-223.

Sifri, C. D. (2008). Quorum sensing: bacteria talk sense. *Clinical Infectious Diseases, 47*(8), 1070-1076.

Singhal, N., Kumar, M., Kanaujia, P. K., & Virdi, J. S. (2015). MALDI-TOF mass spectrometry: an emerging technology for microbial identification and diagnosis. *Frontiers in Microbiology, 6*, 791.

Singla, N., Kaistha, N., Gulati, N., & Chander, J. (2010). *Morganella morganii* could be an important Intensive Care Unit pathogen. *Indian Journal of Critical Care Medicine : Peer-reviewed, Official Publication of Indian Society of Critical Care Medicine, 14*(3), 154-155.

Skandamis, P. N., & Nychas, G. J. (2012). Quorum sensing in the context of food microbiology. *Applied and Environmental Microbiology, 78*(16), 5473-5482.

Sokol, P. A., Sajjan, U., Visser, M. B., Gingues, S., Forstner, J., & Kooi, C. (2003). The CepIR quorum-sensing system contributes to the virulence of *Burkholderia cenocepacia* respiratory infections. *Microbiology, 149*(Pt 12), 3649-3658.

Solano, C., Echeverz, M., & Lasa, I. (2014). Biofilm dispersion and quorum sensing. *Current Opinion in Microbiology, 18*, 96-104.

Stauff, D. L., & Bassler, B. L. (2011). Quorum sensing in *Chromobacterium violaceum*: DNA recognition and gene regulation by the CviR receptor. *Journal of Bacteriology, 193*(15), 3871-3878.

Steindler, L., Devescovi, G., Subramoni, S., & Venturi, V. (2008). A versatile plasmid biosensor useful to identify quorum sensing LuxR-family orphans in bacterial strains. *Journal of Microbiological Methods, 73*(3), 273-275.

Steindler, L., & Venturi, V. (2007). Detection of quorum-sensing *N*-acyl homoserine lactone signal molecules by bacterial biosensors. *FEMS Microbiology Letters, 266*(1), 1-9.

Stewart, J. M., & Quirk, J. R. (2001). Community-acquired pneumonia caused by *Enterobacter asburiae*. *American Journal of Medicine, 111*(1), 82-83.

Subramoni, S., & Venturi, V. (2009). LuxR-family 'solos': bachelor sensors/regulators of signalling molecules. *Microbiology, 155*(5), 1377-1385.

Swartz, M. N. (2002). Human diseases caused by foodborne pathogens of animal origin. *Clinical Infectious Diseases, 34*(Suppl 3), S111-122.

Swift, S., Karlyshev, A. V., Fish, L., Durant, E. L., Winson, M. K., Chhabra, S. R., . . . Stewart, G. S. (1997). Quorum sensing in *Aeromonas hydrophila* and *Aeromonas salmonicida*: identification of the LuxRI homologs AhyRI and AsaRI and their cognate *N*-acylhomoserine lactone signal molecules. *Journal of Bacteriology, 179*(17), 5271-5281.

Swift, S., Winson, M. K., Chan, P. F., Bainton, N. J., Birdsall, M., Reeves, P. J., . . . et al. (1993). A novel strategy for the isolation of luxI homologues: evidence for the widespread distribution of a LuxR:LuxI superfamily in enteric bacteria. *Molecular Microbiology, 10*(3), 511-520.

Tamura, K., Stecher, G., Peterson, D., Filipski, A., & Kumar, S. (2013). MEGA6: molecular evolutionary genetics analysis version 6.0. *Molecular Biology and Evolution, 30*(12), 2725-2729.

Tash, K. (2005). *Rahnella aquatilis* bacteremia from a suspected urinary source. *Journal of Clinical Microbiology, 43*(5), 2526-2528.

Teplitski, M., Warriner, K., Bartz, J., & Schneider, K. R. (2011). Untangling metabolic and communication networks: interactions of enterics with phytobacteria and their implications in produce safety. *Trends in Microbiology, 19*(3), 121-127.

Thomason, L. C., Sawitzke, J. A., Li, X., Costantino, N., & Court, D. L. (2014). Recombineering: genetic engineering in bacteria using homologous recombination. *Current Protocols in Molecular Biology, 106*, 1.16.11-39.

Thorne, S. H., & Williams, H. D. (1999). Cell density-dependent starvation survival of *Rhizobium leguminosarum* bv. phaseoli: identification of the role of an *N*-acyl homoserine lactone in adaptation to stationary-phase survival. *Journal of Bacteriology, 181*(3), 981-990.

Tzouvelekis, L. S., Markogiannakis, A., Psichogiou, M., Tassios, P. T., & Daikos, G. L. (2012). Carbapenemases in *Klebsiella pneumoniae* and other Enterobacteriaceae: an evolving crisis of global dimensions. *Clinical Microbiology Reviews, 25*(4), 682-707.

Ulrich, R. L., Deshazer, D., Brueggemann, E. E., Hines, H. B., Oyston, P. C., & Jeddeloh, J. A. (2004). Role of quorum sensing in the pathogenicity of *Burkholderia pseudomallei. Journal of Medical Microbiology, 53*(Pt 11), 1053-1064.

Ulrich, R. L., Deshazer, D., Hines, H. B., & Jeddeloh, J. A. (2004). Quorum sensing: a transcriptional regulatory system involved in the pathogenicity of *Burkholderia mallei. Infection and Immunity, 72*(11), 6589-6596.

Urbanowski, M. L., Lostroh, C. P., & Greenberg, E. P. (2004). Reversible acyl-homoserine lactone binding to purified *Vibrio fischeri* LuxR protein. *Journal of Bacteriology, 186*(3), 631-637.

Valade, E., Thibault, F. M., Gauthier, Y. P., Palencia, M., Popoff, M. Y., & Vidal, D. R. (2004). The PmlI-PmlR quorum-sensing system in *Burkholderia pseudomallei* plays a key role in virulence and modulates production of the MprA protease. *Journal of Bacteriology, 186*(8), 2288-2294.

Venturi, V., & Ahmer, B. M. M. (2015). Editorial: LuxR solos are becoming major players in cell–cell communication in bacteria. *Frontiers in Cellular and Infection Microbiology, 5*(89).

Viana, E. S., Campos, M. E., Ponce, A. R., Mantovani, H. C., & Vanetti, M. C. (2009). Biofilm formation and acyl homoserine lactone production in *Hafnia alvei* isolated from raw milk. *Biological Research, 42*(4), 427-436.

Waters, C. M., & Bassler, B. L. (2005). Quorum sensing: cell-to-cell communication in bacteria. *Annual Review of Cell and Developmental Biology, 21*, 319-346.

Watson, W. T., Minogue, T. D., Val, D. L., von Bodman, S. B., & Churchill, M. E. A. (2002). Structural basis and specificity of acyl-homoserine lactone signal production in bacterial quorum sensing. *Molecular Cell, 9*(3), 685-694.

Weber, M. M., French, C. L., Barnes, M. B., Siegele, D. A., & McLean, R. J. C. (2010). A previously uncharacterized gene, y*jfO* (*bsmA*), influences *Escherichia coli* biofilm formation and stress response. *Microbiology, 156*(Pt 1), 139-147.

Wellington, E. M., Boxall, A. B., Cross, P., Feil, E. J., Gaze, W. H., Hawkey, P. M., . . . Williams, A. P. (2013). The role of the natural environment in the emergence of antibiotic resistance in gram-negative bacteria. *Lancet Infectious Disease, 13*(2), 155-165.

Whitehead, N. A., Barnard, A. M., Slater, H., Simpson, N. J., & Salmond, G. P. (2001). Quorum-sensing in Gram-negative bacteria. *FEMS Microbiology Reviews, 25*(4), 365-404.

Wilkins, M. R., Gasteiger, E., Bairoch, A., Sanchez, J. C., Williams, K. L., Appel, R. D., & Hochstrasser, D. F. (1999). Protein identification and analysis tools in the ExPASy server. *Methods in Molecular Biology, 112*, 531-552.

Williams, P. (2007). Quorum sensing, communication and cross-kingdom signalling in the bacterial world. *Microbiology, 153*(12), 3923-3938.

Williams, P., Winzer, K., Chan, W. C., & Cámara, M. (2007). Look who's talking: communication and quorum sensing in the bacterial world. *Philosophical Transactions of the Royal Society of London B: Biological Sciences, 362*(1483), 1119-1134.

Winson, M. K., Swift, S., Fish, L., Throup, J. P., Jorgensen, F., Chhabra, S. R., . . . Stewart, G. S. (1998). Construction and analysis of *luxCDABE*-based plasmid sensors for investigating *N*-acyl homoserine lactone-mediated quorum sensing. *FEMS Microbiology Letters, 163*(2), 185-192.

Winson, M. K., Swift, S., Hill, P. J., Sims, C. M., Griesmayr, G., Bycroft, B. W., . . . Stewart, G. S. (1998). Engineering the *luxCDABE* genes from *Photorhabdus luminescens* to provide a bioluminescent reporter for constitutive and promoter probe plasmids and mini-Tn5 constructs. *FEMS Microbiology Letters, 163*(2), 193-202.

Winzer, K., Hardie, K. R., & Williams, P. (2002). Bacterial cell-to-cell communication: sorry, can't talk now — gone to lunch! *Current Opinion in Microbiology, 5*(2), 216-222.

Wolcott, R. D., & Ehrlich, G. D. (2008). Biofilms and chronic infections. *JAMA, 299*(22), 2682-2684.

Wong, C. S., Yin, W. F., Choo, Y. M., Sam, C. K., Koh, C. L., & Chan, K. G. (2012). Coexistence of quorum-quenching and quorum-sensing in tropical marine *Pseudomonas aeruginosa* strain MW3A. *World Journal of Microbiology and Biotechnology, 28*(2), 453-461.

Xie, L., Zeng, J., Luo, H., Pan, W., & Xie, J. (2014). The roles of bacterial GCN5-related *N*-acetyltransferases. *Critical Reviews™ in Eukaryotic Gene Expression, 24*(1), 77-87.

Yan, Q., Power, K., Cooney, S., Fox, E., Gopinath, G., Grim, C., . . . Fanning, S. (2013). Complete genome sequence and phenotype microarray analysis of *Cronobacter sakazakii* SP291: a persistent isolate cultured from a powdered infant formula production facility. *Frontiers in Microbiology, 4*(256).

Yang, M., Sun, K., Zhou, L., Yang, R., Zhong, Z., & Zhu, J. (2009). Functional analysis of three AHL autoinducer synthase genes in *Mesorhizobium loti* reveals the important role of quorum sensing in symbiotic nodulation. *Canadian Journal of Microbiology, 55*(2), 210-214.

Yates, E. A., Philipp, B., Buckley, C., Atkinson, S., Chhabra, S. R., Sockett, R. E., . . . Williams, P. (2002). *N*-acylhomoserine lactones undergo lactonolysis in a pH-, temperature-, and acyl chain length-dependent manner during growth of *Yersinia pseudotuberculosis* and *Pseudomonas aeruginosa*. *Infection and Immunity, 70*(10), 5635-5646.

Yin, W. F., Purmal, K., Chin, S., Chan, X. Y., Koh, C. L., Sam, C. K., & Chan, K. G. (2012). *N*-acyl homoserine lactone production by *Klebsiella pneumoniae* isolated from human tongue surface. *Sensors, 12*(3), 3472-3483.

Zaitseva Iu, V., Popova, A. A., & Khmel, I. A. (2014). Quorum sensing regulation in bacteria of the family Enterobacteriaceae. *Genetika, 50*(4), 373-391.

Zhang, L., Murphy, P. J., Kerr, A., & Tate, M. E. (1993). *Agrobacterium* conjugation and gene regulation by *N*-acyl-L-homoserine lactones. *Nature, 362*(6419), 446-448.

LIST OF PUBLICATIONS AND PAPER PRESENTED

A LIST OF PUBLICATIONS

Lau, Y., Sulaiman, J., Chen, J., Yin, W.-F., & Chan, K.-G. (2013). Quorum sensing activity of *Enterobacter asburiae* isolated from lettuce leaves. *Sensors, 13*(10), 14189.

Lau, Y., Yin, W.-F., & Chan, K.-G. (2014). *Enterobacter asburiae* strain L1: complete genome and whole genome optical mapping analysis of a quorum sensing bacterium. *Sensors, 14*(8), 13913.

B LIST OF PRESENTATION

Lau, Y., & Chan, K.-G. (2014, June). *Enterobacter asburiae*, a novel quorum sensing bacterium. Poster presentation in Monash Science International Symposium 2014 which took place at Monash University, Selangor, Malaysia.